Publisher's PDF, also known as Version of record

Link to published version (if available):
10.1007/s10853-022-06903-8
10.1007/s10853-022-06903-8

Link to publication record in Explore Bristol Research

PDF-document

University of Bristol - Explore Bristol Research
General rights

Review

Current international research into cellulose as a functional nanomaterial for advanced applications

S. J. Eichhorn[1,*], A. Etale[1], J. Wang[1], L. A. Berglund[2], Y. Li[2], Y. Cai[3], C. Chen[4],
E. D. Cranston[5,6], M. A. Johns[5], Z. Fang[7], G. Li[7], L. Hu[8], M. Khandelwal[9],
K.-Y. Lee[10], K. Oksman[11], S. Pinitsoontorn[12], F. Quero[13,14], A. Sebastian[15],
M. M. Titirici[16], Z. Xu[16], S. Vignolini[17], and B. Frka-Petesic[17]

Extended author information available on the last page of the article

ABSTRACT

This review paper provides a recent overview of current international research that is being conducted into the functional properties of cellulose as a nanomaterial. A particular emphasis is placed on fundamental and applied research that is being undertaken to generate applications, which are now becoming a real prospect given the developments in the field over the last 20 years. A short introduction covers the context of the work, and definitions of the different forms of cellulose nanomaterials (CNMs) that are most widely studied. We also address the terminology used for CNMs, suggesting a standard way to classify these materials. The reviews are separated out into theme areas, namely healthcare, water purification, biocomposites, and energy. Each section contains a short review of the field within the theme and summarizes recent work being undertaken by the groups represented. Topics that are covered include cellulose nanocrystals for directed growth of tissues, bacterial cellulose in healthcare, nanocellulose for drug delivery, nanocellulose for water purification, nanocellulose for thermoplastic composites, nanocellulose for structurally colored materials, transparent wood biocomposites, supercapacitors and batteries.

Introduction

The world is facing a very near and present crisis in terms of climate change and the threat to life. A dramatic reduction in global greenhouse gas emissions is needed, and in doing so fossil fuels require significant replacement. Linked to this is a decarbonization of our materials cycle. Our continued reliance on fossil fuels, and in particular oil, for the production of plastics is simply not sustainable. To this end we need to use sources of materials that are renewable, sustainable and have at least the potential to be placed into a closed-loop recycling system. These criteria are often used as a justification for the use of cellulose, which is derived from a

⚫ Springer

renewable resource, i.e., plants, which in addition sequester carbon dioxide from the Earth's atmosphere for its production and can be potentially returned to the Earth at end-of-life. Nevertheless, this perfect view of cellulose is not yet realized in practice, and we are somewhat far yet in reaching this goal.

Cellulose is a carbohydrate polymeric material, containing carbon (C), hydrogen (H) and oxygen (O). It also belongs to a broader class of natural polymeric materials called polysaccharides, some of which have similar structures to cellulose, but also include other atomic groups like nitrogen (N) (*e.g.*, chitin [1]). We would like to address early on a mistake in the previous review [2] where it stated that the repeat unit of cellulose is cellobiose. It is in fact glucose [3], and cellulose is rather unique among carbohydrates in that it can be both synthesized from, and hydrolyzed to, monosaccharides [4]. In synthesis, glucose monomers are polymerized into long chains, forming anhydroglucose units joined via β-1,4 glycosidic linkages, as shown in Fig. 1.

The crystalline forms of cellulose are numerous. For the purposes of this article, the two sub-allomorphs of cellulose type I—cellulose Iα and Iβ [5]—are perhaps the most relevant in that they appear to different degrees in the various types of native cellulose from plants, some animals (tunicates), and bacterial forms. The crystal structures of these allomorphs have been determined with great accuracy, in particular their complex and extensive hydrogen bonding [6, 7]. The hydrogen bonding is often quoted as the reason for the high axial stiffness of cellulose, although this is perhaps sometimes overstated, and quite likely hydrophobic interactions between the planes of the pyranose rings play a role too, but most importantly limit solubility [8]. The recalcitrance of cellulose to common solvents has long been an issue

for its processing, and it is perhaps for this reason, among many, that the material has been traditionally 'structured' by top-down processing, or bottom-up chemical modification or biosynthesis. Recent attempts to self-assemble cellulose-like polymers from enzymatically generated oligomers offer perhaps new ways of producing nanomaterials [9, 10], but these approaches are in their infancy, and not yet suitable for application.
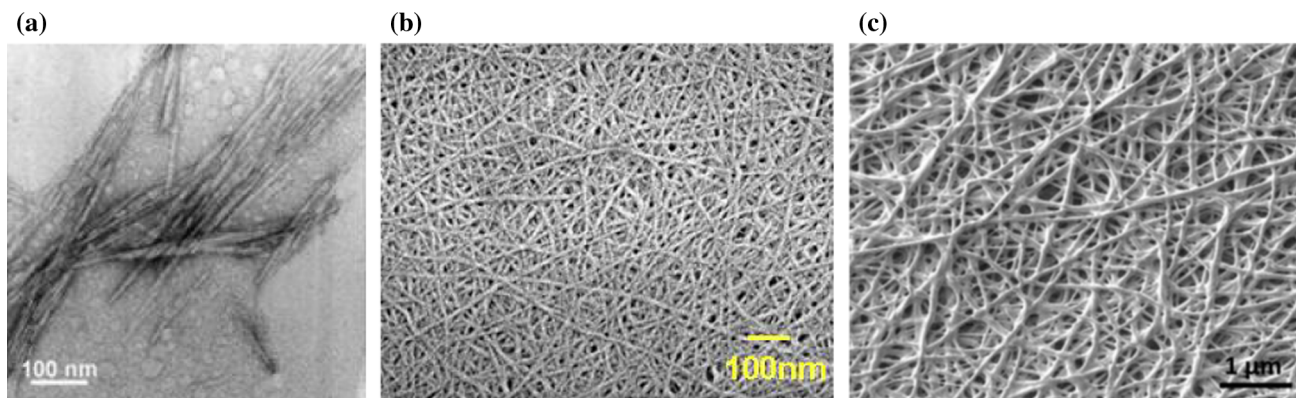
The main forms of cellulose nanomaterials (CNMs) covered in this review are cellulose nanocrystals (CNCs), cellulose nanofibrils (CNFs) and bacterial cellulose (BC); we address the terminology used here in the "Cellulose nanomaterial terminology" section. CNCs are typically produced via the acid hydrolysis of plant-based and other forms of cellulose to produce rod-like particles (see Fig. 2a), although many other production routes are possible. The production and properties of CNCs have been previously reviewed, and readers are referred to that publication for more details [13]. CNFs are typically produced by the mechanical fibrillation of plant cellulose, either via processes such as homogenization, grinding, or excessive beating of pulp. This generates fibrillar materials (see Fig. 2b), and the reader is referred to a previous publication on this subject (where the material is termed 'microfibrillated cellulose') [14]. Finally, BC is typically produced by the gram-negative bacterium *Glucanobacter xylinum* and forms a reticulated network of fibrils, (see Fig. 2c), similar to CNF, but with 'juncture' points between the fibrils. Again, the reader is referred to a previous review of BC, and the other forms of CNFs, for more details [15].

Cellulose is the world's most used material, and it has been exploited for many centuries as wood for fuel and construction, as fibers to produce paper, and textile materials for clothing, ropes, sails and other
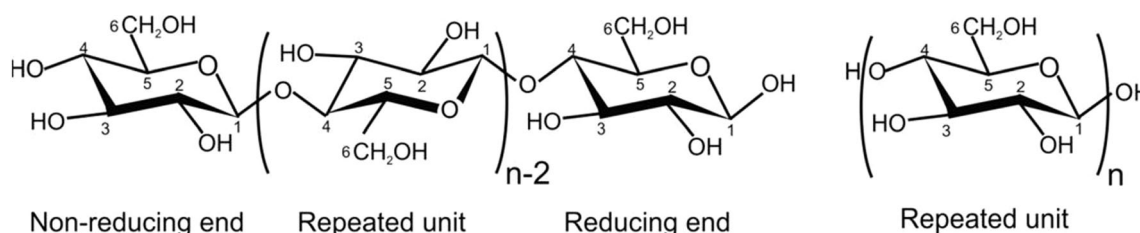
Figure 1 An established convention for the repeated structure of cellulose (left) showing the 'Repeated unit' of glucose (right), with the correct convention for β-1,4 glycosidic linkages and highlighting the non- and reducing ends of the chain. Image reproduced from [3]. Reproduced with permission from [3] (Copyright Springer-Nature, 2017).

Figure 2 Example electron microscope images of cellulose nanomaterials (CNMs); TEM images of **a** cellulose nanocrystals (CNCs) obtained via acid hydrolysis of microcrystalline cellulose [11] **b** cellulose nanofibrils (CNFs) [2] and **c** a scanning electron microscope image of bacterial cellulose (BC) [12]. Figure 2a reproduced from [11] with permission from the American Chemical Society (Copyright American Chemical Society, 2005), Figure 2b from [2] with permission from Springer-Nature (Copyright Springer-Nature, 2010) and Figure 2c from [11] (CC-BY Open Access, 2019).

applications. Our most intimate connection with the material is with wood, and in fact the very word 'material' derives from an old Latin word mātĕria for 'trunk of a tree', which itself derives from the word māter which means 'mother'; many other languages include similar words such as Moeder (Dutch), Maman (French), Māṁ (ਮ) (Punjabi), Mama (Swahili), Maa (媽) (Cantonese), and Mutter (German). The use of this word provides further connection to 'mother earth' a concept that is contained in many indigenous languages and belief systems. Perhaps this connection ought to be regained since we are seeking to protect our planet collectively through sustainability, and through the use of mother nature's material—cellulose.

A review in this journal published in 2010 [2] quoted the English poet Chaucer. It seems apposite to now recall the words of the Japanese Haiku author Matsuo Bashō (1644 – 1694)

"butt of the tree
see in it the cut end
today's moon"

highlighting the mysteries of wood, or perhaps the old Kenyan proverb that '*Sticks in a bundle are unbreakable.*' This proverb might both suggest collaboration is a good thing and that we have had a long history of understanding the mechanical properties of wood. Certainly, our relationships with wood are ancient, and intimately associated with our languages, as already described. Wood itself is also

probably the oldest composite, and it is well known that it possesses a hierarchical structure, which has been well-documented in the literature [16]. The review we present to you contains work that both deconstructs the woody and plant materials into nanomaterials, but also addresses the use and modification of wood itself, making use of its own inherent nanostructure. We therefore present to you a collection of international research on nanocellulose and its application in a variety of fields. It is truly staggering how this material has grown in interest, with publications on 'nanocellulose', and citations to them, growing dramatically over the last decade.

Perhaps it is true to say that many real applications are still yet to materialize. Charreau et al. [17] have, however, recently published data on the numbers of published patents, and their growth since 2010, when the last review in this series was published [2]. This growth in the patent literature is truly dramatic, and nanocellulose is certain to make an impact into many application areas. This review aims to cover research that is a prelude to, and underpins, applications of nanocellulose. Several target areas are covered in the review, namely healthcare, water security, composites, and energy. Recent research in these target areas is discussed, focusing on applications, but also the fundamental research itself that is, and needs to be undertaken to underpin this translation to real products. Each section in this review highlights some work being undertaken by a selected number of

international groups, but also contexts this with current work in the field.

Cellulose nanomaterial terminology

Since 'nanocellulose' emerged onto the scene as a material there has been a proliferation of the terminology used to describe these materials. We will aim to be consistent in our description of nanocellulose and thereby conform to standards that have been recently laid out in another comprehensive review of techniques to analyze what should collectively be called cellulose nanomaterials (CNMs) [18]. This is the acronym we will use to refer to the different forms of 'nanocellulose'. We will use the terms cellulose nanocrystals (CNCs) and cellulose nanofibrils (CNFs) to refer to the rod-like and fibrillar cellulosic materials. Confusingly CNCs have also been called whiskers, needles and nanocrystalline cellulose (NCC), and we will avoid such terms. Bacterial cellulose (BC) will also be used as a term, referring to the fibrillar material produced by the gram-negative bacteria *Glucanobacter xylinum*. We will conform to the international organization for standardization (ISO) on the terminology used for CNMs [19] where possible and to otherwise revert to commonly used terms.

Introduction to nanocellulose in healthcare

Nanocellulose has found suitability in various healthcare applications, for example, tissue engineering and drug delivery, as well as diagnostic devices, wound healing, coatings, drug screening and biosensing [20, 21]. Some key enablers allowing nanocellulose to be used in healthcare applications are its biocompatibility and relatively low cost, as well as its versatility with respect to both the variety of forms available and its ability to be chemically modified. While purity and uniformity of different nanocellulose types (CNFs, CNCs, BC) are dependent on the starting source and production method, they generally offer a reliable, chemically defined, and robust nanomaterial. Plant-based biomaterials can solve some issues present with animal-derived biomaterials where poorly defined, complex mixtures, and high variability from batch to batch suggest advantages of using exogenous components in biomedical applications.

All types of nanocellulose have been evaluated extensively in tissue engineering and drug delivery applications and this section aims to summarize some of the newest advances and trends in the area. For applications in healthcare, BC stands out for its purity (no hemicelluloses, lignin, etc.) and its ability to be manipulated following biotechnological production pathways; in some product development areas like implants, wound healing and cell cultivation/encapsulation, BC has surpassed CNFs and CNCs as reviewed elsewhere [22]. Additionally, we highlight how different architectures like micelles, spheres, patterned surfaces, and 3D-printed shapes, that are based on nanocellulose building blocks, offer advantages such as large surface area, high porosity and enhanced interactions with drugs and cells. While nanocellulose has been shown to have low toxicity [23], there are key variables that have been reported to affect toxicity including size, morphology, crystallinity, surface chemistry and stability [24]. Despite the broad consensus on the low toxicity of the different types of nanocellulose, further studies are recommended to evaluate this property specific to each targeted application, as well as long-term bioaccumulation in the body.

Other important aspects of nanocellulose for healthcare applications are its in vivo biodegradability and bioactivity [23, 25, 26]. High crystallinity celluloses possess low biodegradability and, thus, may limit their use in some bio-applications. Significant efforts have been made to improve biodegradability through chemical modification [27–29] or through higher-order arrangement where the structure degrades but not the nanocellulose itself [30]. It is also known that pure nanocellulose lacks bioactivity [25]. Consequently, many efforts have focused on chemical and physical surface modification routes to provide CNF, CNC, and BC scaffolds with improved bioactivity [25, 26]. Their effect on cell culture parameters has been studied and compared to non-modified nanocellulose forms, demonstrating significant progress.

Owing to the rich chemical, structural, and morphological diversity of nanocellulose, a vast amount of research and commercial translation toward medical applications has been reported. In this section, up-to-date information on the use of nanocellulose for tissue engineering and drug delivery applications is presented. Specifically, the use of CNFs, CNCs and BC as tissue engineering scaffolds

for in vitro cell culture and the effect of surface modification to render nanocellulose bioactive are summarized. This includes the introduction of chemical moieties at the surface of nanocellulose to provide negative or positive surface charges, and the use of amino acids, proteins, and growth factors, to enhance cell uptake/adsorption at the scaffold surface and promote cell adhesion, growth, proliferation, and specific cell morphologies. Additionally, the effect of nano- and microscale anisotropy within nanocellulose scaffolds on cell response and aligned growth is discussed. Nanocellulose offers multiscale control in both 2D and 3D environments, creating new opportunities within tissue engineering. As for drug delivery, the role of nanocellulose as a drug carrier, co-stabilizer, or release modulator in various forms including sheets/films, nanoparticles, and micelles is reported. The use of various types of nanocellulose-based drug delivery systems is presented including examples with hydrophilic and hydrophobic drugs as well as various administration routes such as oral, transdermal, local and triggered-release.

Franck Quero (University of Chile, Chile): tailoring surface chemistry of nanocellulose scaffolds for in vitro cell culture

Cells modify their behavior dependent on the cues that they perceive from their microenvironment [31–33]. One strategy to render the surfaces of several types of nanocellulose more biocompatible and bioactive is through surface modification [25, 26]. Chemical moieties, biomolecules, bio-oligomers and biomacromolecules can be introduced physically or chemically at the surface of nanocellulose to provide cell signals. These include positive or negative surface charges as well as cell receptors such as the amino acid sequence arginine-glycine-aspartic acid. These signals aim at favoring cell uptake/adsorption at the surface of nanocellulose scaffolds, and their effect on cell adhesion, growth, proliferation, and morphology is typically studied.

Research involving the use of BC and CNCs for tissue engineering applications was reviewed by Dugan et al. in 2013 [34]. The surface modification of BC with bioactive peptide sequences using cellulose-binding domains was discussed as a strategy to enhance its bioactivity. The surface charge of CNCs has also been mentioned as a critical factor to provide

their surface with biocompatibility and bioactivity. It is known that mammalian cells possess a net negative charge. As a result, materials with positively charged surfaces could potentially favor cell uptake by electrostatic attraction. On the other hand, materials with negatively charged surfaces would minimize cell uptake due to electrostatic repulsion. The first in vitro study of CNCs with living cells was by Roman et al., where the potential of CNCs as carriers in targeted drug delivery applications was demonstrated [35]. Mahmoud et al. then modified the surface of CNCs with fluorescein isothiocyanate or alternatively rhodamine B isothiocyanate, providing them with negative and positive surface charges, respectively [36]. CNCs modified with positive surface charges were found to be uptaken by human embryonic kidney 293 cells, whereas those modified with negative surface charges were not significantly taken up by both cell types at a physiological pH. The results were explained in terms of cell/material surface electrostatic interactions [36]. Cell uptake mechanisms are, however, more complex, and other scaffold features need to be considered including local nanofiber alignment among others, which are discussed in detail below.

The research group led by Ferraz at Uppsala University explored the effect of nanocellulose surface charge on human dermal fibroblast (HDF) cell culture 2D film scaffolds. In their first work, cationic CNFs and *Cladophora* nanocellulose were obtained by glycidyltrimethylammonium chloride condensation, whereas anionic CNFs and *Cladophora* nanocellulose were obtained by carboxymethylation and TEMPO-oxidation, respectively [37]. The results revealed that anionic CNF films possessed greater cytocompatibility than non-modified and cationic CNF films. On the other hand, anionic *Cladophora* films better promoted cell adhesion and viability compared to non-modified and cationic *Cladophora* films. The improved cell adhesion of HDF onto anionic *Cladophora* films was attributed to local nanofiber alignment.

In a subsequent study, non-modified, anionic, and cationic CNF films were evaluated as 2D scaffolds to direct monocyte/macrophage (MM) responses in the absence or presence of lipopolysaccharide [38]. The results suggested that MM cultured onto anionic CNF films experienced activation toward a proinflammatory phenotype. Non-modified CNF films, however, promoted a mild activation of THP-1 monocyte cells, whereas cationic CNF films behaved

as a bioinert material. None of the materials were able to directly activate the MM toward an anti-inflammatory response.

In a third study by the same group, the effect of the negative surface charge density of TEMPO-oxidized *Cladophora* nanocellulose on the response of HDF and human osteoblastic cells was investigated [39]. From a carboxyl group amount ≥ 260 μmol g^{-1}, equivalent to a threshold ζ-potential value of -36 mV, TEMPO-oxidized *Cladophora* nanocellulose was found to be cytocompatible, demonstrating that bioinert nanomaterials can be turned bioactive by adjusting the magnitude of their surface charge density.

More recently, three primary works have studied the effect of surface charge on cell culture. Films composed of non-modified, anionic, and cationic CNFs were obtained by an evaporation-induced droplet-casting method [40]. Non-modified and cationic CNFs resulted in 2D surfaces with higher degrees of local nanofiber orientation compared to anionic CNFs. With respect to cell viability and proliferation, anionic and cationic CNF surfaces were found to perform similarly compared to a positive control surface. Although the use of fibronectin coating slightly enhanced cell response for all 2D surfaces, uncoated anionic and cationic CNF surfaces were found to support cell growth. Cationic CNF surfaces, along with the presence of CNF alignment, were found to guide cell growth toward a specific orientation direction [40]. In a subsequent study by Pajorova et al. [41], cellulose mesh 3D scaffolds were coated with either cationic, anionic or a 1:1 mixture of cationic and anionic CNFs. Cell adhesion, proliferation, spreading, and morphology were studied by seeding the 3D scaffolds with either HDF or adipose-derived stem cells (ADSC). Anionic CNFs promoted the proliferation of both HDF and ADSC, whereas cationic CNFs enhanced the adhesion of ADSC. The cationic and anionic CNF mixture resulted in promoting combined benefits arising from each CNF type [41]. Lastly, CNFs, CNCs and TEMPO-CNFs with variations in total surface charge were investigated as coatings for cell culture [42]. TEMPO-CNFs with a total surface charge of 1.14 mmol g^{-1} were found to provide the highest cell viability and adhesion compared to the mechanically isolated CNFs without chemical pre-treatment, and CNCs, from which HDF cells were unable to adhere, leading to low viability [42].

Another strategy to render nanocellulose bioactive is by binding either amino acids, peptides, or proteins onto its surface. A first study covalently bound amino acids to the surface of commercial cellulose filter membranes [43]. Cationic amino acids including lysine and arginine were found to enhance cell adhesion, whereas anionic as well as small amino acids significantly reduced cell adhesion. In subsequent work, the surface of α-cellulose fibrous networks was modified by covalent grafting of hydrophilic, aliphatic and aromatic amino acids onto their surface by esterification [44]. Aromatic amino acids, and in particular tryptophan, resulted in enhanced fibroblast cell spreading. Immobilization of collagen peptides onto the surface of dialdehyde BC was proposed by Wen et al. [45] and found to promote enhanced fibroblast cell adhesion and attachment compared to non-modified BC. Another investigation by Barud et al. [46] used silk fibroin proteins to modify the surface of BC, forming a sponge-like scaffold. This was found to facilitate the attachment and growth of L-929 cells, where proteins acted as cell receptors [46].

The research group led by Franck Quero at the University of Chile have produced protein-functionalized cellulose fibrils from the tunic of *Pyura chilensis* by a top-down approach [47]. As illustrated in Fig. 3, the CNFs were used to produce films, which were subsequently evaluated as 2D scaffolds to culture mouse skeletal C2C12 myoblast cells [47]. Membranes having ∼ 3.1% residual proteins at their surface were found to promote higher cell density and spreading as well as a more orientated shape cell morphology compared to membranes constituted of bleached CNFs. In another work by Zhang et al. [48], the real-time cell adsorption of cells onto non-modified and modified CNF films was monitored by multi-parametric surface plasmon resonance. The presence of either human recombinant laminin-L521 (natural protein of the extracellular matrix) or poly-L-lysine at the surface of the CNF films resulted in enhanced attachment of human hepatocellular carcinoma cells compared to non-modified CNF films.

Another method to render the surface of CNFs bioactive has been to modify their surface by polyion complex formation between negatively charged TEMPO-oxidized CNFs and positively charged basic fibroblast growth factors (bFGFS) [49]. In this way, Liu et al. mimicked the interactions that naturally exist between bFGFS and heparin sulfate in the
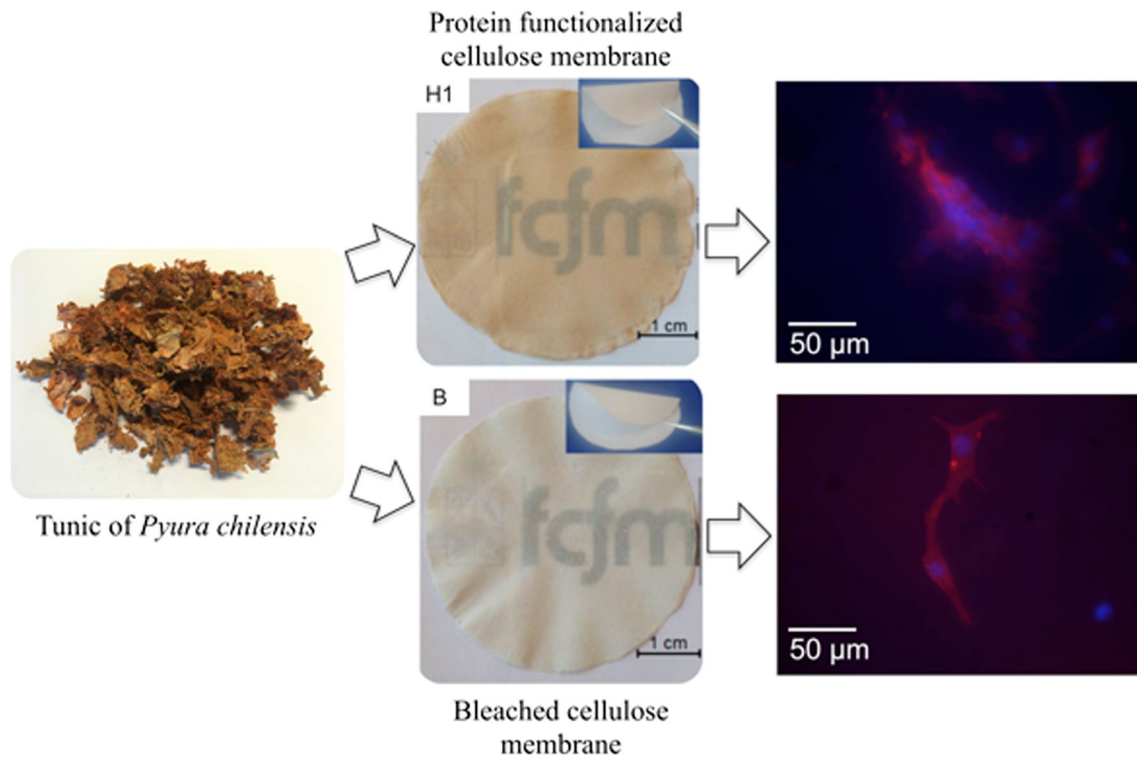
Figure 3 Tunic of *Pyura chilensis* from which CNFs were extracted and used to produce protein functionalized and bleached cellulose membranes (H1 and B, respectively). Fluorescence microscopy images show the differentiation of myoblasts that adhered and grew onto the surface of H1 and B membranes. Reproduced and adapted with permission from [50] (Copyright American Chemical Society, 2019).

extracellular matrix. The scaffold was found to release controlled amount of bFGFS, which was regulated by both CNF surface chemistry and enzymatic deconstruction of the scaffolds. This resulted in significantly enhanced fibroblast cell proliferation [49].

Instead of tailoring the surface chemistry of nanocellulose, other features have been reported to control cell response including multiscale topographical and multicomponent approaches.

These aspects and their specifics are presented in the next subsection and could potentially be translated toward new commercial products in the near future.

Marcus Johns and Emily Cranston (University of British Columbia, Canada): nanocellulose for directional multiscale tissue engineering

Three-dimensional biophysical and biochemical interactions between cells and scaffolds modulate the cell response in terms of proliferation, migration, differentiation, deposition of extracellular matrix proteins, and—ultimately—cell survival. These interactions are dependent on cell surface receptors and, when cell attachment occurs, are regulated by integrin pairs that have a defined nanometric spacing between them [51]. The control of cell alignment via topographical features has been known since the late 1980s/early 1990s [52–54]. Microscale features with step changes>10 μm and spacings>2 μm inhibit cell migration and spreading [55], whilst nanoscale features with dimensions<70 nm and spacings between 70 and 300 nm disrupt focal adhesions [56]. Thus, modification of the tissue engineering scaffold over multiple length scales is significant in defining the response of the cells.

This subsection briefly reviews one particularly promising and emerging area of nanocellulose tissue engineering, namely the design of scaffolds with topographical anisotropy at one, or more, length scales. There are, however, numerous examples in the literature of nanocellulose scaffolds that do not exhibit anisotropy that are well suited to biomedical applications (and tested explicitly in vitro or in vivo) as reviewed elsewhere [20, 25, 57–66] with many
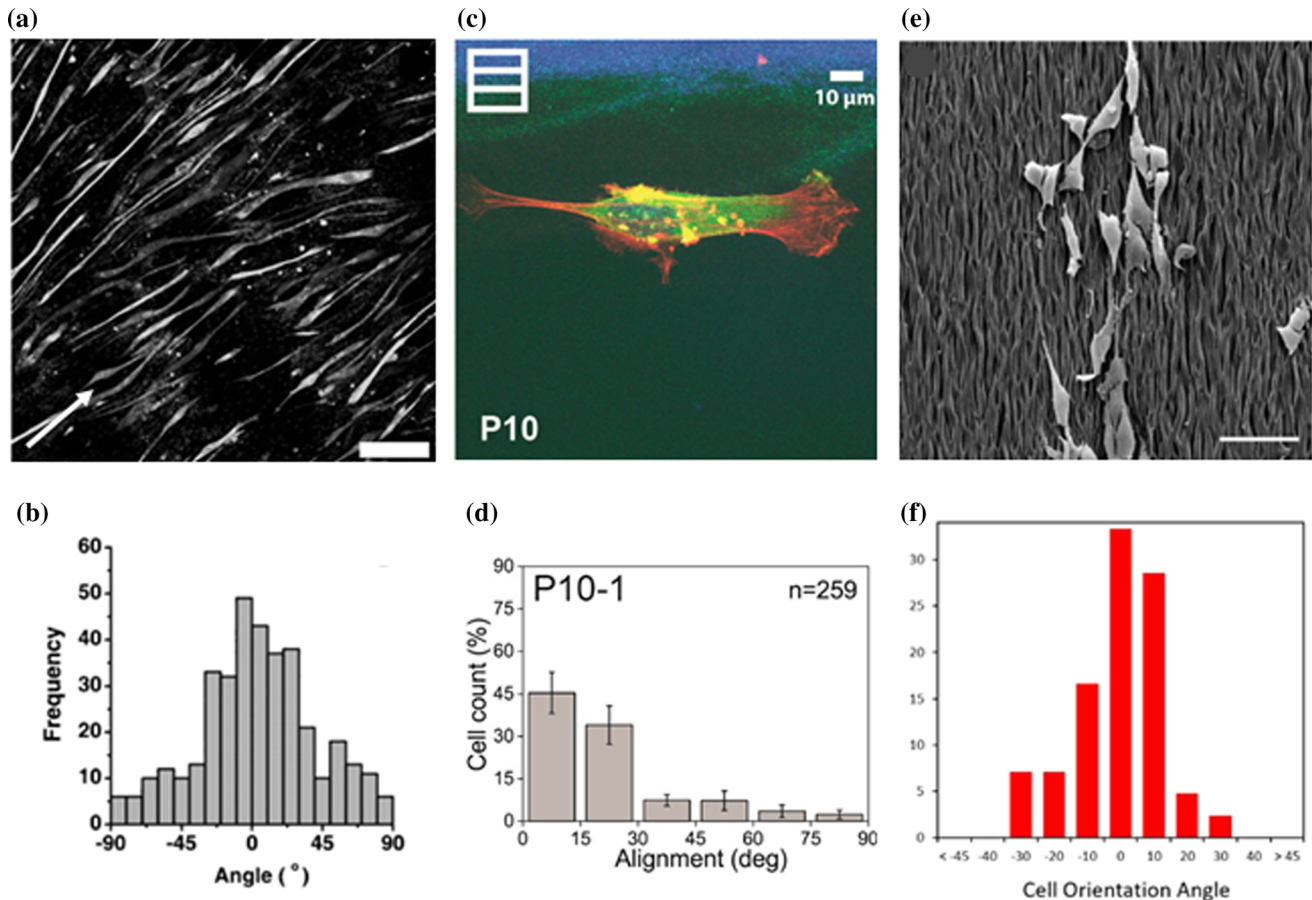
Figure 4 a Myotubes stained for myosin one week after induction of differentiation on aligned CNC surface. Arrow: approx. degree of CNC alignment, scale bar: 250 μm; **b** histogram of myoblast orientation relative to approx. radial axis of CNCs; **c** representative confocal image of human dermal fibroblast adhering to BC substrate with grating microtopography. Orientation of grating reported in top left corner; **d** histogram reporting the cell alignment distribution relative to grating. Error bar:±S.E.; **e** myoblast cell adhesion on uniaxially microscale wrinkled POEGMA-CNC hydrogel sheets with nanoscale parallel-orientated fibers. Scale bar: 50 μm; **f** histogram of cell orientation angle relative to wrinkles. **a, b** Reprinted (adapted) with permission from [93] (Copyright American Chemical Society, 2010). **c, d** Reprinted (adapted) with permission from [97] (Copyright American Chemical Society, 2015). **e, f** Reprinted (adapted) with permission from [109] (Copyright Elsevier, 2021). S.E.=Standard Error.

newer reports focusing on 3D printing specifically [67–71]. Some highlights in the general area of nanocellulose tissue engineering include: 3D scaffolds with controlled bioabsorbability [30, 72]; self-healing hydrogels for cell delivery [73]; scaffolds that maintain stem cell pluripotency [74], or guide cell differentiation [75–79]; hydrogels that support organoid growth [80–83]; and bioinks that enable 3D cell printing [84–92].

Since all nanocellulose types are anisotropic, being fiber or filament-like with diameters at the nanoscale (*e.g.*, BC and CNF), or spindle-like nanoparticles with all dimensions at the nanoscale (*e.g.*, CNCs), the design of tissue scaffolds with, at least, short-range directionality and nano/micro features becomes

possible. Furthermore, long-range directionality and mechanical anisotropy to direct cell response can be achieved via topographical patterning of the scaffold (*e.g.*, soft lithography, 3D printing, templating, electrospinning) or through directed assembly to induce nanoparticle alignment.

In 2010, Dugan et al. [93] were the first to report that the nanoscale structure of CNCs could align myoblast muscle cells (Fig. 4a&b), despite being orders of magnitude smaller than the cells themselves. Straightforward 2D surfaces with spin-coated (radially oriented) CNCs and no other components were sufficient to demonstrate this effect [93]. Similarly, the anisotropic deposition of CNCs onto titanium surfaces guided fibroblast proliferation,

offering new opportunities for integrating implants [94]. Although these features appear too small to enable cell attachment according to earlier literature, it has been recently demonstrated that integrin clusters can form across nanofeatures so long as the feature spacing is <110 nm [95]. It is reasonable to expect that these integrin clusters arrange themselves in line with the features, enabling cell alignment. This work in simple 2D nanocellulose films set the stage for more complex 2D scaffolds and higher dimensionality structures with optimized physicochemical properties and a variety of topographies.

Soft lithographical techniques have been utilized in tissue engineering for almost 20 years [96], however, the first reported use with nanocellulose was demonstrated on BC by Bottan et al. [97] in 2015 (Fig. 4c&d). Since then, the patterning of BC is typically achieved using polydimethylsiloxane with designed structural features >1 µm [97–100]. Spacings of 10 µm between features have been used to direct growth of fibroblasts [97, 99], neuronal cells [98, 100] and muscle cells [100], whilst having a more limited impact on keratinocytes [97, 99]. Importantly, structural control of fibroblast growth via BC scaffolds can influence scar formation in vivo [101]. Jin et al. demonstrated that structured pure BC scaffolds with 10 µm stripes reduced fibroblast proliferation, which limited collagen accumulation. The reduction in collagen, in turn, reduced scar contraction and limited hypertrophic scar formation [101]. Likewise, Boni et al. [99] produced similarly structured BC scaffolds impregnated with silk sericin. The structural features enabled alignment of fibroblasts whilst the silk sericin enhanced fibroblast and keratinocyte proliferation in vitro. However, the structural features limited collagen deposition compared to structurally unmodified BC, which they suggested enhanced the potential to limit fibrosis and scar formation [99]. Thus, soft lithographical modification of BC offers opportunities to produce inexpensive scaffolds and wound dressings with improved healing properties.

Despite previous publications describing increased cell alignment with decreased feature spacing of BC-based materials [97], reports of directly controlling BC 'ribbon' alignment are limited. Wang et al. [102] have recently demonstrated that alignment could be achieved via wet-drawn stretching of the BC film. The gelatin impregnated, aligned films exhibited enhanced mechanical properties and significantly improved fibroblast alignment in vitro, with further enhancement achieved via electric field stimulation [102].

Alternatively, one may produce aligned fibers via electrospinning. He et al. produced aligned regenerated cellulose fibers (with ca. 200 nm diameters) loaded with CNCs and spun from lithium chloride/dimethyl acetamide solution [103]. This composition and processing led to improved tensile properties of the fibers and enabled aligned growth of dental follicle cells [103]. The same scaffolds impregnated with bone morphogenic protein-2 promoted osteogenic differentiation of mesenchymal stem cells in vitro, while anisotropic fiber orientation promoted cell alignment, no significant differences in biomarkers (alkaline phosphatase activity, calcium content) were observed between aligned and unaligned fibers [104]. However, in vivo, the aligned fibers enabled aligned collagen deposition and new cortical bone growth on the external face of the implant. These responses were not observed in the unaligned scaffolds, nor in a similar study using aligned poly(L-lactic acid) nanofibers. As such, the enhanced response in the CNC loaded sample was attributed to the improved mechanical properties observed by the incorporation (and alignment) of CNCs in the scaffold [104].

The improvement of mechanical properties and development of nanoscale anisotropy in multicomponent electrospun and 3D-printed scaffolds via CNC/CNF inclusion has only recently begun to be explored [105–111]. For example, De France et al. reported on the facile production of '2.5D' poly(oligoethylene glycol methacrylate) (POEGMA)/CNC scaffolds that enabled microscale control of 'wrinkled' features, similar to those produced using soft lithography, via controlled thermal shrinkage while independently controlling the alignment of the nanoscale features via electrospinning [109]. Uniaxially (micro) wrinkled features with parallel-oriented (nano) fibers resulted in aligned myoblast growth (Fig. 4e&f), whereby CNC content was used to control the compressive modulus and protein uptake [109]. Similarly, Huang et al. [110] demonstrated that they could align oxidized BC along the direction of extrusion in simple printed structures, which influenced the orientation of lung epithelial stem cells. While research into the nanoscale alignment of nanocellulose in 3D-printed architectures through control of shear is still in the initial stages [112–114], it offers opportunities for the development of scaffolds that exhibit photoresponsive mechanical

properties [115], or change shape depending on the degree of hydration [116].

Nanocellulosic 3D structures with directed cell growth due to anisotropic *microscale* topographies have been achieved via directional freezing to produce aligned pores within cryogels [117, 118] (as opposed to the anisotropy resulting from aligned nanocellulose itself). The effect of pore morphology on cell response is less well defined than that of 2D ridges/grooves. For example, Karageorgiou and Kaplan reported that the optimal pore size to promote osteogenesis was >300 μm [119], while the optimal pore diameter for neuronal cells has often been reported to be <100 μm [120–122]. However, strategies to control pore size and morphology in nanocellulosic cryogels are known, including regulation of the gel composition [123–125]; freeze-casting temperature and/or rate [123, 126]; sol pH [127]; and nanocellulose morphology [126]. Furthermore, Tetik et al. [128] have recently incorporated directional freezing with 3D printing, which enabled the production of controlled 3D geometries with aligned micropores.

Nanoscale anisotropy via alignment of nanocellulose is readily achieved via various techniques [129]. These include shear forces [112, 113, 130–133]; magnetic fields [134–137]; electric fields [138–142]; and material stretching [143–146]. With regard to magnetic alignment in 3D scaffolds, De France et al. [147] showed that anisotropy could be induced in POEGMA-CNC hydrogels with weak magnetic fields capable of aligning CNCs quickly, even within a polymer gel [136]. This enabled alignment of myoblasts in a 3D culture. Echave et al. [137] took this concept further to produce biphasic gelatin hydrogels that mimicked the tendon-bone interface with magnetically aligned CNCs in one section and hydroxyapatite in the other. Adipose-derived stem cells preferentially aligned and expressed tenascin-C (TNC), a tendon tissue-related biomarker, in the CNC section, while cells remained disordered and preferentially expressed osteopontin (OPN), an osteogenic differentiation-related biomarker, in the section containing hydroxyapatite [137].

Unfortunately, there are limited comparative studies investigating cell responses to different nanocellulose morphologies. Kummala et al. [42] have recently examined the response of dermal fibroblasts on different nanocellulose types (i.e., CNCs, a predominantly microfibrillated CNF, and two predominantly nanofibrillated CNFs). While true 'nano'-CNFs supported cell attachment and proliferation, limited cell response was observed on the microfibrillated CNF and CNC surfaces. However, as the authors note, one must consider all the variables involved—including topographical features, surface chemical group type and degree of modification, fibril dimensions, tensile properties, and cell type—to be able to draw conclusions as to the cell response. This requires modeling to isolate cell response to specific parameters, such as the regression modeling performed by Johns et al. [148], and must also take the growth media into consideration as selective molecular adsorption will mediate cell-surface interactions [41, 118].

We conclude that topographically anisotropic nanocellulose scaffolds are promising biobased biomaterials for enabling cell alignment in both 2D and 3D, impacting—for example—wound healing in vitro and stem cell differentiation in vivo. Control of the topographic features at both the microscale and nanoscale through patterning and nanocellulose alignment offers new opportunities in regulating cellular response. Combining these structures with stimuli-dependent chemistry may present future opportunities in dynamic/bio-responsive tissue engineering.

Mudrika Khandelwal (IIT Hyderabad, India) and Anu Sebastian (CIPET: IPT-Kochi, India): nanocellulose-based drug delivery systems

Cellulose has a long history of application in pharmaceutics owing to ease of availability and a good compaction property, primarily as an excipient in oral formulations. Nanocellulose has been shown to play a variety of roles and offer several advantages in drug delivery applications, for example, for its release modulation, as a drug carrier, its improved mechanical properties, better compaction, and appropriate rheological modification [20, 23, 149–151]. It has been shown that the addition of nanocellulose can control the release of incorporated drugs to significantly reduce consumption [152–156]. Nanofibers offer an additional advantage in terms of mechanical support and improvement of shelf life by improving oxidative stability [29]. Novel drug delivery systems such as triggered and targeted forms have emerged using different types of

nanocellulose [157, 158]. Most interestingly, nanocellulose allows easy incorporation of multiscale therapeutic agents such as nanoparticles, drug molecules, supramolecular organization and as a template for the production of other drug carriers [159–162].

In this subsection, the most up-to-date and relevant findings in the literature are summarized in Table 1, describing the nanocellulose type and source, composition or formulation, mode of drug delivery, and key outcomes. The ability of nanocellulose to act as a drug delivery modulator may be attributed to various reasons: aggregation of nanocellulose, interactions between drug molecules and cellulose hydroxyl groups, as well as cellulose's ability to modulate the microstructure and morphology of composite materials. It has been shown that nanocellulose can be successfully used for both water-soluble as well as poorly water-soluble drugs [24, 151, 163]. Nanocellulose can be modified, and in the case of BC, to hasten as well as delay the release of a drug and offer a combination of release profiles [164–167]. Nanocellulose has been utilized for various routes of drug delivery—oral, transdermal, local. There are a few recent reviews on nanocellulose in drug delivery [24, 151, 163, 168]; however, an important emerging concept of triggered or actuated drug delivery remains less discussed [24, 151, 163, 168].

Suitability of nanocellulose for drug delivery

Given the wide variety of nanocellulose types, it can be used in various ways in different drug delivery systems. For example, nanocellulose can be the carrier for the drug or act as a delivery modulating agent. Furthermore, it is important to recognize that nanocellulose can be obtained or processed in the form of nanoparticles, microparticles, tablets, aerogels, hydrogels, and membranes, enabling varied modes of drug delivery [169]. The large surface area and high density of surface hydroxyl groups on nanocellulose make it conducive for hydrophilic drug delivery specifically. For hydrophobic drug delivery, functionalization or the production of composites or hybrid materials has been shown to be useful [152, 170, 171].

Despite many advantages, nanocellulose also has some limitations—namely, moisture sensitivity and low thermal stability [172]. Significant progress has been made to improve these properties through pre-

treatments and surface modifications. Aggregation can be a challenge and may be overcome by deploying electrostatic effects and steric stabilization mechanisms [163]. To summarize, surface modification pathways have emerged as an important step to optimizing nanocellulose in drug delivery to 1) carry the drug; 2) make it suitable for delivering hydrophobic drugs; 3) prevent aggregation; 4) improve processability (i.e., by enhancing thermal stability); and 5) improve shelf life by decreasing moisture sensitivity [162].

Nanocellulose for various routes of drug delivery

Delivery systems must be developed to administer drugs using the most suitable route. Different types of nanocellulose have been used to deliver various classes of drugs including anticancer, anti-inflammatory, analgesics and antibiotics following oral, transdermal, implantable, and local delivery routes, as summarized in Table 1. While oral drug delivery is the most common mode of drug administration, it suffers from challenges such as the need for high and frequent doses, and side effects, which need to be addressed. Nanocellulose has been used for the delivery of, for example, indomethacin, salbutamol sulfate, diclofenac, ampicillin, and ranitidine. It has also been demonstrated that the addition of nanocellulose to these formulations offers several benefits such as an increase in the dissolution rate and oral bioavailability, high drug entrapment efficacy, enabling sustained and controlled drug release, prolonged drug release in fasted state-simulated stomach fluid, and good mechanical and viscoelastic properties [154, 173–176].

Nanocellulose has shown great potential in transdermal as well as topical drug delivery systems where the drugs are administered through the skin to achieve therapeutic concentrations. Thus, it allows the drug to by-pass the gastrointestinal tract and liver metabolism and enables an effect at lower doses. Nanocellulose has enabled release modulation, high drug entrapment, good permeation rates with drugs such as berberine compounds, diclofenac, providone-iodine, hydroquinone, ceftriaxone, and crocin [177–181]. It is important to note that transdermal delivery works better for small molecule drugs.

Another popular approach is implantable systems or local drug delivery systems that release the drug at or near the target site, increasing the effectiveness

Table 1 Nanocellulose-based drug delivery systems (ordered chronologically)

Nanocellulose type and source	Formulation	Delivery route	Drug loading and release profiles	Ref
Plant CNF	Indomethacin, Itraconazole Beclomethasone and CNF	Parenteral, ocular and transdermal delivery	Drug loading is about 20—40%, High entrapment efficiency Sustained drug release due to the formation of a tight fiber network around the encapsulated drug entities Drug release kinetics depends upon the drug type	[186]
BC	Berberine hydrochloride Berberine sulfate and BC	Transdermal delivery	Berberine sulfate retains more drug than berberine hydrochloride Freeze-dried membranes release drug more rapidly in simulated intestinal fluid Sustained release of berberine hydrochloride was slower than for berberine sulfate	[187]
Plant CNF	Indomethacin (IMC), CNF, ethanol	Oral delivery	Self-assembly and recrystallization of IMC on the surface of composite forms a hierarchically ordered CNF/IMC structure resulting in high loading and encapsulation efficiency of the drug and prolonged release	[173]
BC	Diclofenac sodium salt (DCF), BC, and glycerol	Transdermal delivery	Incorporation of diclofenac in BC membranes provided similar permeation rates to those obtained with commercial patches and substantially lower than those observed with a commercial gel	[178]
BC	BC, sodium alginate. ibuprofen (IBU)		Dual stimuli responsive system Ibuprofen exhibits an enhanced drug release and swelling behavior in neutral or alkaline medium and in the presence of an electric stimulus	[157]
Plant CNC	CNC, chitosan, doxorubicin curcumin		Sustained drug release is observed for doxorubicin with enhanced release in acidic pH CNC interacts with hydrophobic drugs like curcumin and can show sustained release	[188]
BC	BC, polyhexanide (PHMB), povidone-iodine (PI)	Transdermal delivery	BC loaded with PI shows a delayed release compared to PHMB due to the high molar mass and structural changes induced by the insertion of PI into BC PHMB-loaded BC exhibits a better therapeutic window than PI-loaded BC	[189]
BC	Doxorubicin, BC, calcium carbonate, carrageenans	Implantable delivery	Drug loading is significantly improved in the hybrid BC system Drug released faster from the hybrid film with decreasing pH Controlled and sustained drug release was observed which can extend for 1 year	[152]
Plant CNF	Polyethyleneimine, CNF, sodium salicylate	Oral delivery	High drug loading is achieved at pH 3 due to electrostatic interactions Surface grafting of PEI with CNF results in sustained drug release pH and temperature-dependent drug release	[190]
Plant CNC	CNC, starch, vitamin B12	Oral delivery	CNC gives a retardant effect when combined with starch Drug release rate is approximately 2.9 times slower than starch microparticles	[191]

Table 1 continued

Nanocellulose type and source	Formulation	Delivery route	Drug loading and release profiles	Ref
Plant CNC	CNC, hydroquinone	Topical delivery	CNC is introduced as a suitable carrier for delivery of the drug to skin	[180]
			Sustained release of drug from the complex is observed	
Plant CNC	CNC, chlorhexidine (CHX)	Topical delivery	Exhibits good antimicrobial activity and sustained drug release	[192]
BC	BC, ceftriaxone	Topical delivery	Double layer and 3D fiber network of BC with high density fiber and entangling	[181]
			High loading capacity and sustained drug release	
Plant CNC	Tris(2-aminoethyl) amine, Fe_3O_4, methotrexate	Local (Intratumoral) delivery	High drug loading, good binding ability, direct target to cancer cells	[182]
			Controlled and sustained drug release, pH-responsive-based drug release	
Nanocellulose Plant cellulose	Gold nanoparticles, polyelectrolyte complexes, diltiazem hydrochloride (DH)	Transdermal delivery	The film incorporated with 4% GNP-NC exhibits improved thermo-mechanical properties, water vapor permeability, drug encapsulation efficiency, and transparency	[193]
BC	BC, salbutamol sulfate (SS)	Oral delivery	BC capsule shells as an alternative to gelatin-based shells allows immediate release	[194]
			Adding release retardant polymer to the core of the capsule sustains the drug delivery	
BC	BC, poloxamer, octenidine	Wound dressing	Drug delivery was sustained over up to 8 days	[195]
			Addition of poloxamers-induced octenidine loaded micelle formation leading to a biphasic and controlled release profile	
BC and Plant CNF	BC, CNF, high amylose starch (RS), pectin (P) Methotrexate (MTX),	Colonic delivery	A better controlled release of MTX is observed from RS/P-NFC film due to its lower porosity	[196]
BC	Poly(N-methacryloyl glycine), BC, diclofenac sodium salt (DCF)	Oral and transdermal delivery	Controlled and pH-responsive drug delivery is observed where drug delivery is fast in the intestinal pH	[197]
Plant CNC	CNC, oxidized CNC (OCNC), chitosan nanoparticles (CHNP), repaglinide (RPG)	Oral delivery	Drug release is dependent on medium pH where enhanced RPG release is observed at pH 1–2 compared to that at pH 6–8	[176]
			Increasing the amount of CNC or OCNC results in slower release of drug with more pronounced effect in case of OCNC	
Plant CNF	Hydroxypropyl methylcellulose (HPMC), CNF, ketorolac tromethamine	Transdermal delivery	HPMC, which is reported to have a faster drug release on contact with biological fluids, attains a slow and steady release on adding CNF	[198]
			Drug release is decreased with the increase of CNF concentration in the composites	
Plant CNC	Alginate, CNC, ampicillin	Oral delivery	Presence of CNC enhances the release profile of Ampicillin from alginate due to the free space	[175]
BC	Nanostructured lipid carriers (NLCs-NH), doxorubicin	Intratumoral delivery	BC-NLCs-NH films revealed sustained drug release, high drug loading	[199]
			Significant decrease in the tumor-to-control ratio of tumor volume ex vivo, with no side effects	

Table 1 continued

Nanocellulose type and source	Formulation	Delivery route	Drug loading and release profiles	Ref
Plant CNC	CNC, alginate (ALG), natural honey, rifampicin,	Oral delivery	The presence of CNC in alginate improves drug entrapment efficiency ALG-CNC nanoparticles (NPs) exhibits pH-dependent swelling characteristics and drug release, which is higher at intestinal pH, sustained drug release profile	[200]
Plant CNC	Alginate, magnetic cellulose nanocrystals (m-CNC)		m-CNC improves swelling degree and decreases drug release rate Initial burst release is observed within the first 30 min and then sustained drug release	[201]
Plant CNC	CNC, PVA, curcumin	Transdermal (wound dressing)	Curcumin release studies show that CNC film provides controlled release of drugs in wounds and a prominent antibacterial activity	[202]
Plant CNF	CNF, anionic CNF, metronidazole , mucin, pectin, chitosan	Transmucosal delivery	Drug release profiles show an initial burst release in all the films, where most films exhibit a fast release of drug in 30 min which is important for the treatment of oral diseases Maximum drug release of 84.7% at 30 min was observed for CNF–mucin	[203]
Plant CNF	CNF, gelatin, dialdehyde starch , 5-fluorouracil (5-FU)	Oral delivery	Drug loading is stabilized by increasing the strength of CNF-gelatin composite with dialdehyde starch as the chemical crosslinker More controlled and sustained drug delivery is achieved with an increase in CNF content, DAS content, and NGDC density, limiting the drug dissolution and diffusion	[204]
BC	BC, crocin	Transdermal delivery	Burst release of crocin was found in direct dissolution method while with Franz diffusion cells, a slow and controlled release of drug is obtained	[177]
Plant CNC	Poloxamer 407, Pilocarpine HCl	Ocular delivery	Increased gel mechanical strength Greater the concentration of CNC, better is the sustained drug release property	[153]
Plant CNF	CNF, NaIO$_4$, NaClO$_2$, piroxicam	Transdermal delivery	Periodate-chlorite oxidation tunes surface charge density of CNF Anisotropic layered nanoporous structure of the membranes (NF-DCC) holds great potential for prolonged drug release	[205]
BC	BC (cultured in standard medium & coconut water), ranitidine	Oral delivery	Drug loading and entrapment efficiency is higher for BNM-CW due to the porous fibrous network of BNM produced in CW media Both systems show slow and sustained release	[154]
BC	BC, methylglyoxal, manuka honey (modified graphene oxide)	Wound dressing	Composite shows thermal stability excellent mechanical strength Excellent antimicrobial activity against broad spectrum bacteria making them promising material in chronic wound dressing	[206]

Table 1 continued

Nanocellulose type and source	Formulation	Delivery route	Drug loading and release profiles	Ref
Plant CNC	CNC-sulfate cetyltrimethylammonium bromide (CTAB), curcumin	Local delivery	Adsorption of CTAB improves the hydrophobicity carrier of CNCs making it suitable as a hydrophobic drug CTAB-CNC system exhibits increased release of curcumin, maximum antioxidant, and anti-inflammatory activities	[207]
BC	Diclofenac sodium, BC with different drying methods	Implantable systems	Two drying methods are used to tune drug release kinetics from bacterial cellulose Swellability (rate, extent), and porosity directly affected the diffusion of the drug Oven-dried BC shows sustained release, while freeze-dried BC showed a burst release	[165]
BC	Diclofenac sodium, BC modified in situ by PEG	Implantable systems	PEG is non-incorporating in situ modifier, PEG2000 increased the overall porosity, pore volume and decreased the specific surface area A huge burst release for PEG modified BC as compared to pristine BC	[164]
BC	Diclofenac sodium, BC	Transdermal delivery	A combination release was obtained from oven-dried and freeze-dried BC	[166]
BC	Hyaluronic acid microneedles, BC, rutin	Transdermal delivery	BC acted as a macromolecular support for the incorporation of active ingredients BC increased the mechanical resistance of HA MNs Rutin introduced into BC kept its antioxidant activity over 24 weeks	[208]

and lowering the required dose. Nanocellulose has been particularly beneficial with local delivery of diclofenac, doxorubicin, and methotrexate [165, 182]. Another local delivery route explored with nanocellulose is ocular drug delivery, which takes advantage of nanocellulose gel properties [153].

Nanocellulose has also been explored to produce stimuli-responsive materials for smart/triggered drug delivery systems. These materials are sensitive to specific stimuli which can be a change in humidity, pH, and light, or the application of an electric or a magnetic field. For example, multi pH/near-infrared responsive polydopamine/CNF composites with calcium ions as crosslinkers have been developed for drug delivery and wound healing applications [183]. The drug tetracycline hydrochloride could be released in a controlled fashion on exposure to Near Infrared (NIR) radiation or lower pH conditions. Such a system also offers a synergetic effect on wound healing and is advantageous as it is easy to

fabricate while providing multi-response and sustained release of the drug. CNF-sodium alginate-based gel macrospheres were developed for intestinal targeted delivery of probiotics, thereby protecting them from the acidic conditions of the stomach [184]. A novel dual stimuli responsive drug delivery system of aminated nanodextran and carboxylated nanocellulose deposited on the surface of modified graphene oxide was prepared by layer-by-layer assembly [158]. It showed that curcumin can destroy HCT116 cells upon exposure to NIR radiation. In this case, the drug was loaded into the nanocomposite based on hydrogen bonding or π-π stacking and was released faster in an acidic environment than at an intestinal pH [158].

A dual responsive hydrogel based on BC and sodium alginate which reacts to changes in pH and electric stimuli has been developed [157]. The model drug, ibuprofen, showed an enhanced release in a neutral or alkaline medium and in the presence of

an electric stimulus [157]. Another BC-based drug delivery system was fabricated by chemical oxidative polymerization of BC and polyaniline [185]. This resulted in a pH-electro sensitive hydrogel that showed a slower release of the drug berberine hydrochloride in acidic conditions thereby protecting the drug before it is released into the small intestine for drug absorption, and it also showed accelerated release on application of an electric potential [185].

Commercialization of healthcare products incorporating nanocellulose

Several companies have been commercializing medical grade products based on BC (*e.g.*, Membracel® by Vuelopharma, Epi Nouvelle$^+$® naturelle by JeNaCell GmbH) and CNFs derived from tunicates (*e. g.*, Ocean TuniCell®) and wood pulp (*e.g.*, UPM Biomedicals). Most of these products are based on non-surface-modified nanocellulose but UPM Biomedicals now sells a cell culture media product named GrowDex®-A that consists of surface-modified CNFs with proteins or peptides. UPM Biomedicals also produces FibDex®, an advanced CNF wound care dressing that has proven to provide efficient wound healing in skin graft donor sites [209]. CELLINK have also developed a series of bioinks based on CNFs and alginate for the 3D printing of tissue engineering cell scaffolds. As such, commercial opportunities exist to move forward with the use of surface-modified nanocellulose toward new commercial products.

Surrounding wound dressings with transdermal drug delivery, application, product development and commercialization of nanocellulose continues to advance significantly. Some commercial products include Biofill®, Bioprocess®, Suprasorb X+PHMB® and Xcell®. Nanocellulose-based drug delivery products such as Gengiflex® membranes for dental implants exist; however, there is a need to push clinical trials and commercialization of nanocellulose further [23, 149]. For widespread acceptance of nanocellulose in drug delivery, a better understanding of the influence and regulation of drug release, interactions between drug molecules and nanocellulose, as well as possible reduction or destruction of drug activity and structure is required. In addition, toxicity needs to be further assessed, likely on a case-by-case basis [210].

Introduction to nanocellulose and water purification

Although water is a basic need for all 7.9 billion of us, access to clean portable water remains a significant challenge globally. The UN estimates that over one million people in developing countries do not have access to clean drinking water and that up to 159 million people around the world consume untreated water from surface water sources [211]. Yet this water is often contaminated by toxic levels of heavy metals, dyes, and hydrocarbons.

This section presents advances in the application of cellulose in water treatment. We classify the use of cellulose for water treatment applications into the following three categories: (i) as the active agent i.e., adsorbent, (ii) as a support for adsorbents or catalysts, and (iii) for the enhancement of photocatalyst performance through reduction of the band gap energy.

As the active agent, negatively charged (-COO$^-$) cellulose materials such as those generated by TEMPO (2,2,6,6-tetramethylpiperidine-1-oxyl radical)-mediated-oxidation or sulfuric acid hydrolysis (-SO$_3^{2-}$) can serve as adsorbents for cationic contaminants (*e.g.*, metal ions [212–214]). The surfaces of cellulose fibers may also be functionalized by amine (-NH$_2^-$), thiol (-SH$^-$), phosphoryl (-PO$_3^{2-}$), or sulfate (-SO$_3^{2-}$) groups to increase the specificity for specific elements [215, 216]. In similar fashion, cationically modified cellulose may be applied as an adsorbent for anionic pollutants (*e.g.*, As(V), As(III), Cr(VI), pesticides, and dyes [217, 218]). These approaches have the advantage of involving relatively simple modifications to the cellulose fibers [217, 218].

The use of cellulose as an adsorbent support takes advantage of the physical properties of cellulose, in particular, its porosity [219]. Pores within and between fibers can act as nucleation and deposition sites for adsorbents, reducing their attrition/ loss, thus increasing the performance and lifespan. Iron oxides, for instance, are excellent adsorbents for arsenic, whose contamination of groundwater poses serious health effects to over 40 million people worldwide [220]. However, recovery from treated water poses a significant challenge to the use of iron oxides for this purpose. Recent work has shown that iron-oxide-cellulose composites can overcome this challenge, increasing both the performance and lifespan of the adsorbent [221]. A similar rationale

has been employed in the design of catalysts for advanced oxidative processes, to allow for reuse/recycling of catalysts [222]. Further, it has also been suggested that cellulose increases catalyst performance by providing settling sites for radicals and pollutants thus increasing their interaction, and the subsequent degradation of the latter [223], in addition to preventing catalyst aggregation of the catalyst, increasing access to active sites on the catalyst surface [224].

A third way by which cellulose has been applied in water treatment has been for the enhancement of the performance of photocatalysts. In the presence of graphitic structures (*e.g.*, cellulose char), electron–hole recombination after exposure of the catalyst to irradiation is hindered, as electrons are instead quickly captured by the cellulose char [225]. Holes created in the conduction band (CB) because of this electron capture result in a higher probability of the formation of $\bullet$OH radicals, while electrons in the biochar combine with oxygen in solution to form superoxide radicals ($\bullet O_2$ -). Cellulose therefore acts as a sustainable and renewable graphitic source, improving catalyst performance. Indeed, Fu et al. [226] found that for the oxidative degradation of orange II by peroxymonosulfate, the graphitization degree had a greater influence than surface area and pore volume of a $MnFe_2O_4$-based catalyst.

## Anita Etale (University of Bristol, UK): nanocellulose for water purification

Using locally available agricultural waste biomass including hemp, and corn stover, various approaches for the preparation of heavy metal adsorbents have been explored. In one study, cellulose-supported iron oxides were prepared and applied for the removal of As(III), As(V) and Cr(VI) ions. Notwithstanding that arsenic is considered carcinogenic even at very low concentrations, over 200 million people in 40 countries around the world are exposed to drinking water with As levels above World Health Organisation guidelines (10 μg L^{-1}) [227]. Although As(V) predominates (as $H_2AsO_4^-$ and $HAsO_4^{2-}$) in oxidizing conditions, in regions of previous gold mining activity which are often characterized by reducing conditions and high sulfate concentrations, arsenic exists predominantly in the more toxic As(III), as $H_3AsO_3^0$ and $H_2AsO_3^-$. Nevertheless, because of

slow redox transformations, both forms often occur in either redox environment [228].

Anita Etale's group has explored two strategies for the use of cellulose in water treatment applications. The first involves using cellulose as a support material for iron oxides which are excellent adsorbents for arsenic [229]. Preliminary work, however, showed them to be prone to dissolution so that the prepared iron oxides 'leached' into treated water compromising both the treatment process and adsorbent lifespan. To address this challenge, iron oxides were deposited on CNF extracted from hemp fibers. Importantly, the CNF are thought to be porous [219]. CNF porosity may be the result of dissolution of lignin and hemicellulose between the lamellae by the chemical pulping process, or mechanical treatments *e.g.*, blending and sonication applied to increase fibril separation. CNF with average pore sizes of ∼ 6 nm have recently been reported [219]. Manninen et al. [230] also reported a cumulative pore volume of 1.7 mL g^{-1} from pore sizes that ranged from<1 – 3 nm in kraft pulp fibers, and from 3 nm to an undefined maximum between the CNF fibers.

The approach to adsorbent synthesis has, therefore, involved exploiting these pore spaces as embedment sites for contaminant adsorbents. In one study, a cellulose-ferrihydrite composite (Fig. 5a) was synthesized by the deposition of iron oxide onto TEMPO-oxidized fibrils at pH 10.5. Iron oxides, including poorly crystalline ones such as ferrihydrite, have a strong affinity for both As(III) and As(V). Adsorption occurred primarily by ligand exchange with surface OH_2 and / or OH^- resulting in bidentate binuclear inner-sphere complexes [229, 231]. This adsorbent displayed efficiencies of>99% for the removal of As in mine drainage contaminated water (Fig. 5b). Further, column experiments showed that 1 g of the adsorbent was needed to treat 1L of contaminated water. The reduction in absorbance intensity from the OH region (1000 cm^{-1}) on FTIR spectra (Fig. 5c) suggests that adsorption of both arsenic species involved some loss of OH as suggested by Jain et al. [229].

A similar approach was employed in Sillanpää's group for the removal of Ni, Cd, Cu, as well as PO_4^{3-} and NO_3^- [232]. Removal of these ions by CNF-calcium hydroxyapatite composites was rapid with> 95% of metal ions adsorbed in the first five minutes of exposure. Removal efficiencies were also high for phosphate ions (>85%) and nitrates (>80%).
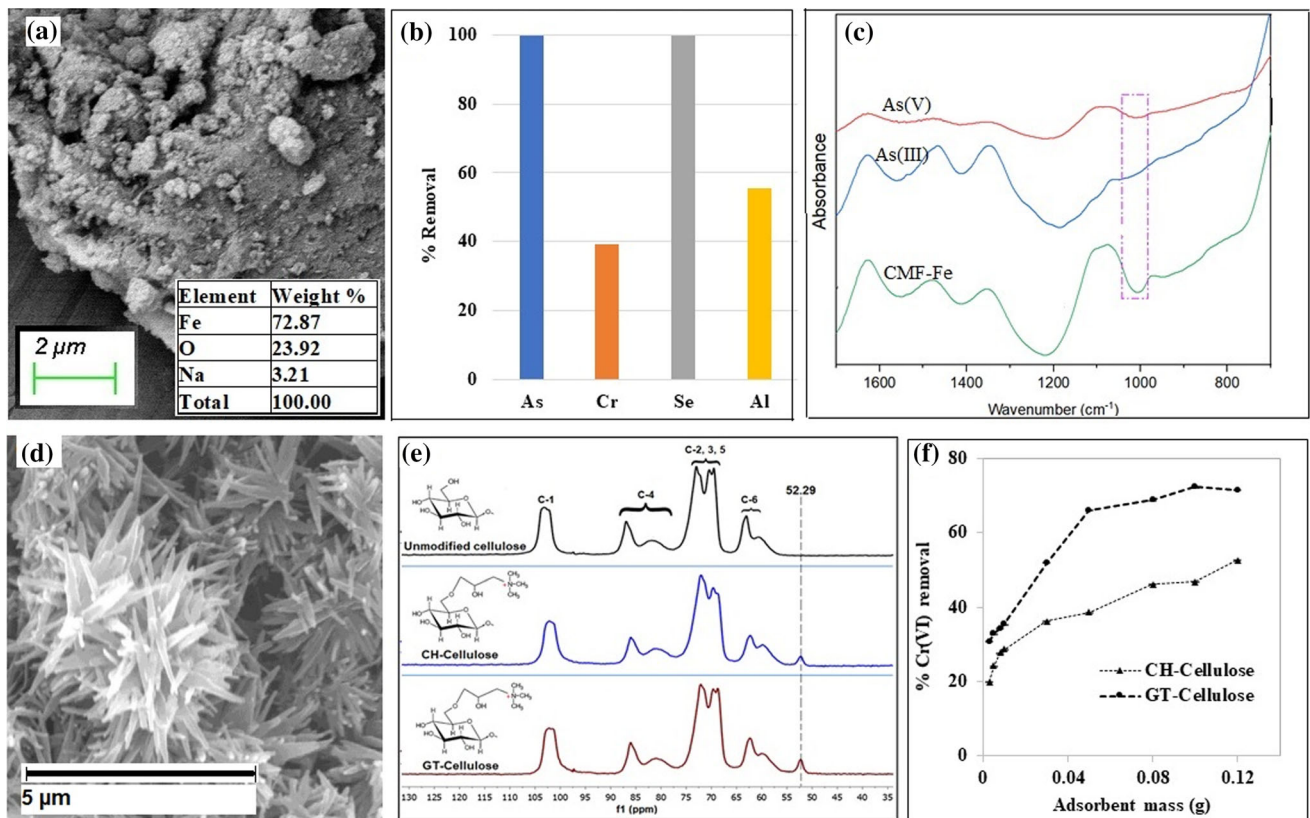
Figure 5 **a** Scanning electron micrograph of CNF-Fe adsorbent. **b** Removal efficiency of the CNF-Fe adsorbent when exposed to mine-drainage contaminated water **c** FTIR spectra of CNF-Fe before adsorption, and after uptake of As(III) and As(V). The box highlights changes in the surface -OH absorption region before and after adsorption. **d** Scanning electron micrograph of succinic anhydride-modified CNF [215]. **e** CP-MAS ^{13}C NMR spectra of unmodified and cationized cellulose with the additional peak at $\sim$ 52 ppm from $(CH_3)_3$ N$^+$- groups of the quaternary amines highlighted **f**r(VI) removal efficiency of cationized cellulose. (d) is reproduced from [215] with permission from Elsevier (Copyright Elsevier, 2013); **e** and **f** are reproduced under the terms of a CC-BY license from [218]. **a**–**c** are unpublished data.

Exposure of the same adsorbent to Cr(VI) contaminated water also revealed similarly high efficiencies between pH 5 and 7: 94% of Cr(VI) ions were removed from solution in the first 5 min [233]. In a separate study, succinic anhydride was deposited onto CNF, and the composite investigated for adsorption of a range of metals (Fig. 5d) [215]. The results showed maximum metal uptakes ranging from 0.72 to 1.95 mmol g^{-1} and following the order Cd>Cu>Zn>Co>Ni. Adsorption was constant between pH 3 and 7 for Zn, Cu, and Cd (>95%), and above 75% for Co and Ni at pH 7. Importantly, 96 - 100% of the adsorption efficiency could be regenerated by sonicating the used composite in 1 M HNO$_3$ for 15 s.

A second approach has been through surface modification of cellulose *e.g.*, via amination [216], thiolation [234], and cationization. This latter approach uses two quaternary ammonium salts: 3-chloro-2-hydroxypropyl trimethyl ammonium chloride (CHPTAC) and glycidyltrimethylammonium chloride (GTMAC), and has been explored (Fig. 5e) and the resulting materials examined for Cr (VI) removal (Fig. 5f), and antibacterial activity. The results showed that at pH 4, 0.1 g of CHPTAC-modified cellulose removed up to 47% of Cr (VI) ions, while 72% was adsorbed by GTMAC-cationized cellulose. GTMAC-cationized also displayed considerable antibacterial effects, reducing the viability of *Escherichia coli* by up to 45% after just 3 h of exposure. However, Cr(VI) uptake in contaminated water (pH 2.7) was diminished to 22% likely due to competition from sulfate and selenate ions [235] which are abundant in mine drainage. Nevertheless, together,

these results suggest that cationized cellulose can be applied in the treatment of Cr(VI)-contaminated mine water particularly if pre-treatments to reduce concentrations of other anions are applied.

Supree Pinitsoontorn (Khon Kaen University, Thailand): carbonized bacterial cellulose aerogel as an efficient sorbent for oil-polluted water

Bacterial cellulose (BC) is a class of nanocellulose with a unique structure and properties, such as a three-dimensional network of intertwined cellulose nanofibers, remarkable mechanical properties, high porosity, and low density [236, 237]. In its original state, BC is a hydrogel with a significant water uptake volume ($\sim$99%) [237]. Freeze-drying removes the water content but still preserves the BC 3D nanofibrous network and transforms a hydrogel into an aerogel. Moreover, pyrolysis of the BC aerogel in an inert gas atmosphere leads to the carbonization of the BC nanofibers, thereby forming a carbon nanofiber aerogel. The carbonized BC (c-BC) aerogel inherits the BC precursor's merits, so it still preserves the 3D continuous architecture, the interconnected nanofibrous network, and an extremely high porosity. The surface area of the carbon nanofibers can reach >400 $m^2\ g^{-1}$, with a sizeable porous volume (ca. 3.00 $cm^3\ g^{-1}$) and an ultra-light weight (4–6 mg cm^{-3}) [238]. Furthermore, high-temperature pyrolysis can induce the hydrophobic/oleophilic properties of the c-BC aerogel, which makes it an ideal material for oil sorption.

Oil pollutants are one of the leading global environmental problems. Every year, the annual spillage of petroleum compounds to the marine environment is over 1.4 million tonnes which has caused catastrophic effects on ecological systems [239, 240]. Therefore, a remedy for oil-spills is urgently needed. Although there are several approaches for treating oil-spills, the most effective approach is via physical adsorption, i.e., the use of oil sorbents, which has been proven to be energy-efficient, highly selective, environmentally friendly, fast, and recyclable [241, 242]. Research over the last decade has reported several types of oil sorbent materials. Carbon aerogels have received considerable attention as one of the most effective materials for adsorption, separation, and recovery of spilled oil [243, 244]. The carbon aerogels can be fabricated from various biomass-based products, such as cotton, bamboo, winter melon, or waste paper [241]. These aerogels have been applied for remedying oil-spills and have successfully demonstrated a large oil sorption capacity of up to 100 times of their weight. However, the preparation processes for such aerogels may involve severe mechanical and chemical pre-treatments, which are high in energy consumption, and subject to environmental concerns. Moreover, high-temperature pyrolysis may cause frangibility and brittleness to those biomass-based carbon aerogels [245], which hinders their practical use for oil recovery. On the other hand, carbon aerogels from carbonized BC (c-BC) have advantages over other biomass-derived materials. The fabrication of c-BC is simple and cheap without any use of harsh chemicals or complicated processes. Also, the natural 3D continuous nanofibrous architectures of BC make the c-BC material mechanically robust and flexible. The c-BC aerogel is typically obtained in a bulky macroscopic form, which is desirable for easy handling and recycling after oil sorption. Plus, the shapes and sizes of the c-BC aerogel are controllable via the bacteria cultivation process and scalable for industrial production.

The application of the c-BC aerogel for oil sorption was firstly reported by pioneering work done by Wu et al. [246]. They showed that pyrolyzing the BC aerogel under an argon atmosphere at 700–1300 °C led to a c-BC aerogel with a density of only 4–6 mg cm^{-3} and a high porosity up to ca. 99.7%. The c-BC aerogel exhibits hydrophobicity and can adsorb a wide range of oils and organic solvents with excellent recyclability by direct combustion. The sorption capacity reached up to 310 times the weight of the c-BC aerogel. Moreover, it was highly flexible and mechanically robust. It could also be compressed to a more than 90% volume reduction and almost recover to its original shape after release, making a 'squeezing' process to recover oil possible [246]. In a recent study, a c-BC aerogel pyrolyzed at 1200 °C was compressed to 99.5% strain, and it was able to be restored elastically to almost its original shape after release [247]. A detailed surface area and pore-size study showed that micropores and mesopores (2–100 nm) occupied a large portion of the pore-size distribution, providing huge spaces for oil sorption and leading to high oil sorption capacity. Furthermore, this c-BC aerogel was an excellent thermal insulator with extremely low thermal conductivity (0.025 W $m^{-1}\ K^{-1}$) comparable to air [247].

Several efforts have been reported to increase the oil sorption capacity of c-BC aerogels by using a composite approach. c-BC was combined with carbon nanofibers derived from polyimide (PI) by freezing the mixture of BC and PI precursor suspension before imidization and pyrolysis [248]. The resultant carbon aerogel consisted of a 3D carbon skeleton with a cellular architecture from carbonized PI, decorated with 1D c-BC nanofibers. This hierarchical structure was advantageous for enhancing the compressive modulus leading to an improved shape-retention ability due to the effective crosslinking between the PI carbon skeleton and the c-BC nanofibers. The aerogel was so stiff that it supported a weight of 200 g without any noticeable deformation. Moreover, the combined 3D carbon skeleton and 1D c-BC nanofibers resulted in a reduced pore size and a narrow pore size distribution, which could be beneficial for oil sorption [248].

Wan et al. fabricated a c-BC aerogel nanocomposite with graphene [249]. To facilitate the uniform distribution of graphene in the BC network, an in situ biosynthesis route under agitated cultivation using a graphene-dispersed culture medium was employed. The spherical BC/graphene hydrogel was carbonized at 800 °C to form a sphere-like c-BC/graphene aerogel. The nanocomposite aerogel exhibited an open honeycomb-like surface pattern consisting of numerous ridges and large cavities, which increased the aerogel's specific surface area and porosity. The unique nanostructure of the sphere-like c-BC/graphene aerogel is the key to enhance the sorption capacity (up to 457 times of its weight) for a wide range of oils and organic solvents [249].

Reduced graphene oxide (rGO) has also been composited in a c-BC aerogel [250]. This was done by freeze-casting and freeze-drying of the GO and BC mixed suspension. The GO nanosheets and BC nanofibers were uniformly assembled into a porous and interconnected 3D network. Subsequent pyrolysis transformed it into rGO/c-BC aerogel with the preserved 3D nanostructure where the c-BC nanofibers were still coated on the rGO sheets. The aerogel density was easily controlled by varying the concentration of the precursor in the suspension and the ratio of GO/BC. The lowest density was found for a GO/BC ratio of 1:1. The oil sorption capacities of the rGO/c-BC aerogel ranged from ~ 300 to 1000 times of its weight, much higher than most carbon sorbents

[250]. The ultrahigh sorption capacity was attributed to its low density and high porosity.

Luo et al. devised a new method of preparing c-BC aerogels containing rGO by a novel BC culturing process [251]. A thin BC pellicle was used as a substrate in the static culture. The solution containing a 2D few-layer rGO (FrGO) suspension was sprayed onto the BC substrate to form a thin layer, onto which BC was grown to consume the sprayed FrGO layer completely. The process was repeated to form a thick BC/FrGO layered structure, which was then freeze-dried and pyrolyzed. The c-BC/FrGO aerogel from the process exhibited an entangled nanostructure between the FrGO sheets and c-BC nanofibers, creating a multi-scaled porous structure and large specific area. As a result, the c-BC/FrGO aerogel exhibited mechanical robustness and an extremely high sorption capacity of 245–598 times its weight for a range of oils and organic solvents [251]. It also showed excellent reusability by both squeezing and combustion, with nearly the same sorption retention.

To assist the collection of a c-BC aerogel for reuse, regeneration, or recycling after oil sorption, functionalizing the aerogel with magnetic properties is a very useful and practical approach. A magnetic functionalized c-BC aerogel can be collected easily in large quantities with the aid of an applied magnetic field. Supree Pinitsoontorn and his team at the Institute of Nanomaterials Research and Innovation for Energy (IN-RIE), Khon Kaen University, have explored that concept by using in situ co-precipitation of magnetic Fe_3O_4 nanoparticles in the BC pellicle before converting it into a magnetic c-BC aerogel [252]. Interestingly, by controlling the concentration of the initial Fe_3O_4 precursors, the c-BC nanofibers were decorated with well-dispersed magnetic nanoparticles with a Fe/Fe_3O_4 core–shell structure (Fig. 6a&b). The core–shell structure increased the magnetization of the NPs due to the large magnetization of the Fe core. This, in turn, improved the magnetic attraction ability when subjected to external magnetic forces. Although magnetic NPs were impregnated in the c-BC structure, the outstanding mechanical properties of the c-BC aerogel were still maintained. The magnetic c-BC aerogel was able to be compressed up to 90% strain and return to its original shape after release. This process was repeated up to 100 successive cycles, and the shape of the aerogel was nearly unchanged from the original state. Moreover, even with the addition of magnetic NPs,
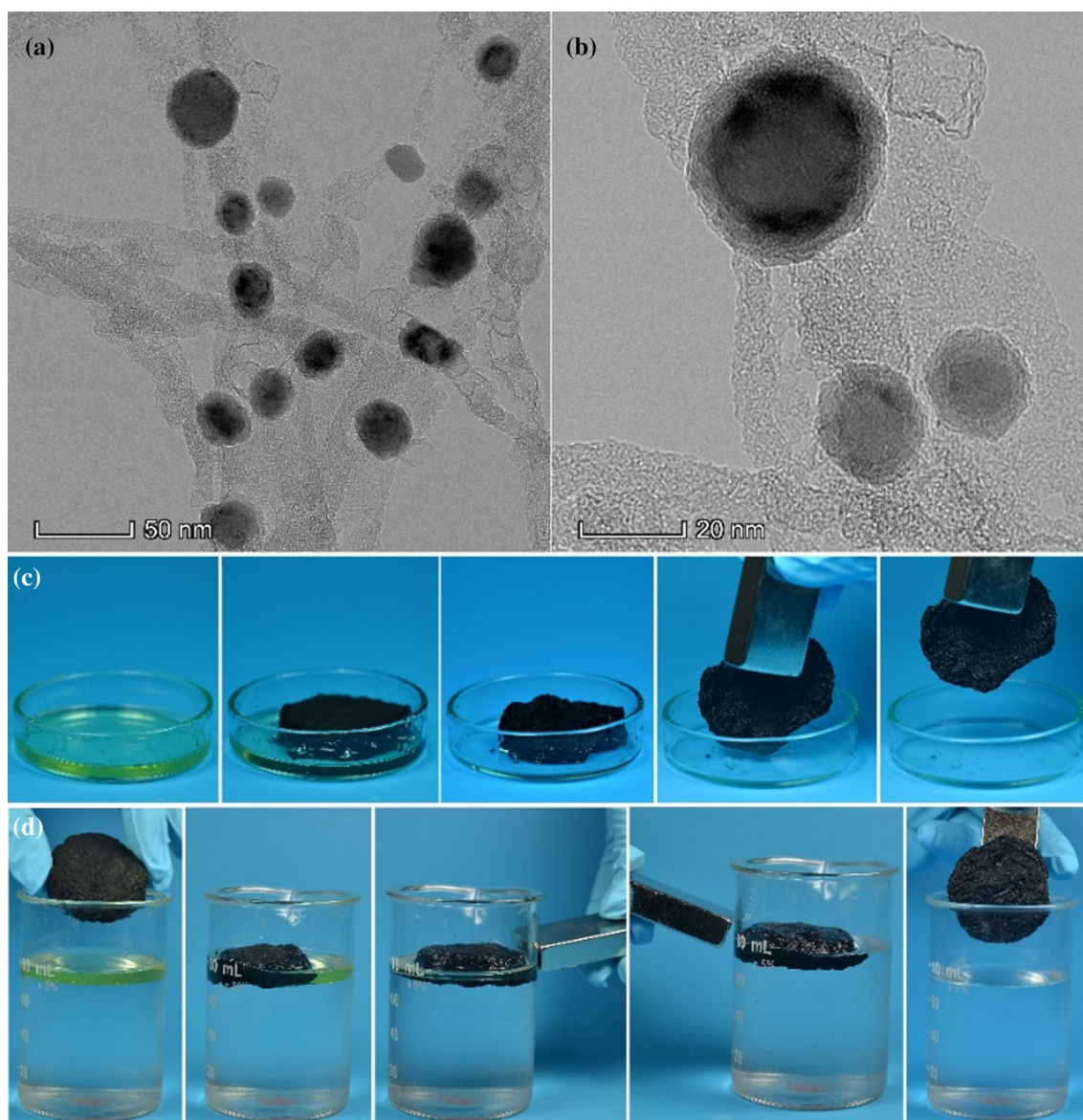
Figure 6 **a**, **b** TEM micrographs of the magnetic c-BC aerogel showing the magnetic Fe/Fe$_3$O$_4$ core–shell nanoparticles anchoring on carbon nanofibers. **c** The sorption experiment and magnetic retrieval after oil sorption. **d** The sorption of oil floating on water, with magnetic manipulation and retraction of the c-BC aerogel. [252]. Image reproduced from [252] with permission from the ACS (Copyright American Chemical Society, 2020).

the magnetic c-BC aerogels had an ultralightweight property with a density of only 7.4 mg cm^{-3}, which is lighter than other magnetic carbon aerogels from several carbon sources [253, 254]. The oil sorption capacity of the magnetic c-BC aerogel was still very high (37–87 times of its weight), which is comparable to other carbon aerogels from various sources [254–256]. Also, it can be rendered recyclable several times by dissolution. The highlight of the magnetic c-BC aerogel is its ability for magnetic retrieval from the liquid after sorption. As shown in Figs. 6c&d, the

motion of the magnetic c-BC aerogel in a liquid can be controlled by an external magnet. The magnetic force can also lift it out of the liquid after use. This functionality is beneficial for manipulating the sorbents in a large area of polluted water, in a practical application of this technology.

The magnetic c-BC aerogel could not just be used for the remediation of an oil-spill but also be applied to other contaminant adsorption situations. Figure 7 shows a series of images demonstrating the dye (indigo carmine) sorption capability of the magnetic
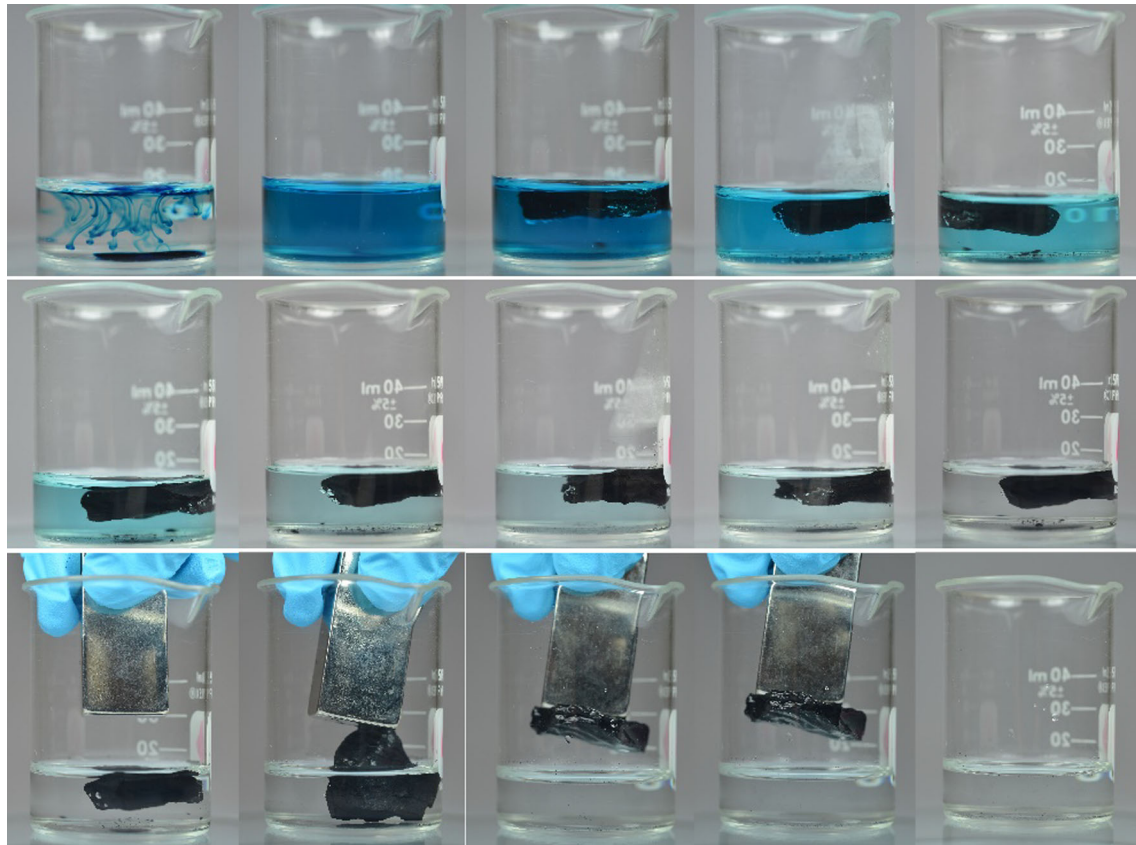
Figure 7 A series of images demonstrating dye sorption using the magnetic c-BC aerogel, which was magnetically retracted afterward [257]. Image reproduced from [257] with permission from Springer-Nature (Copyright Springer-Nature, 2020).

c-BC aerogel [257]. The vivid blue color gradually faded, and the water became clear just like before the dye was added, indicating the complete dye removal, as confirmed by UV–Vis analysis. After the process, the aerogel was magnetically removed from water by a permanent magnet. The dye-adsorbed c-BC aerogel can be regenerated by dissolution followed by oven-drying before reuse. In addition, the magnetic c-BC aerogel can still be utilized in water treatment applications for other contaminants such as bisphenol A and Cr(VI) [258, 259].

Yixiao Cai (Donghua University, China): using cellulose for wastewater treatment for dyes, heavy metals and desalination

In recent years, various semiconductor/cellulose composite materials have been widely used in the degradation of organic dyes in printing and dyeing wastewater, such as metal oxides (TiO_2, ZnO, WO_3), metal sulfides (CdS, ZnS), bismuth-based semiconductors (BiOCl, BiOBr, BiOI, $Bi_4O_5Br_2$), silver-based semiconductors (AgBr, AgI, Ag_3PO_4, $AgVO_4$ and $AgCrO_4$) and non-metallic semiconductors (graphite, carbon nitride).

Some studies combine photocatalysis with other oxidation methods to further strengthen wastewater treatment. Rajagopal et al. [260] prepared microcellulose (MC) and TiO_2 composite materials, combined with hydrogen peroxide photocatalytic degradation (TiO_2+MC+H_2O_2), to decolorized wastewater containing multiple dyes under sunlight. They showed that 99% of high-concentration methylene blue (MB) dye wastewater (200 mg/L) can be degraded within 150 min, and the removal efficiency of Chemical Oxygen Demand (COD) can reach 72%. It was highlighted that the synergy index of H_2O_2 assisted photocatalytic degradation is 3.54, which shows that the above process coupling has a positive synergistic effect. Other research that is being developed by Cai et al. [261] takes advantage of a nanocomposite strategy, rendering stable cellulose-based hybrid materials with diverse functionalities for micropollutant removal. Through synergistic oxidation, *e.g.*,

persulfate activation, photocatalytic water treatment has been proven to obtain practical value and can be further developed industrially [261].

As already discussed, heavy metal ions in water can be removed by adsorption. However, single physical adsorption can only enrich and transfer heavy metals but cannot completely remove them. Semiconductor photocatalysts have redox capabilities, which can change the chemical properties of heavy metal ions to reduce their toxicity. Taking TiO_2 as an example, the mechanism of photocatalysis to remove heavy metal ions is roughly as follows: 1) nano-TiO_2 adsorbs heavy metal ions on its surface, 2) an ultraviolet lamp is excited to generate photogenerated electron–hole pairs, and the electrons transition to the conduction band and transfer to the TiO_2 surface, 3) photogenerated electrons reduce the adsorbed heavy metal ions to low valence states (such as chromium, mercury, lead) or elemental forms (such as silver), the metal ions in the lower valence state further generate compounds and precipitate (such as chromium) or further obtain electrons as elemental substances (such as lead, mercury) and deposit on the surface of TiO_2 particles. However, supporting TiO_2 (or other semiconductor photocatalyst) on the surface of cellulose can improve the removal efficiency of heavy metal ions. Although the adsorption of heavy metal ions by the hydroxyl groups in cellulose contributes to the removal of metal ions, the adsorption effect is weak. For this, researchers usually take advantage of chemical modification or graft copolymerization to introduce effective adsorption active sites on the surface of cellulose [262] such as carboxyl groups, amino groups, and sulfonic acid groups. These groups can selectively recognize and capture various heavy metal ions through electrostatic attraction or complexation and chelation coordination effects [263], thereby improving the photocatalytic removal efficiency.

Interfacial solar evaporation, which utilizes the abundant sunlight to evaporate saltwater, has gained significant attention as an environmentally benign and sustainable approach. Significant efforts have been made in realizing supporting substrates that provide optimal thermal management and unimpeded water transport to foster high-performance interfacial solar evaporation. The high degree of crystallinity of CNMs provides excellent mechanical stability, and their highly dense surface functional groups enable direct deposition or adsorption of various photothermal materials [264, 265]. After subjecting MoS_2/BC bilayered aerogels to vigorous mechanical agitation, no detachment of photothermal materials from a BC matrix was observed, and the bilayered structure remained intact [266]. Besides, CNMs can be easily processed into nanomicroporous structures, and this interconnected porous structure can enhance the light absorption of the photothermal materials loaded onto these structures because of the increased light reflection and scattering within the pores. Jiang et al. prepared carbon nanotube/cellulose composite aerogels as photothermal materials. Owing to the strong hydrogen bonding between the ample hydroxyl groups of CNFs and carboxylic groups of CNTs, these materials were found to be robust. The ultrahigh porosity of the CNF aerogel and high light absorption of CNTs led to a 97.5% light absorbance within the light range from 300 to 1200 nm [267]. In addition, owing to a low thermal conductivity they provide excellent thermal insulation. The thermal conductivity of a sophisticated solar evaporator designed by Li et al. was as low as $0.06 \ W \ m^{-1} \ K^{-1}$. This solar evaporator achieved high evaporation efficiency, up to 85.6% under 1 sun illumination [267].

Introduction to polymer matrix biocomposites from well-dispersed cellulose nanofibers

Cellulose-based plant fibers can be readily used by themselves to form paper, packaging board materials and recently molded fibers [268]. Polymer matrix composites based on the same fibers offer possibilities to improve processing (improved geometrical complexity, rate of processing etc.), extend the range of physical properties, and improve the chemical stability, where the improved moisture stability is particularly important for engineering applications. The use of CNFs as a reinforcement is then of obvious importance: wherein the intrinsic 'fiber' properties should be better than for the plant fibers, specific nanoscale phenomena may occur such as structural improvements to the polymer matrix (crystallinity, orientation, reduced molecular mobility etc.) and it may become easier to fabricate small-scale geometries.

The first effort to make cellulose nanocomposites with a polymer matrix appears to have been the investigation by Boldizar et al. [269]. Poly(vinylacetate) nanocomposite films were prepared from hydrolyzed and homogenized cellulose pulp, with strongly improved mechanical properties. Also, hydrolyzed cellulose pulp was compounded with thermoplastics, injection molded into specimens for mechanical property measurements. The reinforcement effect was better than for pulp fiber reinforcement, possibly due to the higher aspect ratios obtained from the disintegration of the pulp fibers into nanofibers. The cellulose nanocomposites field, however, did not really take off until researchers in Grenoble investigated hydrolyzed CNCs (then called 'cellulose whiskers') as a reinforcement [270, 271], followed by numerous studies, *e.g.*, using nanocelluloses from parenchyma cells (potato tubers etc.), which are covered in a thorough review of the background to the whole field [272]. Yano and coworkers then investigated wood-based CNFs combined with poly(phenol formaldehyde) resins [273] and transparent nanocellulose films with an acrylate polymer matrix [274]. High optical transmittance and high mechanical performance is a highly interesting combination for biocomposites, which provides unique application opportunities, and will be reviewed in more detail in subsequent sections. Another important category of composites for engineering applications is 'cellulose biocomposites' based on thermosets. These are suitable for large-scale production, with nanopaper reinforcement in the form of prefabricated CNF mats. Epoxy and polyester resins typically used for glass fiber composites have been reinforced with a high content of wood CNFs [275, 276], and mechanical properties were competitive with molded glass fiber composites [277]. A large collection of mechanical property data for cellulose nanocomposites have previously been analyzed [278]. The strongest and stiffest nanocomposites were those based on a high content of prefabricated nanopaper reinforcement, and properties scaled with nanopaper properties and volume fraction.

Key research and technical goals for the promotion of nanocellulose applications include scalable processing concepts and processing technologies for cellulose nanocomposites. Numerous technical studies are disappointing in that the mechanical performance does not meet requirements. Properties are simply not good enough to justify substitution of a petroleum-based polymer composite reinforced with glass fibers or mineral fillers. The most common reason for this first problem is that the CNFs are agglomerated in the composite, often into microscale aggregates. Although such a material is based on nanofibers, it is not nanostructured in a true sense. The modulus usually still shows improvement, although the reinforcement can be even lower than for comparable plant fiber composites. Strength is often reduced by the presence of aggregates, since they form stress concentrations which tend to initiate failure at low strain. A second problem is that cellulose nanocomposites are expected to contribute to sustainable development, but energy demand and carbon dioxide emissions related to CNF and nanocomposites fabrication tend to be high [279], which needs to be addressed. Holocellulose-based native CNF is one interesting possibility with low fibrillation energy, despite the lack of chemical modification [280]. Finally, the cost of the nanocomposite material needs to be competitive with alternative materials for a given application. The two last points (sustainability and cost) mean that the possibilities for chemical modification of nanofibers are not endless, contrary to many optimistic statements.

A common preparation route for cellulose nanocomposites is to dissolve the polymer in an organic solvent, mix in the CNF and then do solvent casting. In industry, this process could be used for some coatings, preparation of adhesive films etc., but it is not appropriate for semi-structural composites. The solvents used are frequently expensive and could even be toxic and difficult to recover. Casting from a hydrocolloidal dispersion is possible, though. The polymer matrix can be water-soluble, *e.g.*, starch [281, 282], although this limits the applications. The polymer can also be distributed in the form of water-dispersed nanoparticles, as was demonstrated for PLA [283]. The water-based processing route is again feasible for coatings and adhesives, and also for the preparation of some types of nanocomposite films and barrier layers. Layers of nanocomposite films of around 100 µm in thickness can be stacked, followed by hot-pressing into nanocomposite laminates. There are, however, significant industrial challenges in processing of the colloids. The concentration of nanofibers needs to be higher than the 1–2% typically used in basic research investigations, while preserving CNF dispersion and limiting the use of chemical modification to affordable and sustainable technologies. The removal of a large quantity of water is a

technical difficulty, and a challenge in terms of cost and energy demands.

Melt processing of thermoplastic nanocomposites is of great technical potential. Injection molding of thermoplastic products is an enormous business and preferred in the automotive industry, due to the high processing rates. An important technical problem is the strong viscosity increase arising from the addition of CNF to thermoplastics, which can happen at a low cellulose content. The main reason for this increase is the large aspect ratio and small dimensions of the nanofibers. Yano and coworkers have addressed this by doing some of the pulp fiber disintegration in the compounding process itself [284]. Since mechanical properties scale with cellulose content, one limitation is that a typical reinforcement content is around 10 wt.%, which may be related to melt viscosity problems.

Thermoset nanocomposite processing is also challenging. Bulk mixing between liquid thermoset precursors and CNFs frequently results in their aggregation, simply because of the CNF-CNF affinity in such liquids. CNF reinforcement 'mats' will have nanoscale porosity, which means that good wetting is required for resin impregnation. Thermoset resin wetting of cellulose is, however, difficult since there will be water molecules at hydrophilic CNF surfaces under ambient conditions. Commercial production of glass fiber/epoxy prepreg utilizes organic solvent assisted epoxy impregnation, and this works well also for high content CNF/epoxy [277]. If the nanocellulose reinforcement is modified by acetylation [285] or by green chemistry approaches [286], bulk monomer impregnation is facilitated so that processing may be feasible and similar to industrial liquid molding of thermoset composites.

After more than 25 years of cellulose nanocomposites research, there is an urgent need to address challenges to realize large-scale use of nanostructured cellulose biocomposites (processing, moisture, performance, cost, sustainability, etc.) and intensify research and development on credible applications. In addition, the goals of materials substitution need to be defined: What are the specific reasons for substituting existing materials with polymer matrix cellulose nanocomposites? In the following sections, four cases of importance for the application potential of cellulose nanocomposites are covered: melt compounding of thermoplastic composites for mass markets will be addressed, optically transparent composites based on bacterial cellulose (BC) for impact protection, transparent wood, which is a polymer matrix nanocomposite for building and photonic applications based on nanostructured wood substrates, and finally functional CNM composites with structural color.

Kristiina Oksman (Luleå University of Technology, Sweden): large-scale melt compounding of cellulose nanocomposites

Melt blending is an important manufacturing process, and its development is important for the commercialization of cellulose nanocomposites and associated products such as automotive parts and packaging films. However, many challenges need to be overcome to enable large-scale production [287]. One challenge is the high material cost and complexity of the manufacturing process, which further increases the total cost of the material. In addition, the environmental impact of the manufacturing process is a vital consideration. Since significant amounts of energy are required to manufacture promising biobased cellulose nanocomposites, this has negative implications for product cost and commercial production. For this reason, the use of cellulosic nanomaterials in thermoplastic polymers must be extensively explored. The improvement in mechanical properties associated with the addition nanocellulose has been a research focus; however, the addition of nanocellulose can also result in other benefits. Regardless of the impact on polymer properties, nanomaterial additives must be optimally dispersed, distributed, and, in some cases, oriented within the polymer.

Generally, the manufacturing of nanocomposites is challenging since nanomaterials have a large surface energy and tend to agglomerate. CNMs are usually fabricated via top-down processes in the presence of water; although these materials initially disperse well in the water, once they have dried, redispersal is difficult owing to strong interactions that may include hydrogen bonding amongst other interactions, but ultimately leading to what is commonly termed 'hornification'. CNFs and CNCs form gels at low concentrations (1 wt.%) because of their tendency to form networks; however, gels derived from CNCs are less viscous owing their reduced length. Melt compounding is a high-temperature nanocomposite fabrication process in which polymers are heated

above their melting temperature; this method restricts the use of CNMs as some are sensitive to high temperatures. These specific properties of nanocellulose materials make their use in melt compounding with thermoplastics even more challenging [287].

Many researchers have reviewed this topic; for example, Oksman et al., Wang et al., Zheng and Pilla, and Clemons and Sabo [288–291]. These reviews explore the developments in the extrusion processing of cellulose nanocomposites; Oksman et al. [288] focused on the processing and properties of cellulose nanocomposites, Wang et al. [289] focused on potential industrial processes, Zheng and Pilla [290] focused on melt processing with CNCs, and Clemons and Sabo focused on the wet compounding of cellulose nanocomposites [291].

In melt blending processes, various components, such as polymers, additives, and nanocellulose (reinforcing agents), are mixed in a compounding extruder where high temperatures and high shear forces melt the polymer; a specific screw configuration enables the mixing of the components. Two types of extruders are used in compounding processes: co-rotating and counter-rotating twin-screw extruders. Co-rotating extruders are preferred because they are more effective at mixing and dispersing the components; they also allow a flexible screw design, i.e., screws can be tailored to maximize dispersive, distributive mixing, or minimize shear forces to preserve fiber length. Co-rotating extruders are also more effective at removing moisture and volatiles, which is important if liquids are used as processing aids. The main challenges in the melt processing of cellulose nanocomposites are the controlled feeding of nanocellulose materials into the extruder and the dispersion and distribution of these nanomaterials in the polymer without degrading the cellulose or polymer [287, 288]. Different approaches to the melt processing and associated dispersion of CNMs have been explored, namely, liquid-assisted extrusion or wet feeding, dry feeding, and single- or multi-step processing, including master-batch processing and solid-state processing.

Liquid-assisted extrusion

Liquid-assisted extrusion was developed for nanocomposites derived from clay suspensions and polyamide 6 (PA6) [292] and used for first time on cellulose nanocomposites by Oksman et al. in 2006 [293]. Several reports on liquid-assisted extrusion or wet feeding of cellulose have since been published [294–302].

In liquid-assisted extrusion processes, CNMs are suspended or dispersed in water with or without additives. This suspension is pumped into the extruder that vaporizes the liquid phase and removes it via a venting system [292, 293, 295–301]. Karger-Kocsis et al. [292] listed several benefits of the liquid-assisted feeding of nanomaterials into the extruder, including the absence of the necessity for the surface modification of the nanomaterials—thus avoiding the degradation associated with surface modifiers, reduced health risks owing to the suspension of the nanomaterials in liquid, and their improved dispersion because of 'blow-up' phenomena caused by the pressurized liquid evaporating from the melt, particularly in cases where water is used. Oksman et al. [287] also mentioned the economic and environmental benefits of the liquid-assisted process associated with the absence of supplementary treatment processes such as freeze-drying, which would increase its energy requirements, processing time, and risk to human health. CNCs are extremely small particles that are safer to handle in liquid owing to risks associated with inhalation.

However, if water-dispersed CNMs are directly subjected to high-temperature processing, rapid evaporation can lead to aggregation. Therefore, the use of processing or dispersion aids, that limit or prevent agglomeration during the evaporation of water or solvents, have been explored, such as polyethylene glycol (PEG) [293], triethyl citrate (TEC) [294, 295], and prepolymers such as methyl methacrylate (MMA) [296], polyvinyl alcohol (PVOH) [297], and glycerol triacetate (GTA) [300].

Figure 8 shows a co-rotating extruder setup and screw design used for the fabrication of cellulose nanocomposites. The polymer is fed into the extruder, using a gravimetric feeding system, and melted before the introduction of the nanocellulose-containing liquid phase. Two atmospheric vents and a vacuum vent are used to remove the vaporized liquid phase. A typical temperature profile for the process with polylactic acid (PLA) as the polymer matrix is shown. The screws consist of feeding zones for the polymer and nanocellulose-containing liquid phase, a polymer melting zone, and dispersive and distributive mixing zones ahead of the vacuum vent. The

Figure 8 Co-rotating twin-screw extruder setup and screw design for liquid-feeding, reproduced from Bondeson and Oksman [297] with permission from Elsevier (Copyright Elsevier, 2007).
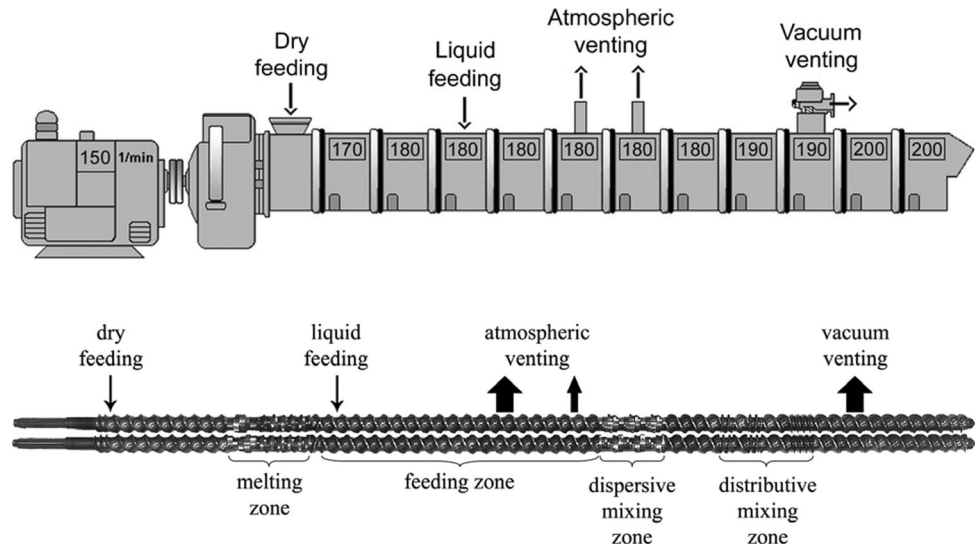
total processing time is 30–50 s depending on the screw speed [297].

Liquid-assisted feeding presents many challenges such as the high viscosity of the nanocellulose suspensions—which hampers blending especially in the case of CNFs—and the high amounts of liquid (water or other solvent) that require removal. A suitable extruder, such as a co-rotating extruder, that effectively removes the liquid (solvent) should be used. The degradation of the polymer is also a common concern in liquid-assisted extrusion; however, provided no oxygen is available during processing, the polymer does not degrade. Herrera et al. [295] showed that the molecular weight of PLA is not affected by the liquid-feeding of CNFs; this result is consistent with that reported by Peng et al. [298], who investigated the reinforcing of PA6.

Geng et al. [296] polymerized MMA-latex onto CNCs (PMMA-CNC) and used this material to prepare a nanocomposite with PLA. A PMMA-CNC–water dispersion was pumped into a twin-screw extruder and mixed with PLA at a low CNC concentration. The nanocomposites were then oriented using a solid-state drawing process. The oriented nanocomposite exhibited an ultrahigh mechanical performance. Furthermore, this nanocomposite, containing well-dispersed CNCs, showed strain-responsive behavior, i.e., birefringence that changed with applied deformation, as shown in Fig. 9.

Peng et al. [298] used a water-assisted extrusion process to compound CNCs and PA6. They found that the addition of CNCs does not significantly affect the mechanical properties of PA6. However, they also found that CNCs act as a nucleation agent for the crystallization of PA6, increasing the cell density and reducing the cell size of the foam during microcellular injection molding. It was also demonstrated that water-assisted extrusion does not significantly affect the molecular weight of PA6. Herrera et al. [295, 299, 300] studied the effect of plasticizers or dispersing aids on the dispersion of CNMs in PLA using a liquid-assisted extrusion process. They found that the addition of plasticizers such as TEC and GTA effectively enhances the dispersion of CNFs and CNCs in PLA. Hietala et al. [301] prepared a liquid mixture of potato starch, plasticizer, and CNFs (up to 20 wt.%) and fabricated thermoplastic starch nanocomposites using a twin-screw extruder. The results were interesting in that the mechanical properties of the composite were similar to those of polyethylene; however, the added CNFs improved the moisture stability of the starch which is typically very moisture sensitive. Yasim-Anuar et al. [302] melt blended low-density polyethylene (LDPE), CNFs, and maleic anhydride–grafted polyethylene (MAPE)—a compatibilizer—using an internal mixer and a twin-screw extruder. They found that a twin-screw extruder better disperses CNFs, up to 3 wt.% fraction, than an internal mixer.

Dry feeding of nanocellulose during extrusion

Several studies have explored the use of dried nanocellulose powders in extrusion processing, *e.g.*, CNCs and CNFs [303–307]. The addition of dried nanocellulose particles is easier to feed, especially if

Figure 9 Cellulose nanocomposite consisting of PLA and CNCs (0.2 wt%) with MMA-modified surfaces to aid dispersion, **a** ultrahigh mechanical properties and **b** strain-responsive birefringence, reproduced from Geng et al. [296] with permission from Elsevier (Copyright Elsevier, 2020).
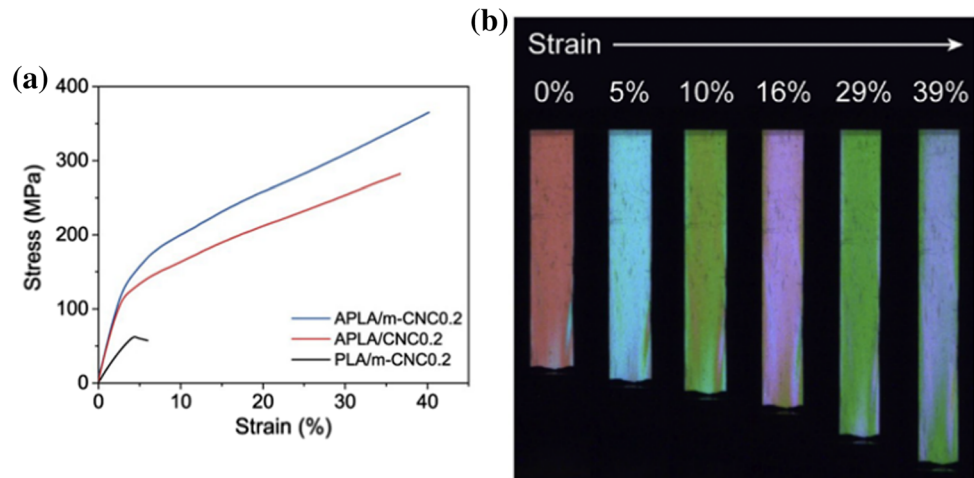
high concentrations are of interest, but there are no studies showing that dry CNCs can be dispersed in melt compounding. Typically, the modulus of a composite prepared using dry nanocellulose increases slightly with increasing nanocellulose content, but its strength is inferior, or similar to that of the neat polymer. For example, Wang et al. [304] used spray-dried CNFs, PP, and maleic anhydride–grafted polypropylene (MAPP)—a compatibilizer—to produce melt-extruded composites containing 3, 10, and 30 wt.% CNFs. The presence of CNFs in PP does not significantly affect its mechanical properties; the modulus and strength of composites containing 30 wt.% CNFs are higher and similar, respectively, to those of neat PP. Microscopy revealed the presence of large CNF agglomerates in the PP matrix. Venkatraman et al. [305] compared the performances of freeze- and spay-dried CNCs in a process considered industrially scalable. A polymer (PA11) and dried CNCs were milled for 6 h before the powdered mixture was extruded or compression molded. Despite being time consuming and energy demanding, both processes produced composites with improved mechanical properties. Leao et al. [306] produced composites consisting of an acrylonitrile butadiene (ABS) matrix and 0.5, 1, and 1.5 wt.% CNCs with different lengths (150 and 220 nm) by twin-screw extrusion and injection molding. The CNCs were shown to increase the tensile modulus of ABS without increasing its strength, and the composite containing 0.5 wt.% CNCs (220 nm) exhibited the highest modulus. Sarul et al. [307] prepared a master batch consisting of spray-dried CNCs and a polymer mixture that was freeze-dried and used to form composites via direct mixing and twin-screw extrusion. The mechanical properties of the composites decreased with increasing CNC content, except in the case of the composites containing 5 wt.% CNCs, which exhibited a slightly increased modulus.

Master-batch processing

A master-batch process where a CNM is introduced in high concentrations into a polymer in solution is another approach for preparing cellulose-based nanocomposites. This mixture—master batch—containing high concentrations of CNMs is dried, crushed, and diluted in the extrusion process to the desired concentration [308–312]. This is a possible approach to the large-scale fabrication of cellulose nanocomposites; however, if solvent exchange is necessary, its environmental impact is significant. For example, it was found that the mixing of water-dispersed polyvinyl acetate (PVAc) latex with CNCs and CNFs at high concentrations (20 wt.%) promoted the dispersion of the CNCs and CNFs in the composite during the subsequent extrusion process [309, 310]. Jonoobi et al. [311] prepared PLA–CNF composites by mixing an organic solvent-dissolved PLA (of different concentrations) with nanocellulose suspensions, drying and then extruding the mixtures using a twin-screw extruder. The resulting composites exhibit excellent mechanical properties and enhanced thermal stability. Jonoobi et al. subsequently investigated the reinforcing effects of acetylated (A_C) CNFs using a similar compounding process and concluded that the acetylation of CNFs does not further improve the nanocomposite properties [311]. Correa et al.

[312] prepared a master batch of PA6 with a high concentration of CNCs by dissolving PA6 in formic acid. The aim was to coat the CNCs with PA6 to improve their thermal stability and enable their application in high-temperature processing. Nanocomposites consisting of PA6 and PA6-coated CNCs (1 wt.%) were prepared using a twin-screw extruder. It was found that, although well dispersed, the effect of the CNCs on the modulus and strength of PA6 was minimal and non-existent, respectively. Evidently, master-batch processing has advanced; however, the requisite solvent exchange and dissolution of the polymer matrix are not sustainable.

Researchers have extensively studied extruded cellulose nanocomposites, conducting interesting research on HDPE, PP, and PA6 nanocomposites, such as Sato et al. [313], Igarashi et al. [284], Suzuki et al. [314], and Semba et al. [315]. Sato et al. [313] compared the wet and dry processing of chemically modified cellulose, using multiple preprocessing steps, including mixing and kneading in an extruder at temperatures below the polymer melting temperature prior to the melt-compounding process. The cellulose and MAPP (compatibilizer) contents were kept constant (at 10 and 4.3 wt.%, respectively), while the degree of chemical modification of the cellulose was varied. They showed that the chemical modification and degree of substitution (DS) of the cellulose significantly affect the material properties and that chemically modified CNFs produce better composites than bead-milled CNFs. The treated cellulose was fibrillated during kneading but not to nanosized fibers.

Igarashi et al. [284] further explored the dry processing of cellulose nanocomposites; preparing dry mixtures of chemically pretreated cellulose pulp, HDPE, MAPP, and $CaCO_3$ using multiple preprocessing steps that were subsequently extruded to obtain composites. The results were similar to those reported by Sato et al. [313], who showed that the cellulose was fibrillated to smaller sizes during processing and that the mechanical properties of the composite were optimized at a DS of 0.43. The dispersion and distribution of the cellulose are shown in X-ray computed tomography images with increasing DS (Fig. 10a-f); Fig. 10d shows the composite with the highest mechanical properties. Although the preprocessing steps fibrillated the cellulose, improving the mechanical properties of the composites, they were time consuming, involving solvent exchange to an organic solvent and multiple washing steps with acetone, ethanol, distilled water, and isopropanol. Moreover, they did not reduce the cellulose to nanosized fibers. The preparation of the dry mixture required multiple steps and its feeding rate into the extruder was only 50 g/h, which is too slow for an industrial process.

Semba et al. [315] prepared nanocomposites consisting of refined A_C cellulose and PA6. These components (PA6 and 10 wt.% A_C cellulose) were mixed in propanol to form a slurry, which was dried and then melt compounded in a twin-screw extruder followed by injection molding. The authors reported a significant increase in the flexural properties of PA6, and the A_C cellulose with DSs of 0.67 and 0.64 produced composites with the highest properties. Furthermore, the A_C cellulose was fibrillated during the extrusion process and the thermal properties and heat deflection temperature of the composite were improved.

High-shear processes

High shear forces have been used in different ways, in wet and dry feeding processes, to improve dispersion, break cellulose agglomerates, and fibrillate cellulose [316–320]. Suzuki et al. [316] fabricated nanocomposites with high cellulose concentrations using a solid-state high-shear process. A wet mixture of cellulose (50 wt.%), powdered PP, and powdered MAPP was blended in a twin-screw extruder with a cooled extruder barrel (0 °C). This process also fibrillated the cellulose to sub-micron sized fibers without melting the polymer. This mixture was then compounded by melt extrusion. The main outcome of this study was the fibrillation of cellulose pulp and the consequent enhanced mechanical properties of the associated composite, compared with those of neat PP.

Solid-state pulverization and melt processing is a multi-step fabrication process that has been employed by Iyer et al. [318] to prepare cellulose nanocomposites. A solid-state mixture of nanocellulose and PP was pulverized (and mixed and dispersed) at low temperature to avoid melting of the polymer before the pulverized homogeneous mixture was compounded through melt processing. They showed that the nanocellulose was well dispersed in PP but that it did not significantly affect its mechanical properties. Venkatraman et al. [319] used
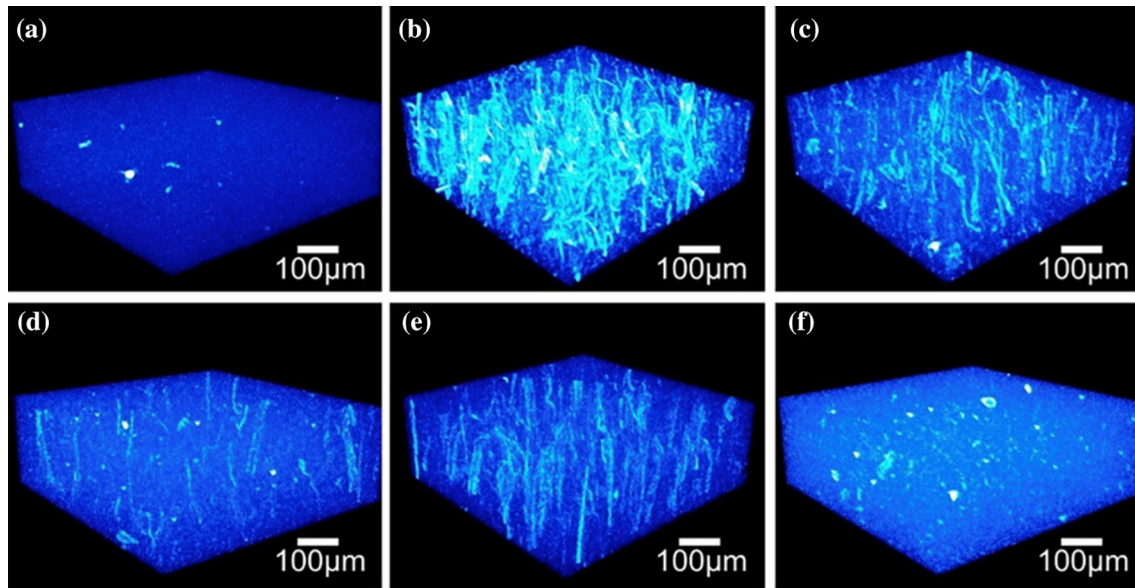
Figure 10 Dispersion of fibrillated cellulose in composites with different DSs. X-ray computed tomography images of **a** neat HDPE; composites containing cellulose **b** DS: 0, **c** DS: 0.22, **d** DS: 0.43, and **e** DS 0.57; and f) bead-milled fibrillated CNFs (DS: 0.44), reproduced from Igarashi et al. [284] with permission from Elsevier (Copyright Elsevier, 2018).

cryo-milling and planetary ball milling to prepare master batches consisting of PA6 and high concentrations of spray-dried CNCs. Master batches of PA6 and 75 wt.% CNCs and PA6 and 90 wt.% CNCs were prepared by ball milling. The powdered master batches were diluted during melt processing to produce composites with CNC contents of 5 and 10 wt.%. The properties of these composites were compared with those of corresponding samples produced by direct milling and compression molding. The results showed that the master-batch process produces a composite with a slightly higher modulus than neat PA6 but does not realize an improvement in strength. This study showed that spray-dried CNCs are difficult to finely disperse in PA6; moreover, the proposed process is very energy demanding as the milling time was 6 h. Olivera et al. [320] also explored the solid-state pulverization of CNFs. They mixed different cellulose nanofibers (10–30 wt.%), with 10 wt.% MAPP and PP, and extrusion mixed and compounded the mixtures at temperatures of 80–100 and 170–180 °C, respectively. They reported improvements in the mechanical properties of the composites, especially for composites containing 30 wt.% cellulose. It has been shown that solid-state high-shear processing can effectively disperse cellulose. However, these processes are very energy demanding and may not be suitable for large-scale applications.

Sridhara and Vilaseca [321] considered batch processing using a thermokinetic mixer to be suitable for scaling up to an industrial level. They fabricated nanocomposites by premixing CNF gel (containing 3 wt.% CNFs) with powdered PA6 to realize composites with CNF contents of 5, 15, and 25 wt.%; these mixtures were dried and melt compounded in a thermokinetic mixer before the resulting materials were milled or pelletized and compression molded. The mechanical properties of the composites increased with an increasing CNF content, and the best properties were found for composites containing 25 wt.% CNFs. This batch process is very fast as the material melts owing to high shear forces within 20 s.

Considering the latest research efforts on the melt processing of cellulose nanocomposites, interest in large-scale processing has increased; however, the expected breakthroughs have not yet materialized. Many processes are time consuming, have high energy and chemical requirements, and are expensive. It is very difficult to finely disperse nanocellulose, at a nanoscale, if composites with high nanocellulose contents (<1 wt.%) are desired. These studies were unable to determine whether cellulose at the nanoscale is a suitable reinforcing material because its dispersion at a nanoscale level is difficult in melt-extruded composites. To date, we have not realized cellulose nanocomposites with properties

that cannot be achieved with micrometer natural-fiber reinforcement.

Techniques to assess the dispersion of CNFs inside thermoplastic composites, and the use of quantitative methods of the determination of dispersion and mixing are few and far between. Some work by Eichhorn and coworkers have shown that both photoluminescence [322], and Raman spectroscopy [323] are very useful in quantifying the spatial distribution and mixing of aggregates in CNF-reinforced thermoplastic composites. The relationship between the size of aggregates, and the mechanical properties of CNF-thermoplastic composites has also similarly been quantified using both photoluminescence, and Raman spectroscopy [324]. It was demonstrated that in spite of the use of a chemical dispersant, in this case tannic acid, sufficiently large aggregates of CNFs still persisted which reduced the fracture toughness of the composites [324]. It is possible that very low concentrations of well-dispersed nanomaterials can impart new functionalities to the polymer (as a nucleation agent etc.) and is expected to be the focus of future research on the melt processing of cellulose nanocomposites.

Koon-Yang Lee (Imperial College, UK): BC nanopaper-enhanced optically transparent composites for impact protection
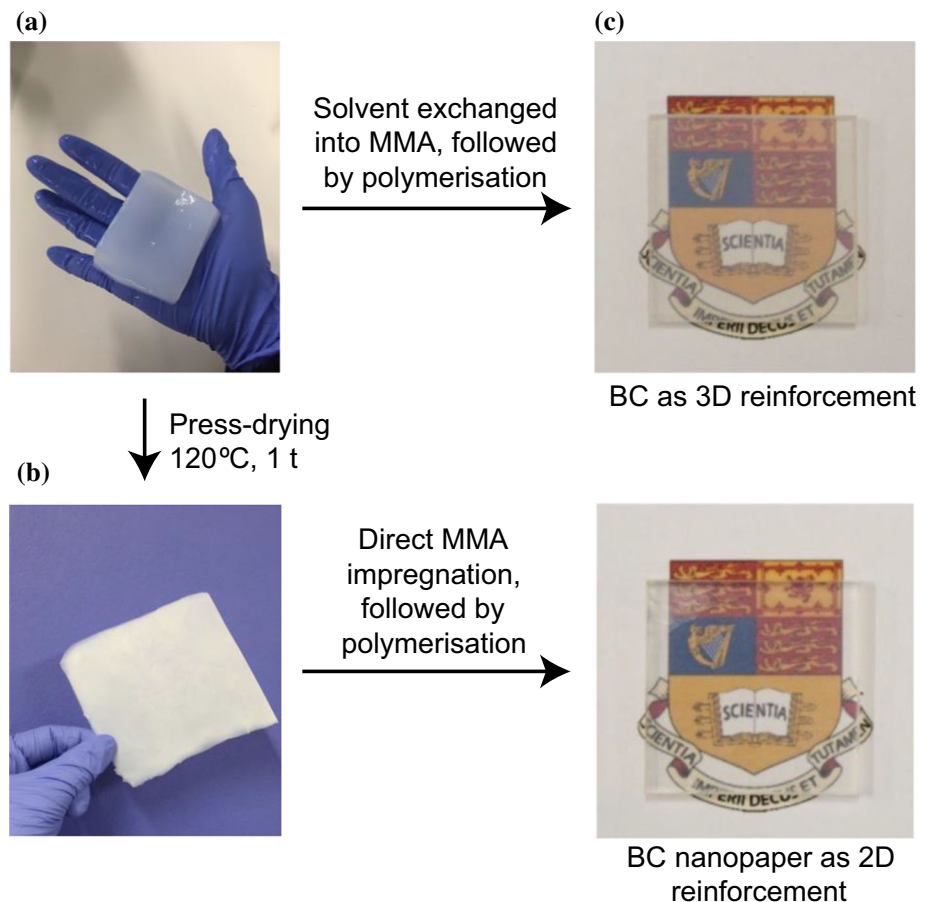
Despite its high Young's modulus and tensile strength, one of the main challenges in the commercialization of nanocellulose as reinforcement for various composite applications is price. A recent market study reported that most producers will sell CNF gel at a price of ~ US$100/kg [325]. Whilst the market price for BC is not widely reported, a recent techno-economic analysis on the large-scale production of BC using an energy-efficient airlift reactor with modified Hestrin-Schramn medium estimated that the breakeven price for manufacturing BC was US$25/kg (a wet BC pellicle containing 99% water) [326]. Nanocellulose is therefore not cost-competitive in the high-volume composite market, especially when a high loading fraction of nanocellulose (>30 vol.-%) is required to achieve significant improvement in mechanical performance [278]. Cheaper sustainable reinforcing fillers, such as wood flour and natural fibers, are available for the composite industry [327–330]. It can be anticipated, however, that the high cost of nanocellulose could be offset by designing high value composites containing only a low loading fraction but still offering dramatically improved mechanical performance that conventional materials cannot achieve. One such area where nanocellulose could make a significant impact is their use to enhance the performance of transparent polymeric amour. The entry level for transparent amours is either monolithic acrylic or laminated polycarbonate/acrylic systems. The next choice up is glass-clad polycarbonate, which offers a significantly higher level of impact protection but at the expense of added weight and cost. There are currently no lightweight polymeric transparent armor solutions that could bridge the gap between the two levels of impact protection.

The research group at Imperial College London is currently working on developing low loading fraction nanocellulose enhanced acrylic systems to close this property–performance gap. BC is an ideal candidate in this context due to its high single nanofiber tensile properties and its similarity to the refractive indices of acrylic resins [274], an essential requirement to achieve high level of optical transparency in a composite system [331]. Furthermore, BC is biosynthesized as pseudo-continuous cellulose nanofiber network [332–334] with a high specific surface area (>50 m^2 g^{-1}) [335–337]. Therefore, the introduction of BC into an acrylic resin could create additional energy-dissipation mechanisms, including fiber-matrix and fiber–fiber debonding, as well as fiber re-orientation and fracture. To produce optically transparent BC-enhanced poly(methyl methacrylate) (PMMA) composites, Santmarti et al. [338] first press-dried BC pellicle (Fig. 11a) into a sheet of a BC nanopaper (Fig. 11b), followed by immersion and polymerization in a cell-cast mold containing a methyl methacrylate (MMA) syrup. Such a composite construct utilizes BC nanopaper as a *two-dimensional* reinforcement. While the starting BC nanopaper was not transparent, the resulting PMMA composite containing the BC nanopaper was optically transparent (Fig. 11c). The light transmittance of a 3 mm thick composite was found to be 73% at a wavelength of 550 nm. Such a high level of optical transparency was due to the low loading fraction of the BC nanopaper used (1 vol.-%), the filling up of the pores within the BC nanopaper structure with PMMA, the similarity between the refractive indices of BC and PMMA, as well as the small lateral size of the BC fibrils.

Figure 11 **a** BC pellicle with a water content of ∼ 99 wt%, **b** press-dried and well-consolidated BC pellicle, followed by methyl methacrylate (MMA) impregnation and polymerization to produce 3-mm-thick BC nanopaper-enhanced PMMA composites, and **c** 3 mm thick BC-PMMA composites produced from the solvent exchange of BC pellicle in water through acetone into MMA, followed by polymerization. The BC loading in all composites was 1 vol%. Reproduced from [338] with permission from the American Chemical Society (Copyright American Chemical Society, 2019).

(a)

(c) Solvent exchanged into MMA, followed by polymerisation

BC as 3D reinforcement

(b) Press-drying 120°C, 1 t

Direct MMA impregnation, followed by polymerisation

BC nanopaper as 2D reinforcement

Significant improvement in the composite performance was achieved even though the BC loading was only 1 vol.-%. The tensile modulus of the resulting BC nanopaper-reinforced PMMA composite was measured to be 4.2 GPa, a 24% increase over the tensile modulus of neat PMMA. The BC nanopaper-reinforced PMMA composite was also found to possess significantly improved fracture resistance and flatwise Charpy impact strength. The initial critical stress intensity factor (K_{Ic}), a measure of resistance to fracture, of the BC nanopaper-reinforced PMMA composite was found to be 1.72 MPa m$^{0.5}$; a 20% increase over the K_{Ic} of neat PMMA. A 20% increase in flatwise Charpy impact strength of the composite was also observed when compared to neat PMMA. Santmarti et al. [338] also investigated whether such improvements could also be achieved if BC was uniformly embedded within the PMMA matrix (i.e., BC as a *three-dimensional* reinforcement). The BC pellicle was first solvent exchanged from water though acetone into MMA, followed by polymerization in a cell-cast mold. While the resulting composite

was also transparent, the mechanical performance of such a composite performed poorly when compared to neat PMMA. The K_{Ic} and flatwise Charpy impact strength were found to be only 0.7 MPa m$^{0.5}$ and 4.7 kJ m^{-2}, respectively; a 50% decrease in K_{Ic} and 25% decrease in flatwise Charpy impact strength compared to neat PMMA.

The mechanical performance of a composite is the volume-weighted average between the mechanical properties of the matrix and the reinforcement [339]. In theory, embedding BC uniformly within a polymer matrix should lead to a PMMA composite with improved performance as the high modulus and strength of a single BC nanofiber can be effectively utilized. However, fractographic analysis revealed the presence of significant matrix embrittlement when BC was embedded uniformly within PMMA (Fig. 12a). When BC was used as a *two-dimensional* reinforcement in the form of BC nanopaper, the effect of matrix embrittlement was minimized due to a reduced BC-PMMA interface. In addition to this, the reinforcing effect of such laminated composite

Figure 12 Fracture surface (single edge notched beam) of the BC-PMMA composites. **a** BC as three-dimensional reinforcement, whereby a rough texture without plastic deformation can be observed and **b** BC nanopaper as two-dimensional reinforcement, where a laminated construct can be observed. The scale bars at low and high magnifications correspond to 0.5 mm and 25 μm, respectively. Reproduction of images from [338] with permission from the American Chemical Society (Copyright American Chemical Society, 2019).
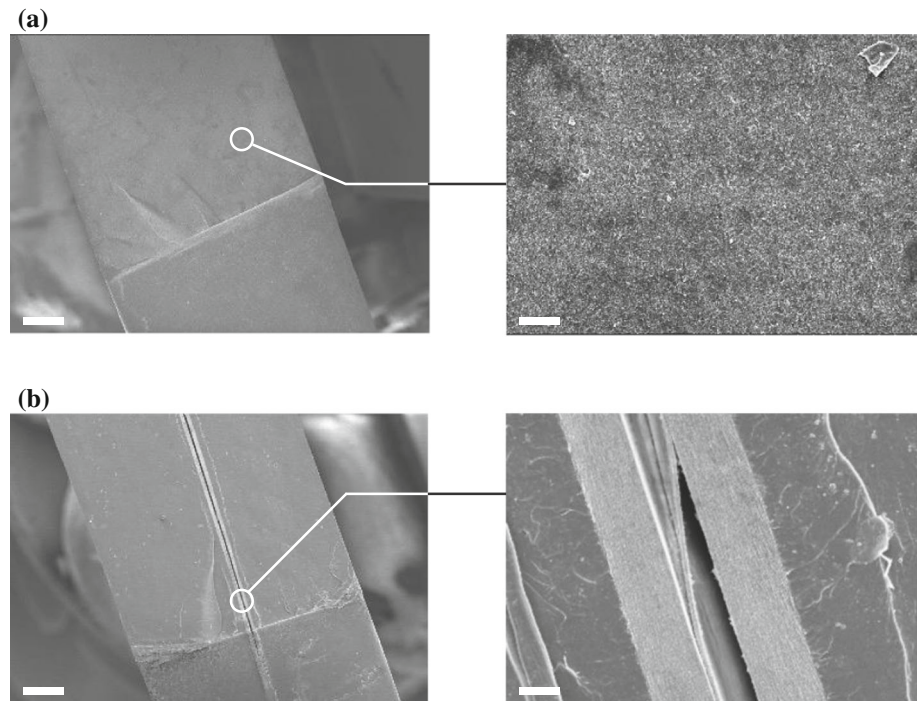
construct stemmed from the mechanical properties of the BC nanopaper (Fig. 12b), which was found to possess a high tensile modulus and strength of 19.6 GPa and 188 MPa, respectively, as well as a high K_{Ic} of 11.9 MPa m$^{0.5}$ [339], which is comparable to a single aramid fiber; reported to be 6.63 MPa m$^{0.5}$ [340]. The use of BC nanopaper also removed the need for complicated solvent exchange or drying steps, reducing the complexity of composite manufacturing. It should be noted that the long dewatering time of BC (or nanocellulose in general) to produce (bacterial) cellulose nanopaper, which is often cited as a bottleneck, could be addressed by reducing the grammage of the nanopaper or to induce flocculation of the nanocellulose by the addition of multivalent salts [341].

Since the loading fraction of BC required to achieve performance enhancement is low, the resulting BC nanopaper-PMMA laminated composite construct is expected to be cost-competitive, increasing its market uptake for advanced composite applications. However, there are still some outstanding issues in using BC nanopaper to enhance the properties of acrylic resins for impact protection that still need to be addressed, especially the effect of moisture on the long-term durability of the laminated construct as moisture is known to cause unpredictable delamination even in commercial transparent armor laminates

under ambient service conditions [342]. Furthermore, the transparency of the BC nanopaper-acrylic laminated construct at elevated temperatures is another major issue requiring further research.

Lars Berglund and Yuanyan Li (KTH, Sweden): transparent wood as an application of nanostructured biocomposites

Cellulose biocomposites are often considered as environmentally friendly materials. The introduction of nanocelluloses is motivated by similar arguments, yet the energy associated with defibrillation of wood fibers into nanocellulose (process energy and energy for chemicals) is very high [343]. Wood substrates offer some advantages in this respect, provided the intrinsic cellulosic nanostructures in wood can be preserved and exploited. The category of wood-polymer composites, however, is not new; wood has been impregnated with formaldehyde-based thermosets and commercialized (Impreg®, Compreg®), and monomers for thermoplastics have also been impregnated and polymerized in wood substrates [344]. The new aspect of many recent studies is that the cellulose nanostructure in the cell wall of the wood substrate has been preserved and targeted for functionalization [345].

Research on transparent cellulose biocomposites started with studies where thin cellulose nanopaper films from nanofibers were impregnated by acrylic monomers and cured [274]. The concept of transparent wood was then suggested for engineering applications [346, 347]. Wood substrates were delignified to remove the light-absorbing lignin component. In the next step, a monomer was impregnated into the substrate, followed by in situ polymerization to form a transparent wood biocomposite. Substrates other than wood have been used subsequently, for instance wood fibers [348] and bamboo [349]. From the point of view of cellulose biocomposites research, these materials are interesting because they combine structural properties (strength, stiffness) and the potential for making large structures with high optical transmittance. Optically transparent biocomposites opens a large field of materials research and opportunities for applications where semi-structural composites have photonic functions.

There are substantial challenges for transparent wood. Although processing is very similar to that of high-strength glass or carbon fiber composites (resin impregnation of a porous reinforcement), the added requirement of avoiding optical defects (voids, microcracks. cellulose agglomerates, etc.) makes it demanding. It is also difficult to achieve high optical transmittance in thick structures of high cellulose content, since light scattering inside the material is substantial. The research and materials development problems are illustrated in Fig. 13. When light reaches the transparent wood surface only a small fraction of it is reflected. Inside transparent wood, however, there is substantial light scattering, both forward- scattering and in other directions. Scattering takes place due to a mismatch in refractive index of

phases, from optical defects (e.g., interfacial debonding) and possibly from Rayleigh scattering inside the cell wall. Very few ballistic photons can go through the material without scattering. Some light may also be absorbed by residual lignin. The detailed mechanisms of light propagation are still under investigation, and the results will support ongoing product development.

Yano and coworkers have prepared load-bearing biocomposites by impregnating delignified wood with polyphenol-formaldehyde thermoset precursors [351]. Li et al. [347] used $NaClO_2$ delignification for their transparent wood substrate to reduce light absorption from lignin whereas Zhu et al. used a kraft pulping approach [346]. Li et al. [352] further developed the possibilities by using a lignin-retaining method, where only lignin chromophores were removed.

Various polymer matrices have been used for transparent wood, where the best approaches involve impregnation of a monomer or thermoset precursor, including acrylic monomers [347, 353], epoxies [346], thiol-enes [354], and polyimide [355]. Although it is well known that the refractive index of the polymer needs to match the refractive index (RI) of the substrate to reduce scattering, the details of the scattering mechanisms are not fully understood. This understanding will contribute to materials development efforts. The need to determine the refractive indices (in two directions) for the wood substrate has led to an experimental determination of their values [356]. This method is important, since chemical modification of the wood substrate will change its RI. Recently, the scattering in real wood microstructures from RI mismatches between the wood substrate and a polymer matrix has been modeled using numerical

Figure 13 **a** Photograph of transparent wood [350] and **b** schematic of light transmission in transparent wood. Images reproduced from [350] under the terms of a CC-BY (Open Access) license.

(a)

(b)
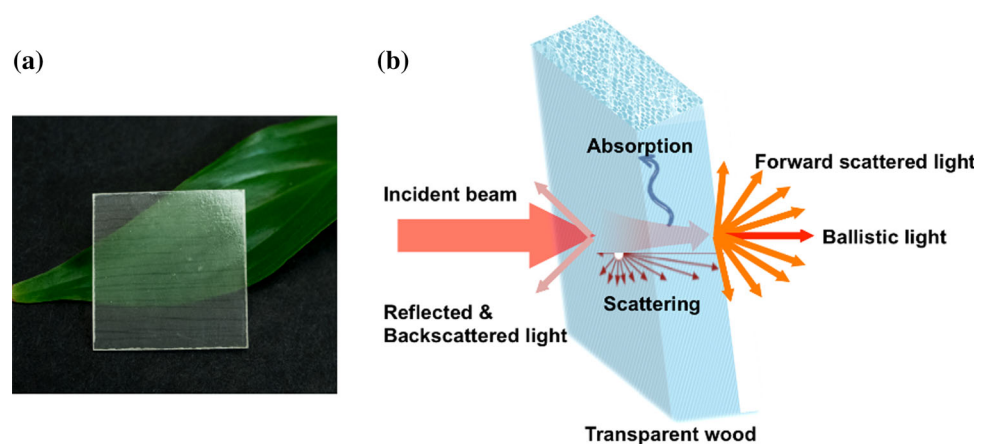
methods and real microstructures [357]. This model can be used to predict haze, transmittance, etc., and also to analyze the effect of different wood substrate morphologies, wood content, and material thickness.

Transparent wood is of particular interest because of its contribution to sustainable development. For this reason, Montanari et al. [358] developed green procedures to modify wood substrates for improved polymer matrix compatibility and reduced moisture sensitivity. Subsequently, a new biobased acrylic polymer matrix was synthesized with a suitable RI, so that a fully biobased transparent wood biocomposite was obtained [359]. One of the challenges was to find chemical approaches which could be used in the chemically heterogeneous environment of a wood substrate.

For building materials applications, the mechanical behavior of transparent wood is important. Jungstedt et al. [360] measured a modulus of 19 GPa and a tensile strength of 263 MPa for birch/PMMA composites with 25 vol% wood substrate reinforcement. The optical transmittance of this composite was still as high as 70% at a thickness of 1.3 mm. Basic optical properties have also been investigated, including anisotropic scattering [361]. Vasileva et al. [362] reported on interesting polarization effects in transparent wood, where the effect depended on the wood species used for the reinforcing substrate. Haze was discussed by Li et al. [363], who pointed out favorable effects from high haze. Haze is defined as the proportion of forward scattered light to the total forwarded light. Broadband high haze (>80%) can create a uniform and consistent light distribution for comfortable living environments [363].

The thickness of transparent wood will have strong effects on optical transmittance, which is important for building applications. Chen et al. [364] investigated this effect since the well-known Beer-Lambert law in principle is not applicable to scattering materials. A model was developed to predict thickness effects, as well as a procedure to determine parameters in this model for specific materials. In a previous study, Li et al. [365] demonstrated how acetylated wood substrates showed improved transmittance so that thicker structures could be prepared. Acetylation will reduce the extent of optical defects, such as wood/polymer interface debonding and cracks. Acetylation also facilitates the amount of acrylic monomer diffusing into the wood cell wall and may influence the refractive index of the wood substrate.

It has been recently demonstrated how the cell wall in wood/PMMA composites prepared by solvent-assisted processing was impregnated by the MMA monomer so that PMMA becomes distributed at the nanoscale inside the wood cell wall [366].

The processing of very large structures is desirable and a requirement for many building applications. A key problem is that the permeability of liquid resins in wood substrates is often quite low. A practical consequence is therefore that thick structures are difficult to impregnate without the formation of significant optical defects. The main strategy suggested is to use lamination of veneer layers, as was demonstrated for plywood structures [367] and subsequently in several other studies [368].

Figure 14 suggests potential applications of transparent wood in smart buildings. High haze is a favorable feature, which allows uniform light distribution and can provide indoor privacy. Although high haze is beneficial for some applications, the possibility for low haze extends the range of product design possibilities. Li et al. [365] reported a smart window concept where indoor privacy was optically tuneable through tailoring of transmittance and haze in thick structures based on clear acetylated transparent wood. Transparent wood is an excellent base for further functionalization by the addition of functional particles and/or polymers. Montanari et al. [369] added phase change materials (PCM) to transparent wood, for heat storage purposes. Energy was adsorbed by the PCM melting during heating. Cooling resulted in heat release by PCM crystallization. Other examples include the addition of Cs_xWO3 particles for heat-shielding since transmission in the near-IR range was reduced [370], and Fe_3O_4 nanoparticles were used for magnetic transparent wood to provide electromagnetic interference shielding [371]. Recently, structural color has also been combined with optical transmittance. Höglund et al. [372] precipitated metal nanoparticles inside the nanoporous wood substrate. This material was then impregnated with a refractive index-matched thiol-ene resin, followed by curing. The resulting composite showed structural color from the plasmonic nanoparticle effect, with only a minor reduction in the optical transmittance. Mechanical properties were well preserved. Another smart window concept is based on the integration of optoelectronic devices. Lang et al. [373] thus prepared electro-chromic windows by building conjugated-polymer-based devices

Figure 14 Examples of potential functions of transparent wood in smart buildings.
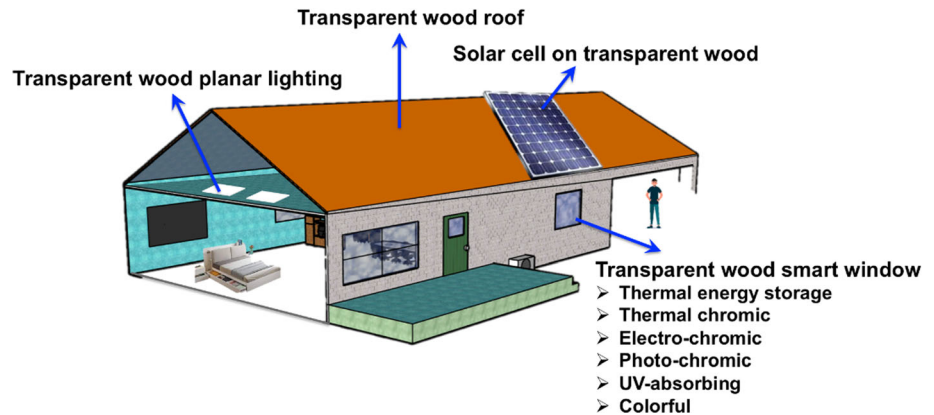
on transparent wood substrates. The device demonstrated vibrant magenta-to-clear switching (ΔE^*= 43.2) between -0.5 and 0.8 V, with a device contrast of 38 $\Delta\%T$ at a 550 nm wavelength.

Another interesting modification possibility is to use stimuli-responsive particles. Li et al. [374] first reported transparent wood from luminescent particles in the form of quantum dots (QDs). Diffused luminescence was revealed under UV irradiation, where the luminescent color obviously depends on the QDs. Other stimuli-responsive properties have been developed, for instance by impregnation of thermo- and photochromic microcapsules [375], and photoluminescent properties through 1,3,3-trimethylindolino-60-nitrobenzopyrylospira-based photoresponsive molecules [376]. One area of applications is the detection of changes in environmental conditions. Liu et al. [374] reported tunable room-temperature phosphorescence through carbon dots doping for formaldehyde gas detection. The main research and development challenge is to obtain a uniform distribution of particles or active polymers despite the tendency for aggregation during processing. In situ particle synthesis [372] is one route to reduce the problems, compared with direct infiltration.

For solar cells, high haze is favorable due to increased length of the light path in the active layer, leading to improved efficiency. Therefore, transparent wood was used as light diffuser layer by direct attachment to a commercial solar cell [377]. Li et al. [378] instead fabricated a perovskite solar cell on a transparent wood substrate, for the purpose of energy positive buildings. Here, the main challenge was the introduction of the conductive layer since high optical transmittance, combined with good interlayer bonding, is required.

Durability and moisture stability are important for load-bearing building applications. One route is cell wall bulking of the wood substrate by acetylation [365] or other anhydrides [358]. This means that also the transparent wood biocomposites, based on such substrates [359, 379], will be durable in a moist environment, although the high cost of polyimides is a limitation. For long-term durability, the yellowing problem known for paper needs to be avoided. Attempts to address this potential problem have been reported [380].

Transparent wood is also attractive for waveguiding photonics applications. Vasileva et al. [381] reported lasing from transparent wood impregnated by luminescent rhodamine 6G molecules. It was found that each fiber functioned as an optical resonator. The output signal is the collective contribution of the fiber-based resonators, which is broadly due to the fiber dimension variations and structural heterogeneity.

Optically transparent biocomposites based on cellulose or wood is a class of semi-structural materials which may combine load-bearing properties with eco-friendly characteristics, high optical transmittance, and photonics functionalities. The optical transmission criterion makes it necessary to improve micro- and nanostructural control during processing of cellulosic biocomposites. In addition, multifunctional biocomposites open new possibilities for applications of wood materials.

Silvia Vignolini and Bruno Frka-Petesic (University of Cambridge, UK): functional CNC composite materials with structural color

One of the most intriguing properties of nanocellulose is its intrinsic molecular chirality and how it can impact its behavior at much larger scales [382], which leads to the ability of CNCs to form functional materials with remarkable optical properties. The ability of CNCs to self-assemble into optically functional materials requires good dispersion in a solvent, usually water, and special care has to be taken to allow for the self-organization of the liquid crystalline order, followed by a removal of the solvent that preserves the acquired organization [383, 384]. While these conditions are usually easily met when casting a pure dispersion in a dish, modifying the formulation or the assembly conditions to gain further functionality without compromising on the assembly abilities represents the main challenge. The formation of colored films using CNCs has been introduced by Revol et al. [385, 386] and continues to be an active field of development, either to increase functionalities of such photonic films or to develop their potential as interference pigments by investigating scaling-up options. In this section, a few recent examples of optical functional materials are reviewed, leading to significant development in these two directions.

Optical functional materials

Plain photonic CNC films are usually brittle, and this has been considered as one of the major limitations to their practical use. Recently, several strategies have been proposed to mitigate their intrinsically poor mechanical resistance. Such strategies usually involve the co-assembly with a plasticizer that does not compromise the self-assembly of the CNCs, such as surfactants [387], a neutral or anionic polymer [388–390], globular proteins [391], resins or sol–gel precursors [392, 393]. Two recent examples from Walters et al. [389] and from Saraiva et al. [390] showed that a common cellulose derivative, hydroxypropyl cellulose (HPC), can be successfully used as a plasticizer for CNC photonic films, significantly preventing crack growth upon bending with respect to plain CNC films (Fig. 15a-c). The tensile testing comparison between CNC/L-HPC 50/50

w/w with plain CNC films showed a clear reduction in stiffness (2.5 GPa vs 14.4 GPa) and maximum tensile strength (18.7 MPa vs 68.7 MPa) as well as a ten-fold increase in maximum strain (4.8% vs 0.5%). However, the addition of HPC, like most non-volatile co-solvents, caused a significant redshift [383, 394], which usually comes with a trade-off on the range of accessible wavelengths. Another recent work involved a combination of bio-sourced and biocompatible silk fibroin (SF) and CNCs, showing improvement of uniformity and adhesion of the film, reminiscent of previous works using PEG to improve mechanical properties, uniformity, and adhesion on substrates (Fig. 15d-g) [388, 395]. The use of silk fibroin thus opens the possibilities of a fully biosourced, protein-based alternative to improve these properties.

Besides the co-assembly route to manufacture composite CNC-based materials, several post-treatments applied to plain CNC films have been also investigated to design original functionalities. Among them, one simple approach consists of immersing a CNC film in a prepolymer solution to produce a polymer-CNC composite. This strategy was used by Espinha et al. [396] to obtain a laminated structure with shape-memory properties. A more interesting and recent example was proposed by Boott et al. [397], whereby a CNC film was swollen and infiltrated with a prepolymer to form a mechano-chromic elastomer (Fig. 16). Importantly, the infiltrated CNC films were initially prepared in the presence of 25%w/w glucose to facilitate later the infiltration of dimethylsulfoxide (DMSO), while specific slow assembly conditions were used to minimize the pitch to compensate for the red-shifting effect of the addition of the infiltrate [398]. After a first immersion in DMSO, two sequential soaking treatments were applied, first of 2,2'-azobis(2-methylpropionitrile) (AIBN)/DMSO solution, and then with the monomer solution (containing ethyl acrylate, 2-hydroxyethyl acrylate and AIBN). The resulting composite elastomer presented clear mechano-chromic behavior upon stretching, visible in ambient light and solely caused by the compression of the pitch in the direction perpendicular to the applied stretch (and not simply relying on birefringence-induced Newton colors like in many other existing reports). A recent follow-up from the same authors proposed the fabrication of similar
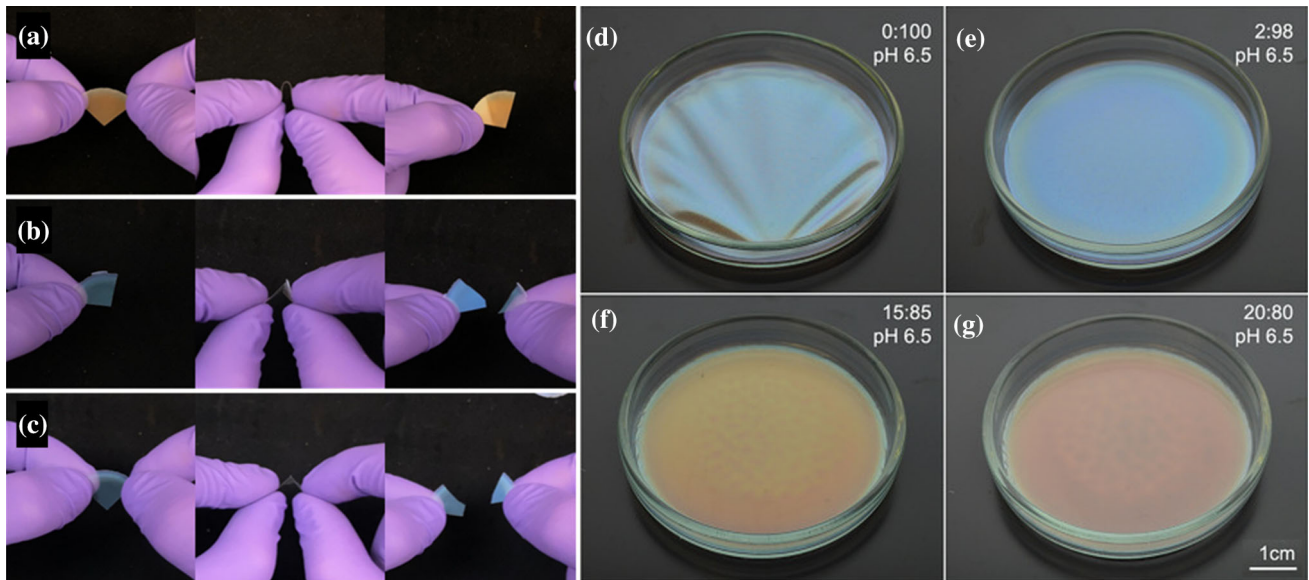
Figure 15 a–c Photographs of CNC/L-HPC composite films before (left), during (middle), and after (right) bending. **a** CNC/L-HPC 50/50 w/w, **b** CNC/L-HPC 80/20 w/w, and **c** CNC/L-HPC 100/0 w/w. (**a–c**) Reprinted from [389] with permission from The American Chemical Society (Copyright American Chemical Society, 2020). **d–g** Macroscopic photographs of silk fibroin (SF) and CNC nanocomposites films obtained by casting suspensions of increasing SF:CNC v/v ratios: (D) 0:100, (E) 2:98, (F) 15:85, (G) 20:80. Reproduced from [391] under the terms of the CC-BY 4.0 license.

elastomers with additional shape-memory properties [399].

Upscaling strategies

The fabrication of CNC-based photonic materials usually involves laboratory scale processes (*e.g.*, small and variable batches, slow processes, casting in Petri dishes) that do not easily translate to the industrial scale, limiting the applicability of CNC-based optical materials in end products.

The use of a roll-to-roll (R2R) approach to deposit CNCs into films has been proposed in the past but without any structural color [400, 401]. The high throughput that is usually desirable makes any fast deposition incompatible with the formation of a cholesteric order; a reduced time suggests a high starting CNC concentration incompatible with a fast colloidal dynamic, and the resulting high shear applied near the slot-die aligns the CNCs in an achiral nematic film [400]. A significant step forward has been made recently by Droguet et al. [402] using R2R deposition to produce several meter-long CNC-based photonic films (Fig. 17a). In this work, a commercially available CNC source was employed (University of Maine Process Development Center) and simple pre-treatments were applied, involving

tip sonication and fractionation. The starting suspension was diluted from *ca* 12%w/w down to 6%w/w and sonicated, after which it was kept at rest until a macro-phase separation led to an upper isotropic phase and a lower cholesteric phase. The upper phase was discarded, and only the cholesteric phase, containing overall longer CNC particles, was deposited on a R2R to reduce the self-assembly time [398, 403, 404]. To reduce further the self-assembly time, the deposited CNC suspension was slowly translated through an in-line hot air dryer ($T = 20 - 60$ °C) at an effective speed of 0.2 mm s^{-1}, allowing the deposited film to be fully dry about a meter and a half from the suspension depositing slot-die, effectively reducing the self-assembly times from days to only a few hours.

The resulting film successfully demonstrated its relevance as a 100%-cellulose water-stable interference pigment after moderate heat treatment, grinding and size-sorting.

Other interesting strategies involve confinement in droplets, either in sessile drops or in water-in-oil (w/o) emulsions. In the first case, selective dewetting was employed to deposit a CNC suspension onto hydrophilic spots with slow evaporation under an oil layer, leading to nearly perfect alignment, without any color distortion as usually caused by the coffee ring
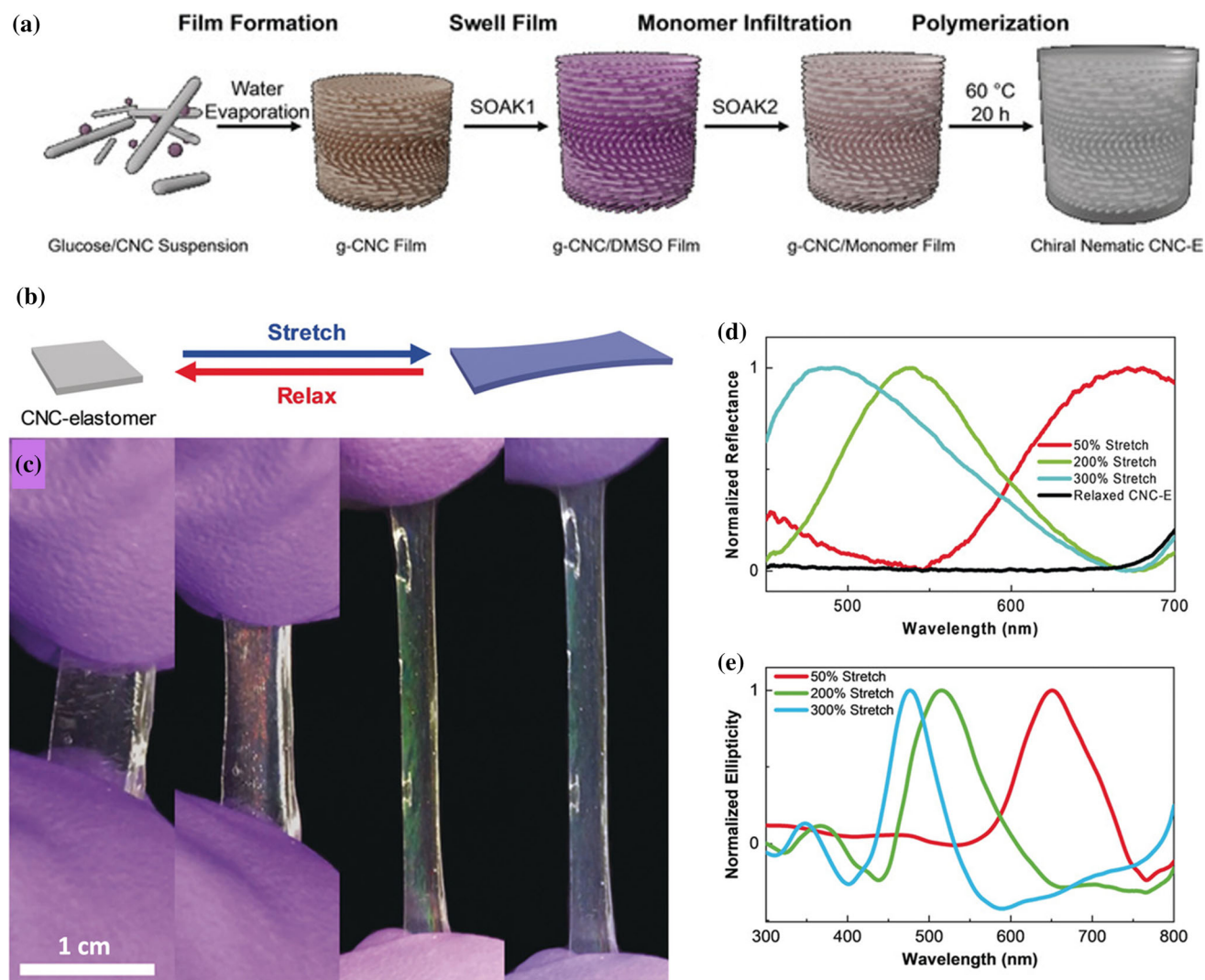
Figure 16 Illustration of CNC-based photonic elastomers prepared by impregnation of a CNC film. **a** preparation, **b** stretching direction **c** mechano-chromic behavior in ambient light (no polarizers) **d** Reflectance and **e** ellipticity. Adapted from [397] under the terms of the CC-BY 4.0 license.

stain (Fig. 17b) [405]. While the self-assembly then takes several days, the order is achieved within half an hour of the deposition, and a much faster assembly is achievable if the drying is completed in air. In the second case, w/o emulsions offer a substrate-free route to self-assembly, whereby the local alignment of the cholesteric is templated by the emulsion droplets themselves, and the need for casting on large surfaces when upscaling is suppressed. While this option was first explored using lab-made CNCs and gave too large a pitch to reflect in the visible [406], the recent optimization of the suspension formulation and exploitation of buckling upon further particle contraction led to a sufficient pitch compression to bring the photonic properties into the visible range

and generate blue, green or red microparticles only made from cellulose (Fig. 17c) [407]. Interestingly, the blue and green hues were obtained by additional desiccation treatment, either via exposure to heat or to polar solvents (isopropanol for green, methanol for blue).

Overall, these alternative strategies open significant routes to industrial manufacturing of CNC-based photonic materials, each of them with specific advantages and disadvantages to adapt to the growing possibilities of co-assembly or post-treatments already available to develop the next generation of CNC-based optical materials.

Figure 17 Photonic CNC films made by exploring different upscaling geometries: **a** via roll-to-roll (R2R), and then converted into glitter after pealing, heating, and grinding (image courtesy of Benjamin E. Droguet); **b** by confined self-assembly into sessile droplets under an oil layer (adapted from [403] under a CC-BY license); **c** by water-in-oil emulsion and additional solvent treatments (images courtesy of Tianheng H. Zhao and Richard M. Parker).
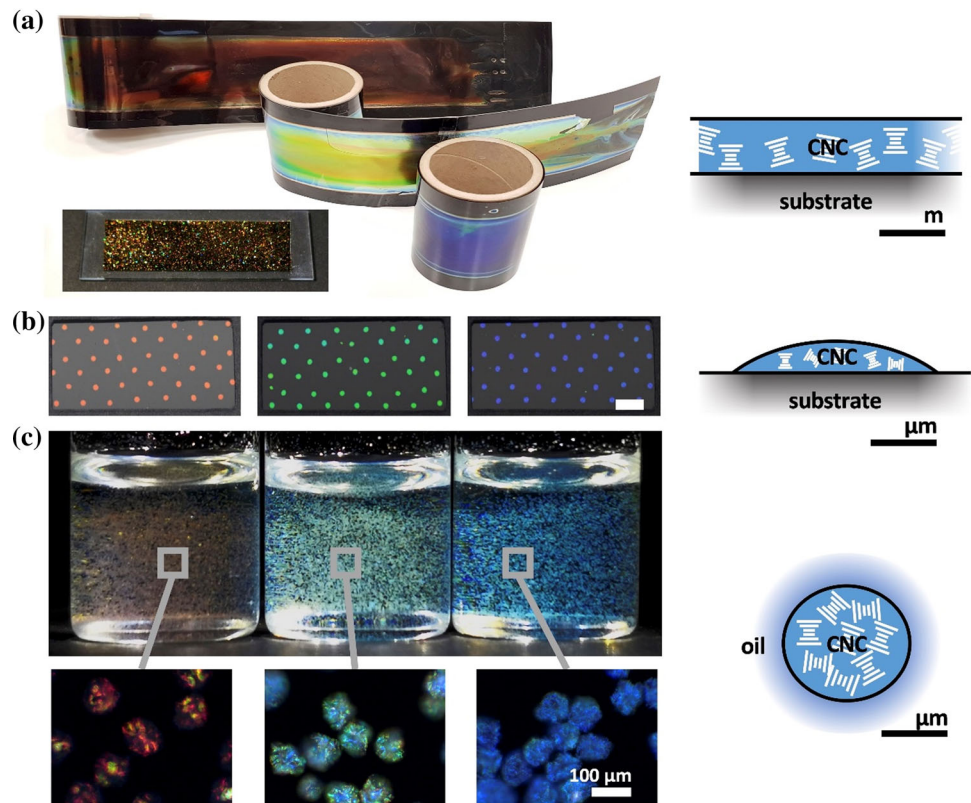
Introduction to energy applications of nanocellulose

Solar cells have the capacity of converting inexhaustible and renewable solar energy into clean electricity and supply modern society with clean energy that promotes the carbon neutrality and sustainable development of our planet [408, 409]. However, at present, only a small market share has been obtained for the electricity produced from solar cells. The widespread application of solar cells in our daily life is rooted in their cost reduction, environmentally friendliness, flexibility, and superior power conversion efficiency (PCE). Incorporation of cellulose paper into solar cells is an alternative solution to address the above issues [377, 410–413]. Solar cells have been demonstrated on common paper for more than fifteen years [414]. However, common cellulose paper has proven to be a poor substrate candidate due to its rough surface, porous structure, and impurities [415], which results in a complicated production procedure and a limited PCE (<1%).

Apart from energy conversion applications like solar cells, nanocellulose can also serve as the basis for the next-generation of sustainable energy storage technologies including supercapacitors and batteries [416]. Since many components of commercial energy storage devices like separators and carbon electrodes are fabricated from fossil fuels, their cost increases year by year with the overutilization of non-renewable raw materials [417]. However, the development of nanocellulose provides a potential but effective scheme to address this issue, where it can be used as the separator or the precursor material for carbon electrodes with enhanced electrochemical performance as well as sustainability [418]. In the near future, all-cellulose-based energy storage devices will be able to play an important role not only for energy conversion like solar cells, but also for energy storage like supercapacitors and batteries.

Zhiqiang Fang (South China University of Technology), Guanhui Li (South China University of Technology), and Liangbing Hu (The University of Maryland): highly transparent nanocellulose film with tailored optical haze for solar cells

By tuning the assembly and type of CNMs it is possible to fully control light transport so to obtain from

transparent to haze to highly scattering materials [419]. Since the first report of transparent nanocellulose films (also named 'cellulose nanopaper') [420], they have emerged as a promising flexible and green substrate candidate for solar cells. This is because of their better optical, mechanical, and barrier properties and surface smoothness compared with standard paper [421, 422]. Hu et al. [423] initially demonstrated the direct fabrication of organic solar cells (OSCs) on a CNF film substrate that showed a PCE of 0.4% (Fig. 18a), and the corresponding I-V curve is displayed in Fig. 18b. Despite the poor device performance, this work first indicated that a CNF film was an attractive substrate for mechanically supporting OSCs. Meanwhile, the same group proposed an optical haze for a transparent CNF film (Fig. 18c & d) and predicted its potential application in solar cells as a functional light management layer.

Previous work had focused on the uses of nanocellulose films as a substrate material for solar cells. A variety of strategies were adopted to enhance the PCE of solar cells on nanocellulose film substrates. These have included the use of CNCs [424] and a mixture with other materials (such as acrylic resin and cellulose derivatives) [425], surface

modifications of nanocellulose film [424], water-free manufacturing techniques [426], the use of novel active materials [427], and exquisite design of the cell configurations [427]. However, at present, the PCE of solar cells on nanocellulose film is still less than 5%, which is much lower than that of devices fabricated on plastic films; these indicate a PCE of over 21% on a laboratory scale [428].

To expedite the practical applications of solar cells on nanocellulose film, constant improvement in their performance should be given high priority. Therefore, future endeavor should focus on rationally engineering barrier properties, water resistance, weather durability, and surface roughness of the order of only a few nanometers over surface areas in the millimeter or even centimeter range. For instance, the mechanical isolation of CNFs from the cell wall of natural cellulose fibers produced microscale fibril bundles and debris in an aqueous suspension, thus increasing the surface roughness of the substrate, significantly deteriorating the device's performance, or even causing device failure.

Transparent nanocellulose film with high optical haze can go beyond the mechanically supporting substrate application and is becoming a functional

Figure 18 **a** OSCs on CNF film and their I-V curve (**b**). **c** The images can be clearly observed when transparent CNF film closely contacts with it, indicating high optical transparency. **d** The underneath images become invisible when the same CNF film is at a distance of 2 inches, suggesting high optical haze [423]. Reprinted with permission from [423] with permission from The Royal Society of Chemistry. (Copyright 2013, Royal Society of Chemistry).
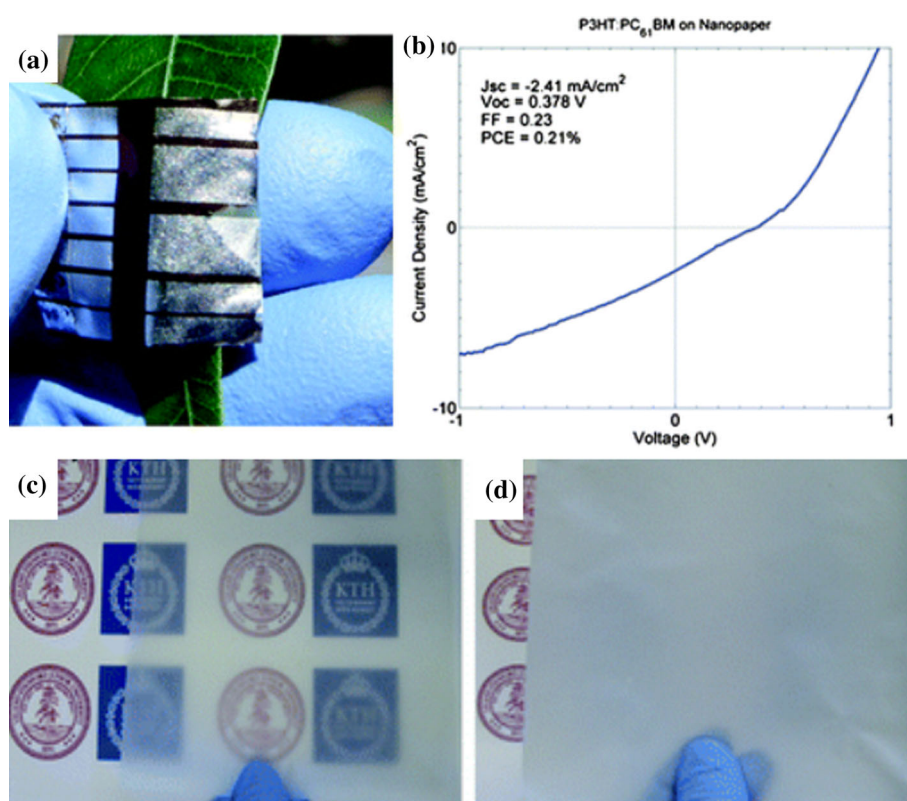
Figure 19 **a** Schematic showing the light scattering behavior of a transparent nanocellulose film. **b** Visual appearance and **c** light scattering behavior of water, purified CNF dispersion, and original CNF dispersion (from left to right). **d** AFM imaging showing the morphologies of original CNFs. Micro-sized fibril bundles and debris are marked with red circles [423, 429] Reproduced from [429] with permission from The American Chemical Society (Copyright 2017, American Chemical Society).
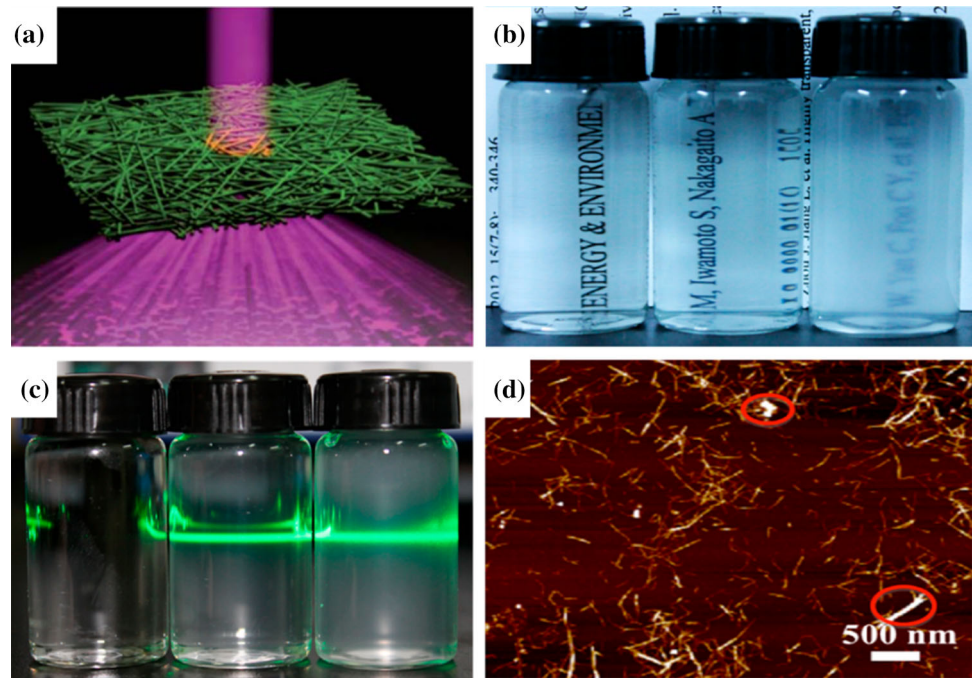
light management layer for solar cells. Generally, high transparency and high transmission haze (light scattering) are mutually exclusive. However, nanocellulose films not only exhibit a ∼90% transparency, but have also showed forward built-in light scattering behavior (Fig. 18a) [423]. These specific optical properties have allowed nanocellulose films to manipulate the propagation direction of transmitted light, which has extended applications toward solar cells as advanced light management layers to improve the efficiencies of light coupling into devices.

The interactions of visible light with nanocellulose plays a significant role in the optical properties of nanocellulose film. Theoretically, visible light can easily pass through nanocellulose films with negligible light scattering because the fibril diameters (3.5 ∼ 30 nm) are much smaller than the wavelength (400-900 nm) of visible light. Therefore, nanocellulose films can display a transparent and clear appearance. However, optical haze is observed in most reported nanocellulose films (Fig. 18c&d). This abnormal phenomenon is primarily due to the existence of scattering particles (*e.g.*, microscale fibril bundles and debris) derived from the incomplete mechanical homogenization of wood fibers.

The presence of micro-sized scattering elements gives rise to refractive index inhomogeneities and increased surface roughness of the as-prepared nanocellulose films, thereby increasing the scattering efficiency and finally indicating an improvement of optical haze. According to Mie theory, when the scattering particles have a diameter equal to or larger than the wavelength of the incident light, most of the transmitted light will be scattered along the incident direction.

Transparent nanocellulose films show forward scattering of light (Fig. 19a). As we can see from Fig. 19b, c and d, the original CNF suspension (rightmost image in Fig. 19b) has a hazy appearance due to the occurrence of micro-sized fibril bundles and debris (Fig. 19d) serving as scattering particles to enhance the transmission haze (Fig. 19c). However, after removing these scattering materials by a centrifugation procedure, the nanocellulose suspension indicated a clear appearance and the green laser could propagate through the suspension with a narrow-angle scattering (middle vials shown in Fig. 19b and c) [429]. Purified nanocellulose showed a uniform distribution of fibril diameters at a nanoscale level, which contributed to the reduced inhomogeneities and surface roughness of the nanocellulose film that suppressed wide-angle light scattering.

Taking inspiration from previous works, Fang et al. [430] reported a highly transparent nanostructured paper with a high haze using micro-/nanocellulose, exhibiting a transparency of >90% and a transmission haze of ∼60% at 550 nm (Fig. 20a). Through 2,2,6,6-
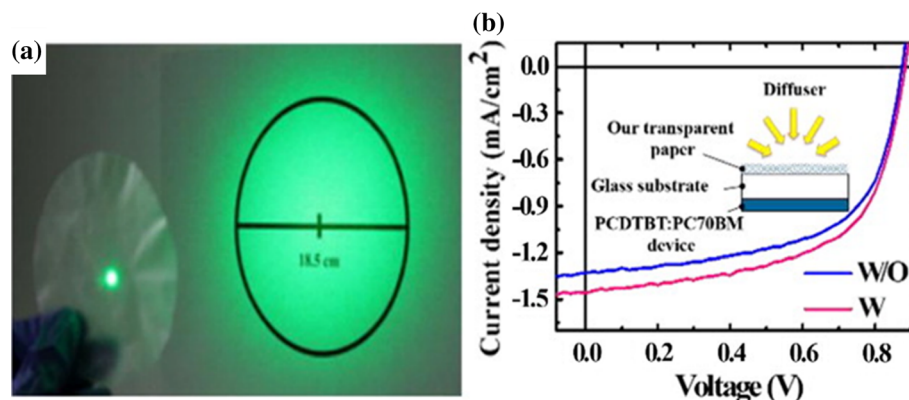
tetramethylpiperidine-1-oxyl (TEMPO) oxidization of wood fibers, micro-/nanocellulose was obtained, where the microscale cellulose fibers functioned as a light scattering source to increase the optical haze while the nanocellulose worked as a filling matrix to improve the transparency. They also demonstrated the use of this nanostructured paper in organic solar cells as a light management layer and a 10% increase of PCE was achieved (Fig. 20b). Since then, microscale cellulose fibers have been the main raw material to prepare highly transparent cellulose film with high haze by bottom-up methods (*e.g.*, filtration [431], impregnation [432, 433], and surface dissolution of fibers) due to their strong light scattering behavior [434].

In conclusion, nanocellulose obtained from mechanical isolation inevitably produces scattering particles. A transparent and hazy film with microscale surface roughness was obtained using the original nanocellulose as a raw material, which can serve as a functional layer for the improvement in the PCE of solar cells. Nanocellulose film without microscale particles (*e.g.*, fibril bundles and debris) is a desired transparent and clear substrate with nanoscale surface roughness for solar cells. Despite much work being devoted to improving the properties of nanocellulose films, their use in solar cells is still in its early stages and is not ready for practical applications. In addition, in comparison with nanocellulose, microscale cellulose fibers are a much more suitable starting material to prepare highly transparent films with high transmission haze for solar cells as a light management layer due to their stronger light scattering behavior.

Zhen Xu and Maria-Magdalena Titirici (Imperial College London, UK), Jing Wang and Stephen Eichhorn (University of Bristol, UK), Chaoji Chen (Wuhan University, China) and Liangbing Hu (University of Maryland, USA): nanocellulose as basis for energy storage

Rechargeable batteries and supercapacitors are the two most popular types of electrochemical energy storage devices, and they have attracted increasing attention and enjoyed great success both in academic research and commercialization over the past few decades [416, 435–437]. With a high aspect ratio, and abundant surface functional groups to interact with ions, nanocellulose is an ideal starting material for energy storage devices based on ion transport [438, 439]. It has been widely investigated as various important functional components in batteries and supercapacitors, such as current collectors, binders, electrolytes/separators, and electrodes [439–442]. The diverse structural tunability of nanocellulose (*e.g.*, pores, fibril orientation, fibril diameter/length, surface functional groups, surface charge, surface energy, and surface wettability, degree of crystallinity, crystal phase structure, etc.) is particularly attractive for the design of high-performance functional components of batteries and supercapacitors. A key design principle is to meet the specific parameters depending on the functions of each component of the device. For example, improving the electrical conductivity of nanocellulose is critical for current collector applications, while separators must be electrically insulating. The combination of a wide potential window, high ionic conductivity and good mechanical properties are critical for developing

high-performance nanocellulose-based electrolytes and separators.

As a common component in batteries and supercapacitors, the properties of binders directly affect the properties of electrodes, particularly their mechanical and electrochemical performances [441–443]. Polyvinylidene fluoride (PVDF) has been one of the most widely used binders in the most recent batteries and supercapacitors. This material, however, requires the use of volatile and toxic/hazardous solvents for processing. Alternatively, biomass-based binders such as nanocellulose, and its derivatives, are 'greener' and safer to use, and therefore are attracting increasing interest from the academic and industrial communities [444]. For example, carboxymethyl cellulose (CMC), as a derivative of the linear polymeric cellulose with the substitution of hydroxyl groups for anionic carboxymethyl groups, is widely used as a water-soluble binder in both the cathodes and anodes of batteries and supercapacitors [441].

Nanocellulose itself can also be used as binder for both cathode and anode electrodes. The high aspect ratio and tunable rheological properties of nanocellulose are desired for electrode manufacturing. Electroactive electrode particles can be wrapped by the high-aspect-ratio nanocellulose fibrils, forming a mechanically robust network. Moreover, at a finer scale, the abundant hydroxyl groups of nanocellulose fibrils can interact with the electroactive electrode particles, providing an excellent binding effect. Kuang et al. [445] demonstrated the excellent binding effect of nanocellulose (or cellulose nanofiber, CNF) in their recent work (Fig. 21). They first prepared a conductive CNF by mixing with carbon black (CB), which was then used as a binder to 'glue' the electroactive electrode (lithium iron phosphate, LFP) particles, forming a 3D interconnected porous foam (Fig. 21a). This 3D interconnected porous foam was further pressed to increase the density of the nanopaper electrode (Fig. 21b). A TEM image of the nanopaper showed that the LFP particles were glued by the CNF/CB network, which provided pathways for ion and electron transport (Fig. 21c). The nanopaper electrode demonstrated not only improved areal capacity over a conventional LFP electrode with similar thickness, but also excellent flexibility (Fig. 21d and e). Alternatively, nanocellulose can also be used as a viscosifier to prepare printable inks for printed electrode fabrication owing to its unique characteristics such as rich hydroxyl groups, negative zeta potential, one-dimensional (1D) fibrous structure, and chemical functionalities [440, 446, 447]. In these printed electrodes, nanocellulose not only acts as a viscosifier during the printing process, but also as a binder to 'glue' the electroactive electrode particles in the dried state.

Nanocellulose-based separators have been widely studied and developed. For instance, mesoporous CNC membranes with high surface areas were prepared by Gonçalves et al. [448] as the separator for environmentally safer lithium-ion batteries (Fig. 22). The obtained nanocellulose-based separators exhibited outstanding wettability when soaked with conventional ester-based and ionic liquid-based electrolytes. Meanwhile, the three-dimensional porous structures formed by nanocellulose can shorten the ion diffusion pathway, thus obtaining a competitive ionic conductivity of 2.7 mS cm^{-1}. Good compatibility of the interface between the electrode and electrolyte can also be obtained, in comparison with commercial separators like glass fiber or polypropylene (PP)/polyethylene (PE) membranes. Coupled with the LiFePO$_4$ cathode, the assembled lithium-ion batteries can deliver a specific capacity of 122 mAh g^{-1} at a 0.5 C and an excellent rate capacity of 85 mAh g^{-1} at 2.0 C, indicating the important role of the three-dimensional porous structures formed by nanocellulose. Meanwhile, the mechanical properties of nanocellulose-based separators are also superior to those of commercial separators according to the literature. In addition, there have been some companies like the Nippon Kodoshi corporation who have fabricated battery separators made from 100% cellulose which exhibit good heat resistance, exceptional porosity, and high liquid retention rates [449]. Therefore, by replacing conventional materials with nanocellulose-based separators, the development of real eco-friendly energy storage devices could be achieved in the near future.

As well as separators, nanocellulose can also be used as flexible substrates. Combined with a coating of conductive nanomaterials (carbon nanotubes, graphene, etc.) on the nanocellulose, free-standing electrodes can be obtained for energy storage devices such as supercapacitors [450].

When employed as the precursors, nanocellulose can also be converted into sustainable carbon materials for next-generation energy storage devices as well. For example, Li et al. [451] prepared hollow hard carbon microtubes derived from renewable
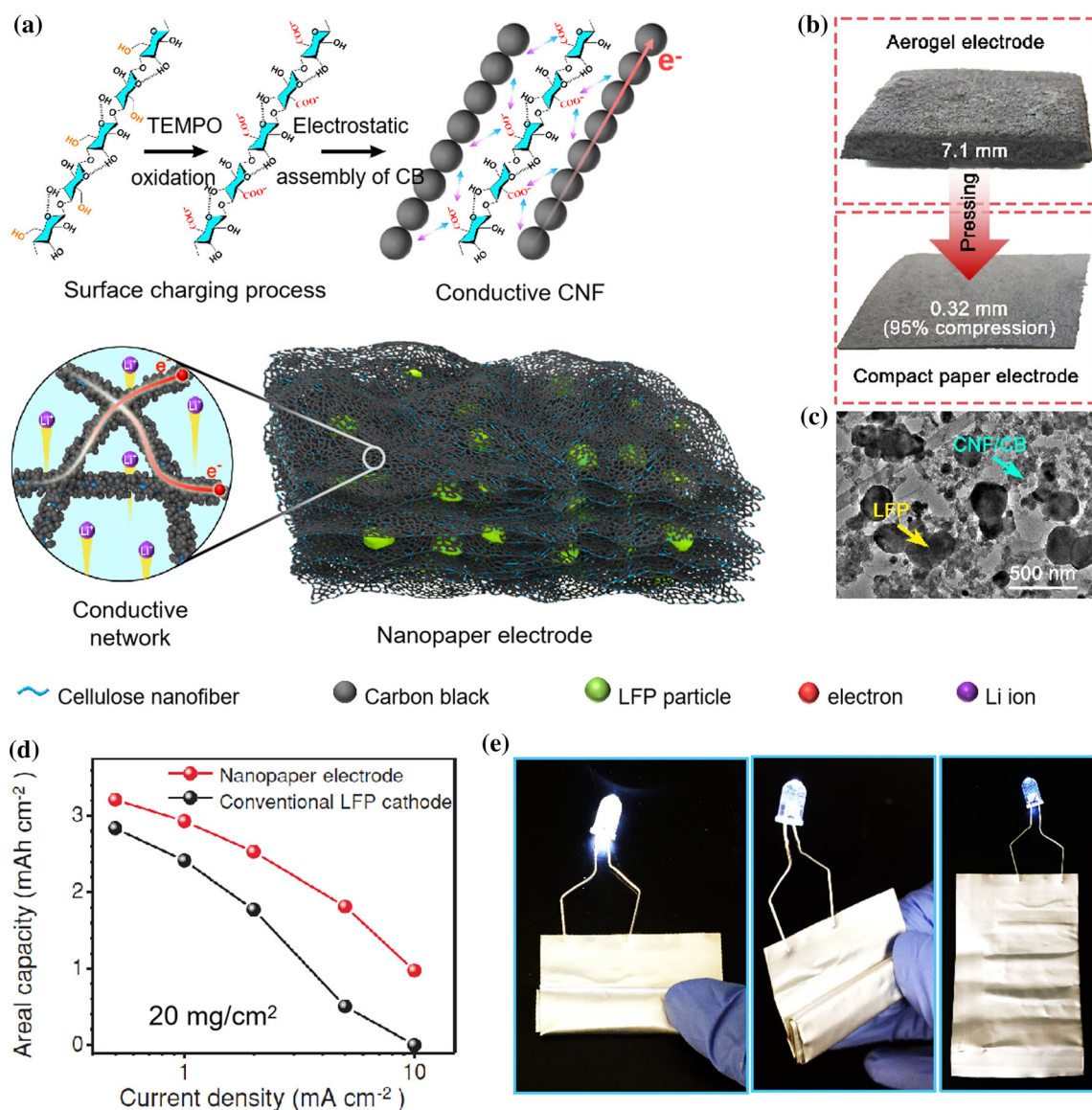
Figure 21 A flexible nanopaper electrode using nanocellulose (also called cellulose nanofiber, CNF) as binder. **a** Schematics illustrating the hierarchical network structure of the nanopaper electrode based on the CNF/CB composite conductive percolation network. The zoom-in shows the decoupled ion/electron transport pathways through the electrode. **b** Photographs of the free-standing nanopaper electrode with 40 mg cm^{-2} LFP loading and high compressibility. **c** TEM image showing the interconnected network of the nanopaper electrode. **d** Areal capacity–current density plots of the nanopaper electrode and conventional LFP cathode. **e** Photographs illustrating the foldability of the pouch cell consisting of the nanopaper electrode as the cathode and Li metal on copper foil as the anode. Reproduced from [445] with permission from John Wiley and Sons (Copyright John Wiley and Sons, 2018).

cotton as high-performance anode materials for the next-generation of sodium-ion batteries, where the resulting hard carbon anodes at 1300 °C delivered an outstanding sodium-ion capacity of 315 mAh g^{-1} at 0.1 C and a good rate capability as a result of their unique turbostratic structures. In addition, Xu et al. [452] developed sustainable hard carbons from CNCs

at a lower carbonization temperature of 1000 °C for use in sodium-ion batteries. The low-cost hard carbon anodes derived from nanocellulose displayed a reversible specific capacity of 256.9 mAh g^{-1} at a current density of 0.1 A g^{-1}, which was superior to the hard carbons obtained from cellulose microfibers at the same carbonization temperature because the
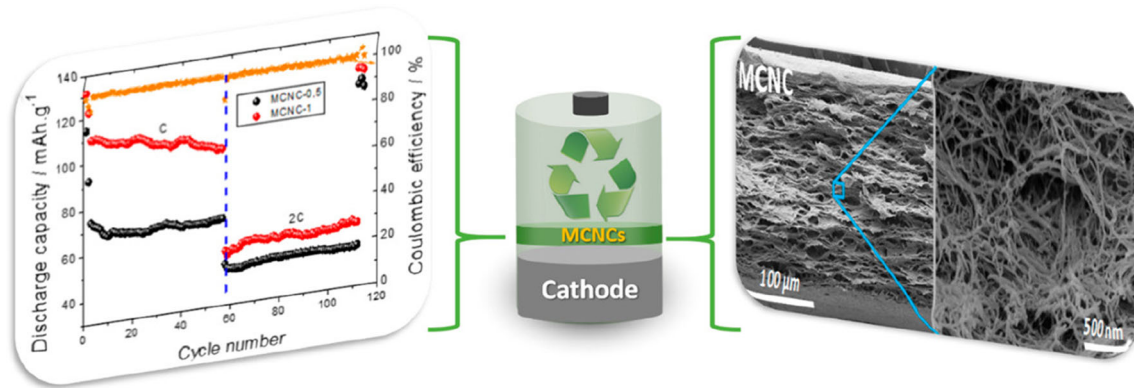
Figure 22 A scanning electron microscopy (SEM) image of mesoporous cellulose nanocrystal (MCNC) membranes and the electrochemical performance of obtained lithium-ion batteries using nanocellulose-based separators [448]. Reproduced from [448] with permission from John Wiley and Sons (Copyright John Wiley and Sons, 2017).

layer-by-layer self-assembly of CNCs during the drying process formed a relatively low surface area to suppress the formation of a solid electrolyte interphase (SEI). The sodium-ion capacity of the hard carbons can compete with commercial graphite anodes for lithium-ion storage by consuming less energy. Sodium-ion batteries have also widely aroused interest from the battery community as promising successors to lithium-ion batteries for grid energy storage based on abundant sodium resources [453]. Therefore, nanocellulose-derived sustainable hard carbons perfectly meet the environmental and electrochemical requirements of eco-friendly sodium-ion batteries.

Meanwhile, all-cellulose-based devices have also been achieved inspired by the hierarchical building blocks of natural cellulose (Fig. 23) [452]. By coupling with the cellulose microfiber-derived porous carbon cathodes using the hydrothermal process and subsequent chemical activation, an all-cellulose-based sodium-ion hybrid capacitor has been assembled [452]. This uses a modified cellulose-based gel electrolyte instead of using oil-based feedstocks, and its capacity reached 58.2 mAh g^{-1} at 0.2 A g^{-1} [452]. The energy density of this all-cellulose-based sodium-ion capacitor reached 139 Wh kg^{-1} at a power density of 478 W kg^{-1}, which can bridge the gap between high-energy batteries and high-power supercapacitors [452].

As we can see, great efforts have been made to develop the next generation of sustainable energy storage devices based on nanocellulose. There are still some challenges that remain to be resolved. For the commercialization of energy storage devices

based on nanocellulose, a large-scale production platform is desirable to be established with decreased energy consumption [454]. In the meantime, how to rationally control the chemical and physical properties of nanocellulose to further enhance the electrochemical performance of devices needs to be considered at a scaled-up level [454]. In addition, most of the development of nanocellulose research in batteries and supercapacitors in the past few decades has been limited to sizes no smaller than the elementary fibril level, while the fundamental science and technologies at the molecular level of nanocellulose deserve further exploration [455]. All in all, the emerging applications of nanocellulose are of obvious benefits to energy storage toward carbon neutrality, but more efforts are needed to overcome existing shortcomings of technologies enabled by nanocellulose.

Conclusions

A review of the use of nanocellulose fibers in a variety of potential applications has been presented, targeting specifically health, water purification, composites and energy. The world needs to move to more sustainable choices for its materials, but not only that it needs to embed sustainability across all sectors of the economy. Nanocellulose has the potential to contribute to sustainability, but there needs to be careful consideration about the ways in which it is used in everyday applications, and there are hurdles to overcome in the embedded energy costs for its production. This review has
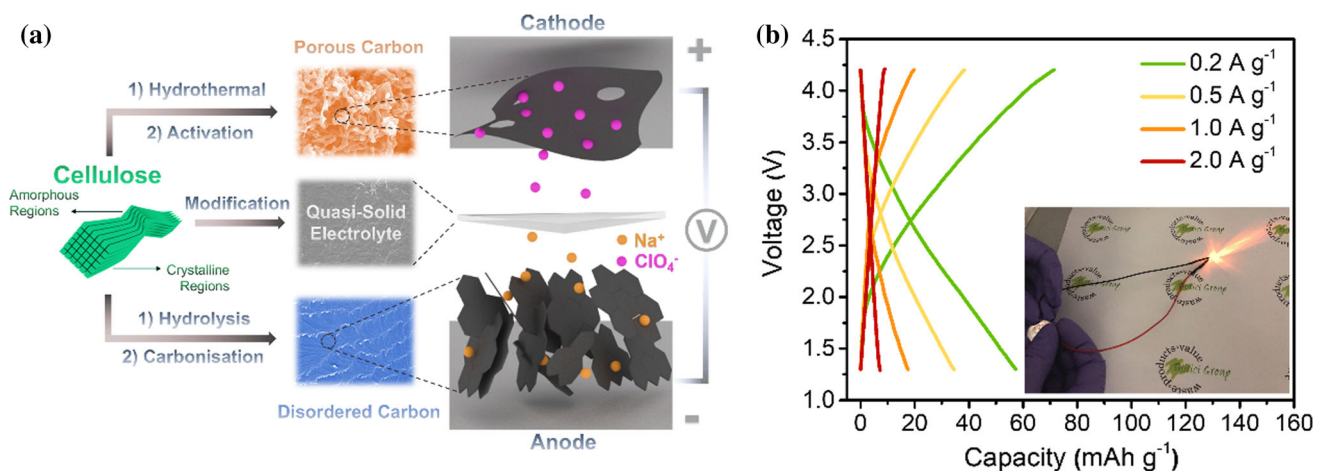
Figure 23 a Schematic illustration of electrodes and electrolytes inspired by hierarchical building blocks of cellulose for sodium-ion capacitors; **b** galvanostatic charge/discharge (GCD) curves of all-cellulose-based capacitors [452]. Reproduced from [452] with permission from John Wiley and Sons (Copyright John Wiley and Sons, 2019).

demonstrated the use of CNMs for the directed growth of tissues, showing that both chemical and topological cues from these materials could be used to judiciously design bespoke tissue for implantation. One of the most common forms of materials for solid dosage pharmaceuticals is cellulose, in the form of microcrystalline cellulose. However, it has been demonstrated that nanocellulose is not just useful for controlled release in a solid dosage format, but also for transdermal and implantable systems. There is potential for nanocellulose to make inroads into commercial products since the barriers of cost are not so restrictive in such applications.

Water purification, and the supply of clean water, is critical to much of the world's population. It has been shown that nanocellulose can be very useful in this respect, and with some chemical modification can help to clean contaminated water. The development of 'smart' aerogel materials that can both clean oil-contaminated water, but also provide a means to remove the materials after use using magnetic properties has great potential for real-world applications. We have also shown that nanocellulose also has the potential to address other forms of water contamination, such as desalination, removal of dyes, and heavy metals.

Polymer composites remain a topic of great interest with respect to nanocellulose. Perhaps one of the most exciting developments in recent times has been the ability to use the inherent nanostructure of wood, combined with suitable resins, to make transparent materials that could have tremendous benefits for

housing and other buildings. These types of application, where carbon can effectively be buried in a building, while also providing a critical function to enhance living, have enormous potential to contribute to sustainability. In terms of the industrial exploitation of composites, it has been made clear that for any advances to be made there are critical issues around dispersion and mixing that need to be addressed. Several in situ methods for the fibrillation of cellulose have been introduced, but much work is required to address mechanical performance. One way to overcome the need to mix the nanocellulose in a polymer is to use a pre-form. Bacterial cellulose networks have been demonstrated to be useful in this respect, although work needs to be done to control the basis weight of the networks, thereby their porosity and the achievable resin penetration. The barrier of cost of the nanocelluloses, over other materials such as talc and conventional fibers, might not be such an issue if the target application is carefully chosen. In niche applications, such as structural colored films, the added functional benefit and the ability to now apply roll-to-roll methods for production have real potential, particularly for packaging applications.

Finally, nanocellulose has real potential for energy storage devices: both as supercapacitors and batteries. Here cost is key, but the potential to make small devices with a high-power delivery, competing with conventional materials, is very much a real prospect. In this way nanocellulose could truly contribute to the development of new sustainable battery systems,

and also with new developments such as the use of sodium-ion-based systems. The use of the material for the anode and separators in the latter has been demonstrated. Large-scale production of such devices is still a barrier for entry into industrial products, but we are close to solutions to these issues, perhaps drawing on the roll-to-roll production methods used for other applications. When it comes to solar cell applications, the efficiency of the devices made with nanocellulose is still not competitive. Nevertheless, the forward scattering provided by nanocellulose fiber networks makes these interesting materials which could be implemented in low-cost devices.

In conclusion then, much has developed in the field of nanocellulose in the last 10 years since the previous review was published. There are now several large-scale manufacturers of materials (both fibrils and nanocrystals), and so the scaled-up production is no longer an issue. What is required now are for applications to be realized, and this can only be aided by a continued use of basic research to underpin these developments.

Open Access

References

[1] O'Sullivan AC (1997) Cellulose: the structure slowly unravels. Cellulose 4(3):173–207. https://doi.org/10.1023/A:1018431705579

[2] Eichhorn SJ, Dufresne A, Aranguren M, Marcovich NE, Capadona JR, Rowan SJ, Weder C, Thielemans W, Roman M, Renneckar S, Gindl W, Veigel S, Keckes J, Yano H, Abe K, Nogi M, Nakagaito AN, Mangalam A, Simonsen J, Benight AS, Bismarck A, Berglund LA, Peijs T (2010) Review: current international research into cellulose nanofibres and nanocomposites. J Mater Sci 45(1):1–33. https://doi.org/10.1007/s10853-009-3874-0

[3] French AD (2017) Glucose, not cellobiose, is the repeating unit of cellulose and why that is important. Cellulose 24 (11):4605–4609. https://doi.org/10.1007/s10570-017-1450-3

[4] Khadem HE (1988) Carbohydrate chemistry: monosaccharides and their oligomers. Academic Press Ltd., New York

[5] Atalla RH, Vanderhart DL (1984) Native cellulose—a composite of 2 distinct crystalline forms. Science 223 (4633):283–285. https://doi.org/10.1126/science.223.4633.283

[6] Nishiyama Y, Langan P, Chanzy H (2002) Crystal structure and hydrogen-bonding system in cellulose 1 beta from synchrotron X-ray and neutron fiber diffraction. J Am Chem Soc 124(31):9074–9082. https://doi.org/10.1021/ja0257319

[7] Nishiyama Y, Sugiyama J, Chanzy H, Langan P (2003) Crystal structure and hydrogen bonding system in cellulose 1(alpha), from synchrotron X-ray and neutron fiber diffraction. J Am Chem Soc 125(47):14300–14306. https://doi.org/10.1021/ja037055w

[8] Lindman B, Karlstrom G, Stigsson L (2010) On the mechanism of dissolution of cellulose. J Mol Liq 156 (1):76–81. https://doi.org/10.1016/j.molliq.2010.04.016

[9] de Andrade P, Munoz-Garcia JC, Pergolizzi G, Gabrielli V, Nepogodiev SA, Iuga D, Fabian L, Nigmatullin R, Johns MA, Harniman R, Eichhorn SJ, Angulo J, Khimyak YZ, Field RA (2021) Chemoenzymatic synthesis of fluorinated cellodextrins identifies a new allomorph for cellulose-like materials**. Chem Eur J 27(4):1374–1382. https://doi.org/10.1002/chem.202003604

[10] Nigmatullin R, de Andrade P, Harniman R, Field RA, Eichhorn SJ (2021) Postsynthesis self- and coassembly of enzymatically produced fluorinated cellodextrins and cellulose nanocrystals. Langmuir 37(30):9215–9221. https://doi.org/10.1021/acs.langmuir.1c01389

[11] Kvien I, Tanem BS, Oksman K (2005) Characterization of cellulose whiskers and their nanocomposites by atomic force and electron microscopy. Biomacromol 6(6):3160–3165. https://doi.org/10.1021/bm050479t

[12] Portela R, Leal CR, Almeida PL, Sobral RG (2019) Bacterial cellulose: a versatile biopolymer for wound dressing

applications. Microb Biotechnol 12(4):586–610. https://doi.org/10.1111/1751-7915.13392

[13] Vanderfleet OM, Cranston ED (2021) Production routes to tailor the performance of cellulose nanocrystals. Nat Rev Mater 6(2):124–144. https://doi.org/10.1038/s41578-020-00239-y

[14] Siro I, Plackett D (2010) Microfibrillated cellulose and new nanocomposite materials: a review. Cellulose 17(3):459–494. https://doi.org/10.1007/s10570-010-9405-y

[15] Klemm D, Kramer F, Moritz S, Lindström T, Ankerfors M, Gray D, Dorris A (2011) Nanocelluloses: a new family of nature-based materials. Angew Chem Int Edn 50(24):5438–5466. https://doi.org/10.1002/anie.201001273

[16] Chen CJ, Kuang YD, Zhu SZ, Burgert I, Keplinger T, Gong A, Li T, Berglund L, Eichhorn SJ, Hu LB (2020) Structure-property-function relationships of natural and engineered wood. Nat Rev Mater 5(9):642–666. https://doi.org/10.1038/s41578-020-0195-z

[17] Charreau H, Cavallo E, Foresti ML (2020) Patents involving nanocellulose: Analysis of their evolution since 2010. Carbohyd Polym 237:116039. https://doi.org/10.1016/j.carbpol.2020.116039

[18] Foster EJ, Moon RJ, Agarwal UP, Bortner MJ, Bras J, Camarero-Espinosa S, Chan KJ, Clift MJD, Cranston ED, Eichhorn SJ, Fox DM, Hamad WY, Heux L, Jean B, Korey M, Nieh W, Ong KJ, Reid MS, Renneckar S, Roberts R, Shatkin JA, Simonsen J, Stinson-Bagby K, Wanasekara N, Youngblood J (2018) Current characterization methods for cellulose nanomaterials. Chem Soc Rev 47(8):2609–2679. https://doi.org/10.1039/c6cs00895j

[19] Nanotechnologies IT (2017) Nanotechnologies—standard terms and their definition for cellulose nanomaterial. https://www.iso.org/standard/68153.html

[20] Subhedar A, Bhadauria S, Ahankari S, Kargarzadeh H (2021) Nanocellulose in biomedical and biosensing applications: a review. Int J Biol Macromol 166:587–600. https://doi.org/10.1016/j.ijbiomac.2020.10.217

[21] Xue Y, Mou Z, Xiao H (2017) Nanocellulose as a sustainable biomass material: structure, properties, present status and future prospects in biomedical applications. Nanoscale 9(39):14758–14781. https://doi.org/10.1039/C7NR04994C

[22] Klemm D, Cranston ED, Fischer D, Gama M, Kedzior SA, Kralisch D, Kramer F, Kondo T, Lindstrom T, Nietzsche S, Petzold-Welcke K, Rauchfuss F (2018) Nanocellulose as a natural source for groundbreaking applications in materials science: today's state. Mater Today 21(7):720–748. https://doi.org/10.1016/j.mattod.2018.02.001

[23] Lin N, Dufresne A (2014) Nanocellulose in biomedicine: Current status and future prospect. Eur Polym J 59:302–325. https://doi.org/10.1016/j.eurpolymj.2014.07.025

[24] Salimi S, Sotudeh-Gharebagh R, Zarghami R, Chan SY, Yuen KH (2019) Production of nanocellulose and its applications in drug delivery: a critical review. ACS Sustain Chem Eng 7:15800–15827. https://doi.org/10.1021/acssuschemeng.9b02744

[25] Jorfi M, Foster EJ (2015) Recent advances in nanocellulose for biomedical applications. J Appl Polym Sci 132 (14):41719–41719. https://doi.org/10.1002/app.41719

[26] Tortorella S, Vetri Buratti V, Maturi M, Sambri L, Comes Franchini M, Locatelli E (2020) Surface-modified nanocellulose for application in biomedical engineering and nanomedicine: a review. Int J Nanomed 15:9909–9937. https://doi.org/10.2147/IJN.S266103

[27] Hou Y, Wang X, Yang J, Zhu R, Zhang Z, Li Y (2018) Development and biocompatibility evaluation of biodegradable bacterial cellulose as a novel peripheral nerve scaffold. J Biomed Mater Res Part A 106(5):1288–1298. https://doi.org/10.1002/jbm.a.36330

[28] Roman M, Haring AP, Bertucio TJ (2019) The growing merits and dwindling limitations of bacterial cellulose-based tissue engineering scaffolds. Curr Opin Chem Eng 24:98–106. https://doi.org/10.1016/j.coche.2019.03.006

[29] Hu Y, Catchmark JM (2011) In vitro biodegradability and mechanical properties of bioabsorbable bacterial cellulose incorporating cellulases. Acta Biomater 7(7):2835–2845. https://doi.org/10.1016/j.actbio.2011.03.028

[30] Osorio DA, Lee BEJ, Kwiecien JM, Wang X, Shahid I, Hurley AL, Cranston ED, Grandfield K (2019) Cross-linked cellulose nanocrystal aerogels as viable bone tissue scaffolds. Acta Biomater 87:152–165. https://doi.org/10.1016/j.actbio.2019.01.049

[31] Janmey PA, Miller RT (2011) Mechanisms of mechanical signaling in development and disease. J Cell Sci 124:9–18. https://doi.org/10.1242/jcs.071001

[32] Walma DAC, Yamada KM (2020) The extracellular matrix in development. Development 147:175596–175596. https://doi.org/10.1242/dev.175596

[33] Rozario T, DeSimone DW (2010) The extracellular matrix in development and morphogenesis: a dynamic view. Dev Biol 341(1):126–140. https://doi.org/10.1016/j.ydbio.2009.10.026

[34] Dugan JM, Collins RF, Gough JE, Eichhorn SJ (2013) Oriented surfaces of adsorbed cellulose nanowhiskers promote skeletal muscle myogenesis. Acta Biomater 9(1):4707–4715. https://doi.org/10.1016/j.actbio.2012.08.050

[35] Roman M, Dong S, Hirani A, Lee YW (2009) Cellulose nanocrystals for drug delivery. In: Polysaccharide materials:

performance by design, vol 1017. American Chemical Society doi:https://doi.org/10.1021/bk-2009-1017.ch004

[36] Mahmoud KA, Mena JA, Male KB, Hrapovic S, Kamen A, Luong JHT (2010) Effect of surface charge on the cellular uptake and cytotoxicity of fluorescent labeled cellulose nanocrystals. ACS Appl Mater Interfaces 2(10):2924–2932. https://doi.org/10.1021/am1006222

[37] Hua K, Carlsson DO, Ålander E, Lindström T, Strømme M, Mihranyan A, Ferraz N (2014) Translational study between structure and biological response of nanocellulose from wood and green algae. RSC Adv 4(6):2892–2903. https://doi.org/10.1039/C3RA45553J

[38] Hua K, Ålander E, Lindström T, Mihranyan A, Strømme M, Ferraz N (2015) Surface chemistry of nanocellulose fibers directs monocyte/macrophage response. Biomacromolecules 16(9):2787–2795. https://doi.org/10.1021/acs.biomac.5b00727

[39] Hua K, Rocha I, Zhang P, Gustafsson S, Ning Y, Strømme M, Mihranyan A, Ferraz N (2016) Transition from bioinert to bioactive material by tailoring the biological cell response to carboxylated nanocellulose. Biomacromolecules 17(3):1224–1233. https://doi.org/10.1021/acs.biomac.6b00053

[40] Skogberg A, Mäki AJ, Mettänen M, Lahtinen P, Kallio P (2017) Cellulose nanofiber alignment using evaporation-induced droplet-casting, and cell alignment on aligned nanocellulose surfaces. Biomacromolecules 18(12):3936–3953. https://doi.org/10.1021/acs.biomac.7b00963

[41] Pajorova J, Skogberg A, Hadraba D, Broz A, Travnickova M, Zikmundova M, Honkanen M, Hannula M, Lahtinen P, Tomkova M, Bacakova L, Kallio P (2020) Cellulose mesh with charged nanocellulose coatings as a promising carrier of skin and stem cells for regenerative applications. Biomacromolecules 21(12):4857–4870. https://doi.org/10.1021/acs.biomac.0c01097

[42] Kummala R, Soto Véliz D, Fang Z, Xu W, Abitbol T, Xu C, Toivakka M (2020) Human dermal fibroblast viability and adhesion on cellulose nanomaterial coatings: Influence of surface characteristics. Biomacromolecules 21(4):1560–1567. https://doi.org/10.1021/acs.biomac.0c00107

[43] Kato R, Kaga C, Kunimatsu M, Kobayashi T, Honda H (2006) Peptide array-based interaction assay of solid-bound peptides and anchorage-dependant cells and its effectiveness in cell-adhesive peptide design. J Biosci Bioeng 101 (6):485–495. https://doi.org/10.1263/jbb.101.485

[44] Kalaskar DM, Gough JE, Ulijn RV, Sampson WW, Scurr DJ, Rutten FJ, Alexander MR, Merry CL, Eichhorn SJ (2008) Controlling cell morphology on amino acid-modified cellulose. Soft Matter 4(5):1059–1065. https://doi.org/10.1039/b719706n

[45] Wen X, Zheng Y, Wu J, Wang L-N, Yuan Z, Peng J, Meng H (2015) Immobilization of collagen peptide on dialdehyde bacterial cellulose nanofibers via covalent bonds for tissue engineering and regeneration. Int J Nanomed 10:4623–4637. https://doi.org/10.2147/IJN.S84452

[46] Barud HO, Barud HD, Cavicchioli M, do Amaral TS, de Oliveira Junior OB, Santos DM, Petersen AL, Celes F, Borges VM, de Oliveira CI, de Oliveira PF (2015) Preparation and characterization of a bacterial cellulose/silk fibroin sponge scaffold for tissue regeneration. Carbohydr Polym 128:41–51https://doi.org/10.1016/j.carbpol.2015.04.007

[47] Quero F, Opazo G, Zhao Y, Feschotte-Parazon A, Fernandez J, Quintro A, Flores M (2018) Top-down approach to produce protein functionalized and highly thermally stable cellulose fibrils. Biomacromolecules 19(8):3549–3559. https://doi.org/10.1021/acs.biomac.8b00831

[48] Zhang X, Viitala T, Harjumäki R, Kartal-Hodzic A, Valle-Delgado JJ, Österberg M (2021) Effect of laminin, poly-lysine and cell medium components on the attachment of human hepatocellular carcinoma cells to cellulose nanofibrils analyzed by surface plasmon resonance. J Colloid Interface Sci 584:310–319. https://doi.org/10.1016/j.jcis.2020.09.080

[49] Liu J, Shi Y, Cheng L, Sun J, Yu S, Lu X, Biranje S, Xu W, Zhang X, Song J, Wang Q, Han W, Zhang Z (2021) Growth factor functionalized biodegradable nanocellulose scaffolds for potential wound healing application. Cellulose 28 (9):5643–5656. https://doi.org/10.1007/s10570-021-03853-3

[50] Quero F, Quintro A, Orellana N, Opazo G, Mautner A, Jaque N, Valdebenito F, Flores M, Acevedo C (2019) Production of biocompatible protein functionalized cellulose membranes by a top-down approach. ACS Biomater Sci Eng 5(11):5968–5978. https://doi.org/10.1021/acsbiomaterials.9b01015

[51] Zhang W, Yang Y, Cui B (2021) New perspectives on the roles of nanoscale surface topography in modulating intracellular signaling. Curr Opin Solid State Mater Sci 25 (1):100873–100873. https://doi.org/10.1016/j.cossms.2020.100873

[52] Clark P, Connolly P, Curtis ASG, Dow JA, Wilkinson CD (1987) Topographical control of cell behaviour I. Simple step cues. Development 99(3):439–448. https://doi.org/10.1242/dev.99.3.439

[53] Clark P, Connolly P, Curtis ASG, Dow JAT, Wilkinson CDW (1990) Topographical control of cell behaviour: II. multiple grooved substrata. Development 108(4):635–644. https://doi.org/10.1242/dev.108.4.635

[54] Clark P, Connolly P, Curtis ASG, Dow JAT, Wilkinson CDW (1991) Cell guidance by ultrafine topography

in vitro. J Cell Sci 99(1):73–77. https://doi.org/10.1242/jcs.99.1.73

[55] Wilkinson CDW, Riehle M, Wood M, Gallagher J, Curtis ASG (2002) The use of materials patterned on a nano- and micro-metric scale in cellular engineering. Mater Sci Eng, C 19(1–2):263–269. https://doi.org/10.1016/S0928-4931(01)00396-4

[56] Biggs MJP, Richards RG, Dalby MJ (2010) Nanotopographical modification: a regulator of cellular function through focal adhesions. Nanomed Nanotechnol Biol Med 6(5):619–633. https://doi.org/10.1016/j.nano.2010.01.009

[57] Luo H, Cha R, Li J, Hao W, Zhang Y, Zhou F (2019) Advances in tissue engineering of nanocellulose-based scaffolds: a review. Carbohyd Polym 224:115144–115144. https://doi.org/10.1016/j.carbpol.2019.115144

[58] Moohan J, Stewart SA, Espinosa E, Rosal A, Rodríguez A, Larrañeta E, Donnelly RF, Domínguez-Robles J (2020) Cellulose nanofibers and other biopolymers for biomedical applications: a review. Appl Sci (Switzerland) 10(1):65–65. https://doi.org/10.3390/app10010065

[59] Bacakova L, Pajorova J, Tomkova M, Matejka R, Broz A, Stepanovska J, Prazak S, Skogberg A, Siljander S, Kallio P (2020) Applications of nanocellulose/nanocarbon composites: Focus on biotechnology and medicine. Nanomaterials 10(2):196–196. https://doi.org/10.3390/nano10020196

[60] Liu W, Du H, Zhang M, Liu K, Liu H, Xie H, Zhang X, Si C (2020) Bacterial cellulose-based composite scaffolds for biomedical applications: a review. ACS Sustain Chem Eng 8(20):7536–7562. https://doi.org/10.1021/acssuschemeng.0c00125

[61] Ferreira FV, Otoni CG, De France KJ, Barud HS, Lona LMF, Cranston ED, Rojas OJ (2020) Porous nanocellulose gels and foams: Breakthrough status in the development of scaffolds for tissue engineering. Mater Today 37:126–141. https://doi.org/10.1016/j.mattod.2020.03.003

[62] Abdul Khalil HPS, Jummaat F, Yahya EB, Olaiya NG, Adnan AS, Abdat M, Nasir NAM, Halim AS, Seeta Uthaya Kumar U, Bairwan R, Suriani AB (2020) A review on micro- to nanocellulose biopolymer scaffold forming for tissue engineering applications. Polymers 12(9):2043–2043. https://doi.org/10.3390/POLYM12092043

[63] Kuhnt T, Camarero-Espinosa S (2021) Additive manufacturing of nanocellulose based scaffolds for tissue engineering: Beyond a reinforcement filler. Carbohyd Polym 252:117159–117159. https://doi.org/10.1016/j.carbpol.2020.117159

[64] Gupta S, Martoïa F, Orgéas L, Dumont PJJ (2018) Ice-templated porous nanocellulose-based materials: current progress and opportunities for materials engineering. Appl Sci (Switzerland) 8:2463. https://doi.org/10.3390/app8122463

[65] Hickey RJ, Pelling AE (2019) Cellulose biomaterials for tissue engineering. Front Bioeng Biotechnol. https://doi.org/10.3389/fbioe.2019.00045

[66] Domingues RMA, Gomes ME, Reis RL (2014) The potential of cellulose nanocrystals in tissue engineering strategies. Biomacromolecules 15(7):2327–2346. https://doi.org/10.1021/bm500524s

[67] Xu W, Wang X, Sandler N, Willför S, Xu C (2018) Three-dimensional printing of wood-derived biopolymers: A review focused on biomedical applications. ACS Sustain Chem Eng 6(5):5663–5680. https://doi.org/10.1021/acssuschemeng.7b03924

[68] Athukoralalage SS, Balu R, Dutta NK, Choudhury NR (2019) 3D bioprinted nanocellulose-based hydrogels for tissue engineering applications: a brief review. Polymers 11(5):898–898. https://doi.org/10.3390/polym11050898

[69] Bhattacharyya A, Janarthanan G, Noh I (2021) Nano-bio-materials for designing functional bioinks towards complex tissue and organ regeneration in 3D bioprinting. Addit Manuf 37:101639–101639. https://doi.org/10.1016/j.addma.2020.101639

[70] Ee LY, Yau Li SF (2021) Recent advances in 3D printing of nanocellulose: structure, preparation, and application prospects. Nanoscale Adv 3(5):1167–1208. https://doi.org/10.1039/D0NA00408A

[71] Muthukrishnan L (2021) Imminent antimicrobial bioink deploying cellulose, alginate, EPS and synthetic polymers for 3D bioprinting of tissue constructs. Carbohyd Polym 260:117774. https://doi.org/10.1016/j.carbpol.2021.117774

[72] Wang X, Wang Q, Xu C (2020) Nanocellulose-based inks for 3D bioprinting: Key aspects in research development and challenging perspectives in applications—a mini review. Bioengineering 7(2):40. https://doi.org/10.3390/bioengineering7020040

[73] Zhang S, Huang D, Lin H, Xiao Y, Zhang X (2020) Cellulose nanocrystal reinforced collagen-based nanocomposite hydrogel with self-healing and stress-relaxation properties for cell delivery. Biomacromolecules 21(6):2400–2408. https://doi.org/10.1021/acs.biomac.0c00345

[74] Das R, Fernandez JG (2020) Cellulose nanofibers for encapsulation and pluripotency preservation in the early development of embryonic stem cells. Biomacromolecules 21(12):4814–4822. https://doi.org/10.1021/acs.biomac.0c01030

[75] Krontiras P, Gatenholm P, Hagg DA (2015) Adipogenic differentiation of stem cells in three-dimensional porous bacterial nanocellulose scaffolds. J Biomed Mater Res Part

B Appl Biomater 103(1):195–203. https://doi.org/10.1002/jbm.b.33198

[76] Bordoni M, Karabulut E, Kuzmenko V, Fantini V, Pansarasa O, Cereda C, Gatenholm P (2020) 3d printed conductive nanocellulose scaffolds for the differentiation of human neuroblastoma cells. Cells 9(3):682–682. https://doi.org/10.3390/cells9030682

[77] Tang A, Ji J, Li J, Liu W, Wang J, Sun Q, Li Q (2021) Nanocellulose/pegda aerogels with tunable poisson's ratio fabricated by stereolithography for mouse bone marrow mesenchymal stem cell culture. Nanomaterials 11(3):1–18. https://doi.org/10.3390/nano11030603

[78] Poorna MR, Sudhindran S, Thampi MV, Mony U (2021) Differentiation of induced pluripotent stem cells to hepatocyte-like cells on cellulose nanofibril substrate. Colloids Surf B 198:111466–111466. https://doi.org/10.1016/j.colsurfb.2020.111466

[79] Guo R, Li J, Chen C, Xiao M, Liao M, Hu Y, Liu Y, Li D, Zou J, Sun D, Torre V, Zhang Q, Chai R, Tang M (2021) Biomimetic 3D bacterial cellulose-graphene foam hybrid scaffold regulates neural stem cell proliferation and differentiation. Colloids Surf B 200:111590–111590. https://doi.org/10.1016/j.colsurfb.2021.111590

[80] Krüger M, Oosterhoff LA, van Wolferen ME, Schiele SA, Walther A, Geijsen N, De Laporte L, van der Laan LJW, Kock LM, Spee B (2020) Cellulose nanofibril hydrogel promotes hepatic differentiation of human liver organoids. Adv Healthcare Mater 9(6):1901658–1901658. https://doi.org/10.1002/adhm.201901658

[81] Curvello R, Kerr G, Micati DJ, Chan WH, Raghuwanshi VS, Rosenbluh J, Abud HE, Garnier G (2021) Engineered plant-based nanocellulose hydrogel for small intestinal organoid growth. Adv Sci 8(1):2002135–2002135. https://doi.org/10.1002/advs.202002135

[82] Curvello R, Garnier G (2021) Cationic cross-linked nanocellulose-based matrices for the growth and recovery of intestinal organoids. Biomacromolecules 22(2):701–709. https://doi.org/10.1021/acs.biomac.0c01510

[83] Curvello R, Alves D, Abud HE, Garnier G (2021) A thermo-responsive collagen-nanocellulose hydrogel for the growth of intestinal organoids. Mater Sci Eng C 124:112051–112051. https://doi.org/10.1016/j.msec.2021.112051

[84] Martínez Ávila H, Schwarz S, Rotter N, Gatenholm P (2016) 3D bioprinting of human chondrocyte-laden nanocellulose hydrogels for patient-specific auricular cartilage regeneration. Bioprinting 1–2:22–35. https://doi.org/10.1016/j.bprint.2016.08.003

[85] Müller M, Öztürk E, Arlov Ø, Gatenholm P, Zenobi-Wong M (2017) Alginate sulfate–nanocellulose bioinks for cartilage bioprinting applications. Ann Biomed Eng 45 (1):210–223. https://doi.org/10.1007/s10439-016-1704-5

[86] Möller T, Amoroso M, Hägg D, Brantsing C, Rotter N, Apelgren P, Lindahl A, Kölby L, Gatenholm P In vivo chondrogenesis in 3D bioprinted human cell-laden hydrogel constructs. In: Plastic and Reconstructive Surgery - Global Open, 2017. Lippincott Williams and Wilkins. doi: https://doi.org/10.1097/GOX.0000000000001227

[87] Henriksson I, Gatenholm P, Hägg DA (2017) Increased lipid accumulation and adipogenic gene expression of adipocytes in 3D bioprinted nanocellulose scaffolds. Biofabrication 9(1):15022–15022. https://doi.org/10.1088/1758-5090/aa5c1c

[88] Nguyen D, Hgg DA, Forsman A, Ekholm J, Nimkingratana P, Brantsing C, Kalogeropoulos T, Zaunz S, Concaro S, Brittberg M, Lindahl A, Gatenholm P, Enejder A, Simonsson S (2017) Cartilage tissue engineering by the 3D bioprinting of iPS cells in a nanocellulose/alginate bioink. Sci Rep 7(1):1–10. https://doi.org/10.1038/s41598-017-00690-y

[89] Apelgren P, Amoroso M, Lindahl A, Brantsing C, Rotter N, Gatenholm P, Kölby L (2017) Chondrocytes and stem cells in 3D-bioprinted structures create human cartilage in vivo. PLoS ONE 12(12):e0189428–e0189428. https://doi.org/10.1371/journal.pone.0189428

[90] Ojansivu M, Rashad A, Ahlinder A, Massera J, Mishra A, Syverud K, Finne-Wistrand A, Miettinen S, Mustafa K (2019) Wood-based nanocellulose and bioactive glass modified gelatin-alginate bioinks for 3D bioprinting of bone cells. Biofabrication 11(3):35010–35010. https://doi.org/10.1088/1758-5090/ab0692

[91] Gatenholm B, Lindahl C, Brittberg M, Simonsson S (2020) Collagen 2A type B induction after 3D bioprinting chondrocytes in situ into osteoarthritic chondral tibial lesion. Cartilage 13(2_suppl):1755S-1769S. https://doi.org/10.1177/1947603520903788

[92] Säljö K, Orrhult LS, Apelgren P, Markstedt K, Kölby L, Gatenholm P (2020) Successful engraftment, vascularization, and In vivo survival of 3D-bioprinted human lipoaspirate-derived adipose tissue. Bioprinting 17:e00065–e00065. https://doi.org/10.1016/j.bprint.2019.e00065

[93] Dugan JM, Gough JEJE, Eichhorn SJSJ (2010) Directing the morphology and differentiation of skeletal muscle cells using oriented cellulose nanowhiskers. Biomacromolecules 11(9):2498–2504. https://doi.org/10.1021/bm100684k

[94] Vilaça A, Domingues RMA, Tiainen H, Mendes BB, Barrantes A, Reis RL, Gomes ME, Gomez-Florit M (2021) Multifunctional surfaces for improving soft tissue integration. Adv Healthcare Mater 10(8):2001985. https://doi.org/10.1002/adhm.202001985

[95] Changede R, Cai HG, Wind SJ, Sheetz MP (2019) Integrin nanoclusters can bridge thin matrix fibres to form cell-matrix adhesions. Nat Mater 18(12):1366–1375. https://doi.org/10.1038/s41563-019-0460-y

[96] Kane RS, Takayama S, Ostuni E, Ingber DE, Whitesides GM (1999) Patterning proteins and cells using soft lithography. Biomaterials 20(23–24):2363–2376. https://doi.org/10.1016/s0142-9612(99)00165-9

[97] Bottan S, Robotti F, Jayathissa P, Hegglin A, Bahamonde N, Heredia-Guerrero JA, Bayer IS, Scarpellini A, Merker H, Lindenblatt N, Poulikakos D, Ferrari A (2015) Surface-structured bacterial cellulose with guided assembly-based biolithography (GAB). ACS Nano 9(1):206–219. https://doi.org/10.1021/nn5036125

[98] Geisel N, Clasohm J, Shi X, Lamboni L, Yang J, Mattern K, Yang G, Schafer KH, Saumer M (2016) Microstructured multilevel bacterial cellulose allows the guided growth of neural stem cells. Small 12(39):5407–5413. https://doi.org/10.1002/smll.201601679

[99] Boni BOO, Lamboni L, Bakadia BM, Hussein SA, Yang G (2020) Combining silk sericin and surface micropatterns in bacterial cellulose dressings to control fibrosis and enhance wound healing. Eng Sci 10:68–77. https://doi.org/10.30919/es8d906

[100] Lamboni L, Xu C, Clasohm J, Yang J, Saumer M, Schäfer KH, Yang G (2019) Silk sericin-enhanced microstructured bacterial cellulose as tissue engineering scaffold towards prospective gut repair. Mater Sci Eng C 102:502–510. https://doi.org/10.1016/j.msec.2019.04.043

[101] Jin M, Chen W, Li Z, Zhang Y, Zhang M, Chen S (2018) Patterned bacterial cellulose wound dressing for hypertrophic scar inhibition behavior. Cellulose 25(11):6705–6717. https://doi.org/10.1007/s10570-018-2041-7

[102] Wang L, Mao L, Qi F, Li X, Wajid Ullah M, Zhao M, Shi Z, Yang G (2021) Synergistic effect of highly aligned bacterial cellulose/gelatin membranes and electrical stimulation on directional cell migration for accelerated wound healing. Chem Eng J 424:130563–130563. https://doi.org/10.1016/j.cej.2021.130563

[103] He X, Xiao Q, Lu C, Wang Y, Zhang X, Zhao J, Zhang W, Zhang X, Deng Y (2014) Uniaxially aligned electrospun all-cellulose nanocomposite nanofibers reinforced with cellulose nanocrystals: Scaffold for tissue engineering. Biomacromolecules 15(2):618–627. https://doi.org/10.1021/bm401656a

[104] Zhang X, Wang C, Liao M, Dai L, Tang Y, Zhang H, Coates P, Sefat F, Zheng L, Song J, Zheng Z, Zhao D, Yang M, Zhang W, Ji P (2019) Aligned electrospun cellulose scaffolds coated with rhBMP-2 for both in vitro and in vivo bone tissue engineering. Carbohyd Polym 213:27–38. https://doi.org/10.1016/j.carbpol.2019.02.038

[105] Xu W, Molino BZ, Cheng F, Molino PJ, Yue Z, Su D, Wang X, Willför S, Xu C, Wallace GG (2019) On low-concentration inks formulated by nanocellulose assisted with gelatin methacrylate (GelMA) for 3D printing toward wound healing application. ACS Appl Mater Interfaces 11(9):8838–8848. https://doi.org/10.1021/acsami.8b21268

[106] Li Z, Ramos A, Li MC, Li Z, Bhatta S, Jeyaseelan A, Li Y, Wu Q, Yao S, Xu J (2020) Improvement of cell deposition by self-absorbent capability of freeze-dried 3D-bioprinted scaffolds derived from cellulose material-alginate hydrogels. Biomed Phys Eng Expr 6(4):45009–45009. https://doi.org/10.1088/2057-1976/ab8fc6

[107] Erkoc P, Uvak I, Nazeer MA, Batool SR, Odeh YN, Akdogan O, Kizilel S (2020) 3D printing of cytocompatible gelatin-cellulose-alginate blend hydrogels. Macromol Biosci 20(10):2000106–2000106. https://doi.org/10.1002/mabi.202000106

[108] Hivechi A, Bahrami SH, Siegel RA, B. Milan P, Amoupour M, (2020) In vitro and in vivo studies of biaxially electrospun poly(caprolactone)/gelatin nanofibers, reinforced with cellulose nanocrystals, for wound healing applications. Cellulose 27(9):5179–5196. https://doi.org/10.1007/s10570-020-03106-9

[109] De France KJ, Xu F, Toufanian S, Chan KJW, Said S, Stimpson TC, González-Martínez E, Moran-Mirabal JM, Cranston ED, Hoare T (2021) Multi-scale structuring of cell-instructive cellulose nanocrystal composite hydrogel sheets via sequential electrospinning and thermal wrinkling. Acta Biomater 128:250–261. https://doi.org/10.1016/j.actbio.2021.04.044

[110] Huang L, Yuan W, Hong Y, Fan S, Yao X, Ren T, Song L, Yang G, Zhang Y (2021) 3D printed hydrogels with oxidized cellulose nanofibers and silk fibroin for the proliferation of lung epithelial stem cells. Cellulose 28(1):241–257. https://doi.org/10.1007/s10570-020-03526-7

[111] Patel DK, Dutta SD, Shin WC, Ganguly K, Lim KT (2021) Fabrication and characterization of 3D printable nanocellulose-based hydrogels for tissue engineering. RSC Adv 11(13):7466–7478. https://doi.org/10.1039/d0ra09620b

[112] Siqueira G, Kokkinis D, Libanori R, Hausmann MK, Gladman AS, Neels A, Tingaut P, Zimmermann T, Lewis JA, Studart AR (2017) Cellulose nanocrystal inks for 3D printing of textured cellular architectures. Adv Func Mater 27(12):1604619–1604619. https://doi.org/10.1002/adfm.201604619

[113] Hausmann MK, Rühs PA, Siqueira G, Läuger J, Libanori R, Zimmermann T, Studart AR (2018) Dynamics of cellulose

nanocrystal alignment during 3D printing. ACS Nano 12 (7):6926–6937. https://doi.org/10.1021/acsnano.8b02366

[114] Prince E, Alizadehgiashi M, Campbell M, Khuu N, Albulescu A, De France K, Ratkov D, Li Y, Hoare T, Kumacheva E (2018) Patterning of structurally anisotropic composite hydrogel sheets. Biomacromolecules 19 (4):1276–1284. https://doi.org/10.1021/acs.biomac.8b00100

[115] Müller LAE, Zimmermann T, Nyström G, Burgert I, Siqueira G (2020) Mechanical properties tailoring of 3D printed photoresponsive nanocellulose composites. Adv Func Mater 30(35):2002914–2002914. https://doi.org/10.1002/adfm.202002914

[116] Fourmann O, Hausmann MK, Neels A, Schubert M, Nyström G, Zimmermann T, Siqueira G (2021) 3D printing of shape-morphing and antibacterial anisotropic nanocellulose hydrogels. Carbohyd Polym 259:117716–117716. https://doi.org/10.1016/j.carbpol.2021.117716

[117] Camarero-Espinosa S, Rothen-Rutishauser B, Weder C, Foster EJ (2016) Directed cell growth in multi-zonal scaffolds for cartilage tissue engineering. Biomaterials 74:42–52. https://doi.org/10.1016/j.biomaterials.2015.09.033

[118] Courtenay JC, Filgueiras JG, Deazevedo ER, Jin Y, Edler KJ, Sharma RI, Scott JL (2019) Mechanically robust cationic cellulose nanofibril 3D scaffolds with tuneable biomimetic porosity for cell culture. J Mater Chem B 7 (1):53–64. https://doi.org/10.1039/c8tb02482k

[119] Karageorgiou V, Kaplan D (2005) Porosity of 3D biomaterial scaffolds and osteogenesis. Biomaterials 26 (27):5474–5491. https://doi.org/10.1016/j.biomaterials.2005.02.002

[120] Bozkurt A, Deumens R, Beckmann C, Olde Damink L, Schügner F, Heschel I, Sellhaus B, Weis J, Jahnen-Dechent W, Brook GA, Pallua N (2009) In vitro cell alignment obtained with a Schwann cell enriched microstructured nerve guide with longitudinal guidance channels. Biomaterials 30(2):169–179. https://doi.org/10.1016/j.biomaterials.2008.09.017

[121] Jurga M, Dainiak MB, Sarnowska A, Jablonska A, Tripathi A, Plieva FM, Savina IN, Strojek L, Jungvid H, Kumar A, Lukomska B, Domanska-Janik K, Forraz N, McGuckin CP (2011) The performance of laminin-containing cryogel scaffolds in neural tissue regeneration. Biomaterials 32 (13):3423–3434. https://doi.org/10.1016/j.biomaterials.2011.01.049

[122] Pawar K, Mueller R, Caioni M, Prang P, Bogdahn U, Kunz W, Weidner N (2011) Increasing capillary diameter and the incorporation of gelatin enhance axon outgrowth in alginate-based anisotropic hydrogels. Acta Biomater 7

(7):2826–2834. https://doi.org/10.1016/j.actbio.2011.04.006

[123] Chau M, De France KJ, Kopera B, Machado VR, Rosenfeldt S, Reyes L, Chan KJW, Förster S, Cranston ED, Hoare T, Kumacheva E (2016) Composite hydrogels with tunable anisotropic morphologies and mechanical properties. Chem Mater 28(10):3406–3415. https://doi.org/10.1021/acs.chemmater.6b00792

[124] Chen B, Zheng Q, Zhu J, Li J, Cai Z, Chen L, Gong S (2016) Mechanically strong fully biobased anisotropic cellulose aerogels. RSC Adv 6(99):96518–96526. https://doi.org/10.1039/c6ra19280g

[125] Kumar A, Rao KM, Han SS (2017) Synthesis of mechanically stiff and bioactive hybrid hydrogels for bone tissue engineering applications. Chem Eng J 317:119–131. https://doi.org/10.1016/j.cej.2017.02.065

[126] Yin K, Divakar P, Wegst UGK (2019) Plant-derived nanocellulose as structural and mechanical reinforcement of freeze-cast chitosan scaffolds for biomedical applications. Biomacromol 20(10):3733–3745. https://doi.org/10.1021/acs.biomac.9b00784

[127] Pan ZZ, Govedarica A, Nishihara H, Tang R, Wang C, Luo Y, Lv W, Kang FY, Trifkovic M, Yang QH (2021) pH-dependent morphology control of cellulose nanofiber/graphene oxide cryogels. Small 17(3):2005564–2005564. https://doi.org/10.1002/smll.202005564

[128] Tetik H, Zhao K, Shah N, Lin D (2021) 3D freeze-printed cellulose-based aerogels: Obtaining truly 3D shapes, and functionalization with cross-linking and conductive additives. J Manuf Process 68:445–453. https://doi.org/10.1016/j.jmapro.2021.05.051

[129] Zhu Q, Yao Q, Sun J, Chen H, Xu W, Liu J, Wang Q (2020) Stimuli induced cellulose nanomaterials alignment and its emerging applications: a review. Carbohydr Polym 230:115609. https://doi.org/10.1016/j.carbpol.2019.115609

[130] Haywood AD, Weigandt KM, Saha P, Noor M, Green MJ, Davis VA (2017) New insights into the flow and microstructural relaxation behavior of biphasic cellulose nanocrystal dispersions from RheoSANS. Soft Matter 13 (45):8451–8462. https://doi.org/10.1039/c7sm00685c

[131] Rosén T, Brouzet C, Roth SV, Lundell F, Söderberg LD (2018) Three-dimensional orientation of nanofibrils in axially symmetric systems using small-angle X-ray scattering. J Phys Chem C 122(12):6889–6899. https://doi.org/10.1021/acs.jpcc.7b11105

[132] Brouzet C, Mittal N, Lundell F, Söderberg LD (2019) Characterizing the orientational and network dynamics of polydisperse nanofibers on the nanoscale. Macromolecules 52(6):2286–2295. https://doi.org/10.1021/acs.macromol.8b02714

[133] Xu Y, Atrens AD, Stokes JR (2019) Liquid crystal hydroglass formed via phase separation of nanocellulose colloidal rods. Soft Matter 15(8):1716–1720. https://doi.org/10.1039/C8SM02288G

[134] Cranston ED, De France KJ, Yager KG, Hoare T (2016) Cooperative ordering of cellulose nanocrystals in a magnetic field. TAPPI Int Conf Nanotechnol Renew Mater 32:7564–7571. https://doi.org/10.1021/acs.langmuir.6b01827

[135] Dhar P, Kumar A, Katiyar V (2016) Magnetic cellulose nanocrystal based anisotropic polylactic acid nanocomposite films: Influence on electrical, magnetic, thermal, and mechanical properties. ACS Appl Mater Interfaces 8 (28):18393–18409. https://doi.org/10.1021/acsami.6b02828

[136] De France KJ, Yager KG, Chan KJW, Corbett B, Cranston ED, Hoare T (2017) Injectable anisotropic nanocomposite hydrogels direct in situ growth and alignment of myotubes. Nano Lett 17(10):6487–6495. https://doi.org/10.1021/acs.nanolett.7b03600

[137] Echave MC, Domingues RMA, Gómez-Florit M, Pedraz JL, Reis RL, Orive G, Gomes ME (2019) Biphasic hydrogels integrating mineralized and anisotropic features for interfacial tissue engineering. ACS Appl Mater Interfaces 11(51):47771–47784. https://doi.org/10.1021/acsami.9b17826

[138] Bordel D, Putaux JL, Heux L (2006) Orientation of native cellulose in an electric field. Langmuir 22(11):4899–4901. https://doi.org/10.1021/la0600402

[139] Kadimi A, Benhamou K, Ounaies Z, Magnin A, Dufresne A, Kaddami H, Raihane M (2014) Electric field alignment of nanofibrillated cellulose (NFC) in silicone oil: Impact on electrical properties. ACS Appl Mater Interfaces 6 (12):9418–9425. https://doi.org/10.1021/am501808h

[140] Frka-Petesic B, Radavidson H, Jean B, Heux L (2017) Dynamically controlled iridescence of cholesteric cellulose nanocrystal suspensions using electric fields. Adv Mater 29 (11):1606208–1606208. https://doi.org/10.1002/adma.201606208

[141] Xu S, Liu D, Zhang Q, Fu Q (2018) Electric field-induced alignment of nanofibrillated cellulose in thermoplastic polyurethane matrix. Compos Sci Technol 156:117–126. https://doi.org/10.1016/j.compscitech.2017.12.017

[142] Wise HG, Takana H, Ohuchi F, Dichiara AB (2020) Field-assisted alignment of cellulose nanofibrils in a continuous flow-focusing system. ACS Appl Mater Interfaces 12 (25):28568–28575. https://doi.org/10.1021/acsami.0c07272

[143] Sehaqui H, Ezekiel Mushi N, Morimune S, Salajkova M, Nishino T, Berglund LA (2012) Cellulose nanofiber orientation in nanopaper and nanocomposites by cold drawing. ACS Appl Mater Interfaces 4(2):1043–1049. https://doi.org/10.1021/am2016766

[144] Osorio-Madrazo A, Eder M, Rueggeberg M, Pandey JK, Harrington MJ, Nishiyama Y, Putaux JL, Rochas C, Burgert I (2012) Reorientation of cellulose nanowhiskers in agarose hydrogels under tensile loading. Biomacromolecules 13(3):850–856. https://doi.org/10.1021/bm201764y

[145] Wang B, Torres-Rendon JG, Yu J, Zhang Y, Walther A (2015) Aligned bioinspired cellulose nanocrystal-based nanocomposites with synergetic mechanical properties and improved hygromechanical performance. ACS Appl Mater Interfaces 7(8):4595–4607. https://doi.org/10.1021/am507726t

[146] Pullawan T, Wilkinson AN, Eichhorn SJ (2013) Orientation and deformation of wet-stretched all-cellulose nanocomposites. J Mater Sci 48(22):7847–7855. https://doi.org/10.1007/s10853-013-7404-8

[147] De France KJ, Yager KG, Hoare T, Cranston ED (2016) Cooperative ordering and kinetics of cellulose nanocrystal alignment in a magnetic field. Langmuir 32(30):7564–7571. https://doi.org/10.1021/acs.langmuir.6b01827

[148] Johns MA, Bae Y, Guimarães FEG, Lanzoni EM, Costa CAR, Murray PM, Deneke C, Galembeck F, Scott JL, Sharma RI (2018) Predicting ligand-free cell attachment on next-generation cellulose–chitosan hydrogels. ACS Omega 3(1):937–945. https://doi.org/10.1021/acsomega.7b01583

[149] Huang Y, Zhu C, Yang J, Nie Y, Chen C, Sun D (2014) Recent advances in bacterial cellulose. Cellulose 21(1):1–30. https://doi.org/10.1007/s10570-013-0088-z

[150] Hasan N, Rahman L, Kim S-H, Cao J, Arjuna A, Lallo S, Jhun BH, Yoo J-W (2020) Recent advances of nanocellulose in drug delivery systems. J Pharm Investig 50(6):553–572. https://doi.org/10.1007/s40005-020-00499-4

[151] Yuan Q, Bian J, Ma M-G (2021) Advances in biomedical application of nanocellulose-based materials: a review. Curr Med Chem 28:1–21. https://doi.org/10.2174/0929867328666201130124501

[152] Cacicedo ML, Cesca K, Bosio VE, Porto LM, Castro GR (2015) Self-assembly of carrageenin-CaCO3 hybrid microparticles on bacterial cellulose films for doxorubicin sustained delivery. J Appl Biomed 13(3):239–248. https://doi.org/10.1016/j.jab.2015.03.004

[153] Orasugh JT, Dutta S, Das D, Pal C, Zaman A, Das S, Dutta K, Banerjee R, Ghosh SK, Chattopadhyay D (2019) Sustained release of ketorolac tromethamine from poloxamer 407/cellulose nanofibrils graft nanocollagen based ophthalmic formulations. Int J Biol Macromol 140:441–453. https://doi.org/10.1016/j.ijbiomac.2019.08.143

[154] Xuan Nguyen T, Van Pham M, Cao CB (2020) Development and evaluation of oral sustained-release ranitidine delivery system based on bacterial nanocellulose material produced by komagataeibacter xylinus. Int J Appl Pharm 12(3):48–55. https://doi.org/10.22159/ijap.2020v12i3.37218

[155] Auvinen VV, Virtanen J, Merivaara A, Virtanen V, Laurén P, Tuukkanen S, Laaksonen T (2020) Modulating sustained drug release from nanocellulose hydrogel by adjusting the inner geometry of implantable capsules. J Drug Deliv Sci Technol 57:101625–101625. https://doi.org/10.1016/j.jddst.2020.101625

[156] Pachuau L (2020) Nanocellulose and nanohydrogel-mediated sustained drug delivery: smart medical technology. In: Sustainable nanocellulose and nanohydrogels from natural sources. Elsevier, pp 115–130. doi:https://doi.org/10.1016/b978-0-12-816789-2.00005-5

[157] Shi X, Zheng Y, Wang G, Lin Q, Fan J (2014) pH- and electro-response characteristics of bacterial cellulose nanofiber/sodium alginate hybrid hydrogels for dual controlled drug delivery. RSC Adv 4(87):47056–47065. https://doi.org/10.1039/c4ra09640a

[158] Anirudhan TS, Sekhar VC, Shainy F, Jefin TP (2019) Effect of dual stimuli responsive dextran/nanocellulose polyelectrolyte complexes for chemophotothermal synergistic cancer therapy. Int J Biol Macromol 135:776–789. https://doi.org/10.1016/j.ijbiomac.2019.05.218

[159] Adepu S, Khandelwal M (2018) Broad-spectrum antimicrobial activity of bacterial cellulose silver nanocomposites with sustained release. J Mater Sci 53(3):1596–1609. https://doi.org/10.1007/s10853-017-1638-9

[160] Adepu S, Khandelwal M (2020) Bacterial cellulose with microencapsulated antifungal essential oils: a novel double barrier release system. Materialia 9:100585–100585. https://doi.org/10.1016/j.mtla.2020.100585

[161] Vikulina A, Voronin D, Fakhrullin R, Vinokurov V, Volodkin D (2020) Naturally derived nano- and micro-drug delivery vehicles: Halloysite, vaterite and nanocellulose. New J Chem 44(15):5638–5655. https://doi.org/10.1039/c9nj06470b

[162] Li L, Yu C, Yu C, Chen Q, Yu S (2021) Nanocellulose as template to prepare rough-hydroxy rich hollow silicon mesoporous nanospheres (R-nCHMSNs) for drug delivery. Int J Biol Macromol 180:432–438. https://doi.org/10.1016/j.ijbiomac.2021.03.031

[163] Raghav N, Sharma MR, Kennedy JF (2021) Nanocellulose: a mini-review on types and use in drug delivery systems. Carbohydr Polym Technol Appl 2:100031–100031. https://doi.org/10.1016/j.carpta.2020.100031

[164] Adepu S, Khandelwal M (2021) Drug release behaviour and mechanism from unmodified and in situ modified bacterial cellulose. Proc Indian Natl Sci Acad 87:110–120. https://doi.org/10.1007/s43538-021-00012-x

[165] Adepu S, Khandelwal M (2020) Ex-situ modification of bacterial cellulose for immediate and sustained drug release with insights into release mechanism. Carbohyd Polym 249:116816–116816. https://doi.org/10.1016/j.carbpol.2020.116816

[166] Adepu S, Kalyani P, Khandelwal M (2021) Bacterial cellulose-based drug delivery system for dual mode drug release. Trans Indian Natl Acad Eng 6(2):265–271. https://doi.org/10.1007/s41403-020-00192-w

[167] Beekmann U, Schmölz L, Lorkowski S, Werz O, Thamm J, Fischer D, Kralisch D (2020) Process control and scale-up of modified bacterial cellulose production for tailor-made anti-inflammatory drug delivery systems. Carbohyd Polym 236:116062–116062. https://doi.org/10.1016/j.carbpol.2020.116062

[168] Pötzinger Y, Kralisch D, Fischer D (2017) Bacterial nanocellulose: the future of controlled drug delivery? Ther Deliv 8(9):753–761. https://doi.org/10.4155/tde-2017-0059

[169] Moscovici M, Hlevca C, Casarica A, Pavaloiu RD (2017) Nanocellulose and nanogels as modern drug delivery systems. In: Nanocellulose and nanohydrogel matrices: Biotechnological and biomedical applications. Wiley Blackwell, pp 209–269. doi:https://doi.org/10.1002/9783527803835.ch9

[170] Alkhatib Y, Blume G, Thamm J, Steiniger F, Kralisch D, Fischer D (2021) Overcoming the hydrophilicity of bacterial nanocellulose: Incorporation of the lipophilic coenzyme Q10 using lipid nanocarriers for dermal applications. Eur J Pharm Biopharm 158:106–112. https://doi.org/10.1016/j.ejpb.2020.10.021

[171] Ching YC, Gunathilake TMSU, Chuah CH, Ching KY, Singh R, Liou NS (2019) Curcumin/Tween 20-incorporated cellulose nanoparticles with enhanced curcumin solubility for nano-drug delivery: characterization and in vitro evaluation. Cellulose 26(9):5467–5481. https://doi.org/10.1007/s10570-019-02445-6

[172] Siqueira G, Bras J, Dufresne A (2010) Cellulosic bio-nanocomposites: a review of preparation, properties and applications. Polymers 2(4):728–765. https://doi.org/10.3390/polym2040728

[173] Gao J, Li Q, Chen W, Liu Y, Yu H (2014) Self-assembly of nanocellulose and indomethacin into hierarchically ordered structures with high encapsulation efficiency for sustained release applications. ChemPlusChem 79(5):725–731. https://doi.org/10.1002/cplu.201300434

[174] Sultan S, Mathew AP (2018) 3D printed scaffolds with gradient porosity based on a cellulose nanocrystal hydrogel.

Nanoscale 10(9):4421–4431. https://doi.org/10.1039/c7nr08966j

[175] Poonguzhali R, Khaleel Basha S, Sugantha Kumari V (2018) Synthesis of alginate/nanocellulose bionanocomposite for in vitro delivery of ampicillin. Polym Bull 75 (9):4165–4173. https://doi.org/10.1007/s00289-017-2253-2

[176] Abo-Elseoud WS, Hassan ML, Sabaa MW, Basha M, Hassan EA, Fadel SM (2018) Chitosan nanoparticles/cellulose nanocrystals nanocomposites as a carrier system for the controlled release of repaglinide. Int J Biol Macromol 111:604–613. https://doi.org/10.1016/j.ijbiomac.2018.01.044

[177] Abba M, Ibrahim Z, Chong CS, Zawawi NA, Kadir MRA, Yusof AHM, Razak SIA (2019) Transdermal delivery of crocin using bacterial nanocellulose membrane. Fibers Polym 20(10):2025–2031. https://doi.org/10.1007/s12221-019-9076-8

[178] Silva NHCS, Rodrigues AF, Almeida IF, Costa PC, Rosado C, Neto CP, Silvestre AJD, Freire CSR (2014) Bacterial cellulose membranes as transdermal delivery systems for diclofenac: in vitro dissolution and permeation studies. Carbohyd Polym 106(1):264–269. https://doi.org/10.1016/j.carbpol.2014.02.014

[179] Song JE, Jun SH, Park SG, Kang NG (2020) A semi-dissolving microneedle patch incorporating TEMPO-oxidized bacterial cellulose nanofibers for enhanced transdermal delivery. Polymers 12(9):1873–1873. https://doi.org/10.3390/POLYM12091873

[180] Taheri A, Mohammadi M (2015) The use of cellulose nanocrystals for potential application in topical delivery of hydroquinone. Chem Biol Drug Des 86(1):882–886. https://doi.org/10.1111/cbdd.12466

[181] Lazarini SC, de Aquino R, Amaral AC, Corbi FCA, Corbi PP, Barud HS, Lustri WR (2016) Characterization of bilayer bacterial cellulose membranes with different fiber densities: a promising system for controlled release of the antibiotic ceftriaxone. Cellulose 23(1):737–748. https://doi.org/10.1007/s10570-015-0843-4

[182] Rahimi M, Shojaei S, Safa KD, Ghasemi Z, Salehi R, Yousefi B, Shafiei-Irannejad V (2017) Biocompatible magnetic tris(2-aminoethyl)amine functionalized nanocrystalline cellulose as a novel nanocarrier for anti-cancer drug delivery of methotrexate. New J Chem 41 (5):2160–2168. https://doi.org/10.1039/C6NJ03332F

[183] Liu Y, Sui Y, Liu C, Liu C, Wu M, Li B, Li Y (2018) A physically crosslinked polydopamine/nanocellulose hydrogel as potential versatile vehicles for drug delivery and wound healing. Carbohyd Polym 188:27–36. https://doi.org/10.1016/j.carbpol.2018.01.093

[184] Zhang H, Yang C, Zhou W, Luan Q, Li W, Deng Q, Dong X, Tang H, Huang F (2018) A pH-responsive gel macrosphere based on sodium alginate and cellulose nanofiber for potential intestinal delivery of probiotics. ACS Sustain Chem Eng 6(11):13924–13931. https://doi.org/10.1021/acssuschemeng.8b02237

[185] Li S, Jasim A, Zhao W, Fu L, Ullah MW, Shi Z, Yang G (2018) Fabrication of pH-electroactive bacterial cellulose/polyaniline hydrogel for the development of a controlled drug release system. ES Mater Manuf 1:41–49. https://doi.org/10.30919/esmm5f120

[186] Kolakovic R, Peltonen L, Laukkanen A, Hirvonen J, Laaksonen T (2012) Nanofibrillar cellulose films for controlled drug delivery. Eur J Pharm Biopharm 82(2):308–315. https://doi.org/10.1016/j.ejpb.2012.06.011

[187] Huang L, Chen X, Nguyen TX, Tang H, Zhang L, Yang G (2013) Nano-cellulose 3D-networks as controlled-release drug carriers. J Mater Chem B 1(23):2976–2984. https://doi.org/10.1039/c3tb20149j

[188] Mohanta V, Madras G, Patil S (2014) Layer-by-layer assembled thin films and microcapsules of nanocrystalline cellulose for hydrophobic drug delivery. ACS Appl Mater Interfaces 6(22):20093–20101. https://doi.org/10.1021/am505681e

[189] Wiegand C, Moritz S, Hessler N, Kralisch D, Wesarg F, Müller FA, Fischer D, Hipler UC (2015) Antimicrobial functionalization of bacterial nanocellulose by loading with polihexanide and povidone-iodine. J Mater Sci Mater Med 26(10):1–14. https://doi.org/10.1007/s10856-015-5571-7

[190] Zhao J, Lu C, He X, Zhang X, Zhang W, Zhang X (2015) Polyethylenimine-grafted cellulose nanofibril aerogels as versatile vehicles for drug delivery. ACS Appl Mater Interfaces 7(4):2607–2615. https://doi.org/10.1021/am507601m

[191] Mauricio MR, Da Costa PG, Haraguchi SK, Guilherme MR, Muniz EC, Rubira AF (2015) Synthesis of a microhydrogel composite from cellulose nanowhiskers and starch for drug delivery. Carbohyd Polym 115:715–722. https://doi.org/10.1016/j.carbpol.2014.07.063

[192] Barbosa AM, Robles E, Ribeiro JS, Lund RG, Carreño NLV, Labidi J (2016) Cellulose nanocrystal membranes as excipients for drug delivery systems. Materials 9(12):1002–1002. https://doi.org/10.3390/ma9121002

[193] Anirudhan TS, Nair SS, Sekhar VC (2017) Deposition of gold-cellulose hybrid nanofiller on a polyelectrolyte membrane constructed using guar gum and poly(vinyl alcohol) for transdermal drug delivery. J Membr Sci 539:344–357. https://doi.org/10.1016/j.memsci.2017.05.054

[194] Ullah H, Badshah M, Mäkilä E, Salonen J, Shahbazi MA, Santos HA, Khan T (2017) Fabrication, characterization

and evaluation of bacterial cellulose-based capsule shells for oral drug delivery. Cellulose 24(3):1445–1454. https://doi.org/10.1007/s10570-017-1202-4

[195] Alkhatib Y, Dewaldt M, Moritz S, Nitzsche R, Kralisch D, Fischer D (2017) Controlled extended octenidine release from a bacterial nanocellulose/poloxamer hybrid system. Eur J Pharm Biopharm 112:164–176. https://doi.org/10.1016/j.ejpb.2016.11.025

[196] Meneguin AB, Ferreira Cury BS, dos Santos AM, Franco DF, Barud HS, da Silva Filho EC (2017) Resistant starch/pectin free-standing films reinforced with nanocellulose intended for colonic methotrexate release. Carbohyd Polym 157:1013–1023. https://doi.org/10.1016/j.carbpol.2016.10.062

[197] Saïdi L, Vilela C, Oliveira H, Silvestre AJD, Freire CSR (2017) Poly(N-methacryloyl glycine)/nanocellulose composites as pH-sensitive systems for controlled release of diclofenac. Carbohyd Polym 169:357–365. https://doi.org/10.1016/j.carbpol.2017.04.030

[198] Orasugh JT, Saha NR, Rana D, Sarkar G, Mollick MMR, Chattoapadhyay A, Mitra BC, Mondal D, Ghosh SK, Chattopadhyay D (2018) Jute cellulose nano-fibrils/hydroxypropylmethylcellulose nanocomposite: A novel material with potential for application in packaging and transdermal drug delivery system. Ind Crops Prod 112:633–643. https://doi.org/10.1016/j.indcrop.2017.12.069

[199] Cacicedo ML, Islan GA, León IE, Álvarez VA, Chourpa I, Allard-Vannier E, García-Aranda N, Díaz-Riascos ZV, Fernández Y, Schwartz S, Abasolo I, Castro GR (2018) Bacterial cellulose hydrogel loaded with lipid nanoparticles for localized cancer treatment. Colloids Surf B 170:596–608. https://doi.org/10.1016/j.colsurfb.2018.06.056

[200] Thomas D, Latha MS, Thomas KK (2018) Synthesis and in vitro evaluation of alginate-cellulose nanocrystal hybrid nanoparticles for the controlled oral delivery of rifampicin. J Drug Deliv Sci Technol 46:392–399. https://doi.org/10.1016/j.jddst.2018.06.004

[201] Supramaniam J, Adnan R, Mohd Kaus NH, Bushra R (2018) Magnetic nanocellulose alginate hydrogel beads as potential drug delivery system. Int J Biol Macromol 118:640–648. https://doi.org/10.1016/j.ijbiomac.2018.06.043

[202] Tong WY, bin Abdullah AYK, binti Rozman NAS, bin Wahid MIA, Hossain MS, Ring LC, Lazim Y, Tan WN (2018) Antimicrobial wound dressing film utilizing cellulose nanocrystal as drug delivery system for curcumin. Cellulose 25 (1):631–638 https://doi.org/10.1007/s10570-017-1562-9

[203] Laurén P, Paukkonen H, Lipiäinen T, Dong Y, Oksanen T, Räikkönen H, Ehlers H, Laaksonen P, Yliperttula M,

Laaksonen T (2018) Pectin and mucin enhance the bioadhesion of drug loaded nanofibrillated cellulose films. Pharm Res 35(7):1–14. https://doi.org/10.1007/s11095-018-2428-z

[204] Li J, Wang Y, Zhang L, Xu Z, Dai H, Wu W (2019) Nanocellulose/gelatin composite cryogels for controlled drug release. ACS Sustain Chem Eng 7(6):6381–6389. https://doi.org/10.1021/acssuschemeng.9b00161

[205] Plappert SF, Liebner FW, Konnerth J, Nedelec JM (2019) Anisotropic nanocellulose gel–membranes for drug delivery: tailoring structure and interface by sequential periodate–chlorite oxidation. Carbohyd Polym 226:115306–115306. https://doi.org/10.1016/j.carbpol.2019.115306

[206] Yang M, Ward J, Choy KL (2020) Nature-inspired bacterial cellulose/methylglyoxal (BC/MGO) nanocomposite for broad-spectrum antimicrobial wound dressing. Macromol Biosci 20(8):2000070–2000070. https://doi.org/10.1002/mabi.202000070

[207] Raghav N, Mor N, Gupta RD, Kaur R, Sharma MR, Arya P (2020) Some cetyltrimethylammonium bromide modified polysaccharide supports as sustained release systems for curcumin. Int J Biol Macromol 154:361–370. https://doi.org/10.1016/j.ijbiomac.2020.02.317

[208] Fonseca DFS, Vilela C, Pinto RJB, Bastos V, Oliveira H, Catarino J, Faísca P, Rosado C, Silvestre AJD, Freire CSR (2021) Bacterial nanocellulose-hyaluronic acid microneedle patches for skin applications: In vitro and in vivo evaluation. Mater Sci Eng C 118:111350–111350. https://doi.org/10.1016/j.msec.2020.111350

[209] Koivuniemi R, Hakkarainen T, Kiiskinen J, Kosonen M, Vuola J, Valtonen J, Luukko K, Kavola H, Yliperttula M (2020) Clinical study of nanofibrillar cellulose hydrogel dressing for skin graft donor site treatment. Adv Wound Care 9(4):199–210. https://doi.org/10.1089/wound.2019.0982

[210] Seabra AB, Bernardes JS, Fávaro WJ, Paula AJ, Durán N (2018) Cellulose nanocrystals as carriers in medicine and their toxicities: a review. Carbohyd Polym 181:514–527. https://doi.org/10.1016/j.carbpol.2017.12.014

[211] WHO, UNICEF (2017) Progress on drinking water, sanitation and hygiene: 2017 update and SDG baselines. Geneva

[212] Georgouvelas D, Abdelhamid HN, Li J, Edlund U, Mathew AP (2021) All-cellulose functional membranes for water treatment: Adsorption of metal ions and catalytic decolorization of dyes. Carbohyd Polym 264:118044–118044. https://doi.org/10.1016/j.carbpol.2021.118044

[213] Abou-zeid RE, Dacrory S, Ali KA, Kamel S (2018) Novel method of preparation of tricarboxylic cellulose nanofiber for efficient removal of heavy metal ions from aqueous

solution. Int J Biol Macromol 119:207–214. https://doi.org/10.1016/j.ijbiomac.2018.07.127

[214] Ram B, Chauhan GS (2018) New spherical nanocellulose and thiol-based adsorbent for rapid and selective removal of mercuric ions. Chem Eng J 331:587–596. https://doi.org/10.1016/j.cej.2017.08.128

[215] Hokkanen S, Eveliina R, Sillanpää M (2013) Removal of heavy metals from aqueous solutions by succinic anhydride modified mercerized nanocellulose. Chem Eng J 223:40–47

[216] Hokkanen S, Repo E, Suopajärvi T, Liimatainen H, Niinimaa J, Sillanpää M (2014) Adsorption of Ni(II), Cu(II) and Cd(II) from aqueous solutions by amino modified nanostructured microfibrillated cellulose. Cellulose 21(3):1471–1487. https://doi.org/10.1007/s10570-014-0240-4

[217] Huang X, Dognani G, Hadi P, Yang M, Job AE, Hsiao BS (2020) Cationic dialdehyde nanocellulose from sugarcane bagasse for efficient chromium(VI) removal. ACS Sustain Chem Eng 8(12):4734–4744. https://doi.org/10.1021/acssuschemeng.9b06683

[218] Etale A, Nhlane D, Mosai A, Mhlongo J, Khan A, Rumbold K, Nuapia Y (2021) Synthesis and application of cationised cellulose for removal of Cr(VI) from acid mine-drainage contaminated water. AAS Open Res 4:4. https://doi.org/10.12688/aasopenres.13182.1

[219] El Achaby M, Ruesgas-Ramón M, Fayoud NEH, Figueroa-Espinoza MC, Trabadelo V, Draoui K, Ben Youcef H (2019) Bio-sourced porous cellulose microfibrils from coffee pulp for wastewater treatment. Cellulose 26(6):3873–3889. https://doi.org/10.1007/s10570-019-02344-w

[220] Sudhakar C, Anil Kumar A, Bhuin RG, Sen Gupta S, Natarajan G, Pradeep T (2018) Species-specific uptake of arsenic on confined metastable 2-line ferrihydrite: a combined Raman-X-ray photoelectron spectroscopy investigation of the adsorption mechanism. ACS Sustain Chem Eng 6(8):9990–10000. https://doi.org/10.1021/acssuschemeng.8b01217

[221] Mukherjee S, Kumar AA, Sudhakar C, Kumar R, Ahuja T, Mondal B, Srikrishnarka P, Philip L, Pradeep T (2019) Sustainable and affordable composites built using microstructures performing better than nanostructures for arsenic removal. ACS Sustain Chem Eng 7(3):3222–3233. https://doi.org/10.1021/acssuschemeng.8b05157

[222] Du M, Du Y, Feng Y, Li Z, Wang J, Jiang N, Liu Y (2019) Advanced photocatalytic performance of novel BiOBr/BiOI/cellulose composites for the removal of organic pollutant. Cellulose 26(9):5543–5557. https://doi.org/10.1007/s10570-019-02474-1

[223] Gan L, Zhong Q, Geng A, Wang L, Song C, Han S, Cui J, Xu L (2019) Cellulose derived carbon nanofiber: A

promising biochar support to enhance the catalytic performance of CoFe2O4 in activating peroxymonosulfate for recycled dimethyl phthalate degradation. Sci Total Environ 694:133705–133705. https://doi.org/10.1016/j.scitotenv.2019.133705

[224] Chen L, Yang S, Zuo X, Huang Y, Cai T, Ding D (2018) Biochar modification significantly promotes the activity of Co3O4 towards heterogeneous activation of peroxymonosulfate. Chem Eng J 354:856–865. https://doi.org/10.1016/j.cej.2018.08.098

[225] Geng A, Meng L, Han J, Zhong Q, Li M, Han S, Mei C, Xu L, Tan L, Gan L (2018) Highly efficient visible-light photocatalyst based on cellulose derived carbon nanofiber/BiOBr composites. Cellulose 25(7):4133–4144. https://doi.org/10.1007/s10570-018-1851-y

[226] Fu H, Ma S, Zhao P, Xu S (2018) Zhan S (2019) Activation of peroxymonosulfate by graphitized hierarchical porous biochar and MnFe2O4 magnetic nanoarchitecture for organic pollutants degradation: Structure dependence and mechanism. Chem Eng J 360:157–170. https://doi.org/10.1016/j.cej.2018.11.207

[227] Nordstrom DK (2002) Public health—worldwide occurrences of arsenic in ground water. Science 296(5576):2143–2145. https://doi.org/10.1126/science.1072375

[228] Glasser NR, Oyala PH, Osborne TH, Santini JM, Newman DK (2018) Structural and mechanistic analysis of the arsenate respiratory reductase provides insight into environmental arsenic transformations. Proc Natl Acad Sci USA 115(37):E8614–E8623. https://doi.org/10.1073/pnas.1807984115

[229] Jain A, Raven KP, Loeppert RH (1999) Arsenite and arsenate adsorption on ferrihydrite: Surface charge reduction and net OH- release stoichiometry. Environ Sci Technol 33(8):1179–1184. https://doi.org/10.1021/es980722e

[230] Manninen MA, Nieminen KL, Maloney TC (2013) The swelling and pore structure of microfibrillated cellulose. In: XVth Fundamental RESEARCH SYMPOSIUM, Cambridge. doi:https://doi.org/10.15376/frc.2013.2.765.THE

[231] Muller K, Ciminelli VST, Dantas MSS, Willscher S (2010) A comparative study of As(III) and As(V) in aqueous solutions and adsorbed on iron oxy-hydroxides by Raman spectroscopy. Water Res 44(19):5660–5672. https://doi.org/10.1016/j.watres.2010.05.053

[232] Hokkanen S, Repo E, Westholm LJ, Lou S, Sainio T, Sillanpaa M (2014) Adsorption of Ni2+, Cd2+, PO43- and NO3- from aqueous solutions by nanostructured microfibrillated cellulose modified with carbonated hydroxyapatite. Chem Eng J 252:64–74. https://doi.org/10.1016/j.cej.2014.04.101

[233] Hokkanen S, Bhatnagar A, Repo E, Lou S, Sillanpaa M (2016) Calcium hydroxyapatite microfibrillated cellulose composite as a potential adsorbent for the removal of Cr (VI) from aqueous solution. Chem Eng J 283:445–452. https://doi.org/10.1016/j.cej.2015.07.035

[234] Wang J, Liu M, Duan C, Sun JP, Xu YW (2019) Preparation and characterization of cellulose-based adsorbent and its application in heavy metal ions removal. Carbohyd Polym 206:837–843. https://doi.org/10.1016/j.carbpol.2018.11.059

[235] Wu CH, Lo SL, Lin CF (2000) Competitive adsorption of molybdate, chromate, sulfate, selenate, and selenite on gamma-Al2O3. Colloid Surfaces A-Physicochem Eng Aspects 166(1–3):251–259. https://doi.org/10.1016/s0927-7757(99)00404-5

[236] Wang J, Tavakoli J, Tang Y (2019) Bacterial cellulose production, properties and applications with different culture method—a review. Carbohyd Polym 219:63–76. https://doi.org/10.1016/J.CARBPOL.2019.05.008

[237] Sharma C, Bhardwaj NK (2019) Bacterial nanocellulose: Present status, biomedical applications and future perspectives. Mater Sci Eng C-Mater Biol Appl 104:109963–109963. https://doi.org/10.1016/j.msec.2019.109963

[238] Huang Y, Huang X, Ma M, Hu C, Seidi F, Yin S, Xiao H (2021) Recent advances on the bacterial cellulose-derived carbon aerogels. J Mater Chem C 9(3):818–828. https://doi.org/10.1039/D0TC05433J

[239] Jeddi MK, Laitinen O, Liimatainen H (2019) Magnetic superabsorbents based on nanocellulose aerobeads for selective removal of oils and organic solvents. Mater Des 183:108115–108115. https://doi.org/10.1016/j.matdes.2019.108115

[240] Schrope M (2011) Oil spill: deep wounds. Nature 472 (7342):152–154. https://doi.org/10.1038/472152a

[241] Ge J, Zhao H-YY, Zhu H-WW, Huang J, Shi L-AA, Yu S-HH (2016) Advanced sorbents for oil-spill cleanup: recent advances and future perspectives. Adv Mater 28 (47):10459–10490

[242] Liu HZ, Geng BY, Chen YF, Wang HY (2017) Review on the aerogel-type oil sorbents derived from nanocellulose. ACS Sustain Chem Eng 5(1):49–66. https://doi.org/10.1021/acssuschemeng.6b02301

[243] Chen B, Ma QL, Tan CL, Lim T-TT, Huang L, Zhang H (2015) Carbon-based sorbents with three-dimensional architectures for water remediation. Small 11(27):3319–3336

[244] Gupta S, Tai NH (2016) Carbon materials as oil sorbents: a review on the synthesis and performance. J Mater Chem A 4(5):1550–1565. https://doi.org/10.1039/c5ta08321d

[245] Zhou SF, Zhou LH, Zhang YP, Sun J, Wen JL, Yuan Y (2019) Upgrading earth-abundant biomass into three-dimensional carbon materials for energy and environmental applications. J Mater Chem A 7(9):4217–4229. https://doi.org/10.1039/c8ta12159a

[246] Wu ZY, Li C, Liang HW, Chen JF, Yu SH (2013) Ultralight, flexible, and fire-resistant carbon nanofiber aerogels from bacterial cellulose. Angew Chem-Int Edn 52(10):2925–2929. https://doi.org/10.1002/anie.201209676

[247] Cheng Z, Li JP, Wang B, Zeng JS, Xu J, Gao WH, Zhu SY, Hu FG, Dong JR, Chen KF (2020) Scalable and robust bacterial cellulose carbon aerogels as reusable absorbents for high-efficiency oil/water separation. ACS Appl Bio Mater 3(11):7483–7491. https://doi.org/10.1021/acsabm.0c00708

[248] Lai FL, Miao YE, Zuo LZ, Zhang YF, Liu TX (2016) Carbon aerogels derived from bacterial cellulose/polyimide composites as versatile adsorbents and supercapacitor electrodes. ChemNanoMat 2(3):212–219. https://doi.org/10.1002/cnma.201500210

[249] Wan YZ, Zhang FS, Li CZ, Xiong GY, Zhu Y, Luo HL (2015) Facile and scalable production of three-dimensional spherical carbonized bacterial cellulose/graphene nanocomposites with a honeycomb-like surface pattern as potential superior absorbents. J Mater Chem A 3 (48):24389–24396. https://doi.org/10.1039/c5ta07464a

[250] Li C, Wu ZY, Liang HW, Chen JF, Yu SH (2017) Ultralight multifunctional carbon-based aerogels by combining graphene oxide and bacterial cellulose. Small 13 (25):1700453–1700453. https://doi.org/10.1002/smll.201700453

[251] Luo HL, Xie J, Wang J, Yao FL, Yang ZW, Wan YZ (2018) Step-by-step self-assembly of 2D few-layer reduced graphene oxide into 3D architecture of bacterial cellulose for a robust, ultralight, and recyclable all-carbon absorbent. Carbon 139:824–832. https://doi.org/10.1016/j.carbon.2018.07.048

[252] Ieamviteevanich P, Palaporn D, Chanlek N, Poo-arporn Y, Mongkolthanaruk W, Eichhorn SJ, Pinitsoontorn S (2020) Carbon nanofiber aerogel/magnetic core–shell nanoparticle composites as recyclable oil sorbents. ACS Appl Nano Mater 3:3939–3950. https://doi.org/10.1021/acsanm.0c00818

[253] Gui XC, Zeng ZP, Lin ZQ, Gan QM, Xiang R, Zhu Y, Cao AY, Tang ZK (2013) Magnetic and highly recyclable macroporous carbon nanotubes for spilled oil sorption and separation. ACS Appl Mater Interfaces 5(12):5845–5850. https://doi.org/10.1021/am4015007

[254] Liu RL, Li XQ, Liu HQ, Luo ZM, Ma J, Zhang ZQ, Fu Q (2016) Eco-friendly fabrication of sponge-like magnetically

carbonaceous fiber aerogel for high-efficiency oil-water separation. RSC Adv 6(36):30301–30310. https://doi.org/10.1039/c6ra02794f

[255] Ge X, Yang W, Wang J, Long DH, Ling LC, Qiao WM (2015) Flexible carbon nanofiber sponges for highly efficient and recyclable oil absorption. RSC Adv 5(86):70025–70031. https://doi.org/10.1039/c5ra09021k

[256] Han SJ, Sun QF, Zheng HH, Li JP, Jin CD (2016) Green and facile fabrication of carbon aerogels from cellulose-based waste newspaper for solving organic pollution. Carbohyd Polym 136:95–100. https://doi.org/10.1016/j.carbpol.2015.09.024

[257] Sriplai N, Mongkolthanaruk W, Eichhorn SJJ, Pinitsoontorn S (2020) Magnetic bacterial cellulose and carbon nanofiber aerogel by simple immersion and pyrolysis. J Mater Sci 55(9):4113–4126. https://doi.org/10.1007/s10853-019-04295-w

[258] Thaveemas P, Chuenchom L, Kaowphong S, Techasakul S, Saparpakorn P, Dechtrirat D (2021) Magnetic carbon nanofiber composite adsorbent through green in-situ conversion of bacterial cellulose for highly efficient removal of bisphenol A. Bioresource Technology 333:125184. https://doi.org/10.1016/j.biortech.2021.125184

[259] Ma B, Chaudhary JP, Zhu JG, Sun BJ, Huang Y, Sun DP (2020) Ni nanoparticle-carbonized bacterial cellulose composites for the catalytic reduction of highly toxic aqueous Cr(VI). J Mater Sci Mater Electron 31(9):7044–7052. https://doi.org/10.1007/s10854-020-03270-5

[260] Rajagopal S, Paramasivam B, Muniyasamy K (2020) Photocatalytic removal of cationic and anionic dyes in the textile wastewater by H2O2 assisted TiO2 and micro-cellulose composites. Sep Purif Technol 252:117444. https://doi.org/10.1016/j.seppur.2020.117444

[261] Cai Y, Chen Y, Ge S, Qu X, Sheng N, Yang L, Chen S, Wang H, Hagfeldt A (2021) Co-doped magnetic N-TiO2-x/rGO heterojunction@cellulose nanofibrous flakelet for enhanced photocatalytic oxidation and facile separation: efficient charge separation and self-floatability. Chem Eng J 425:131462. https://doi.org/10.1016/j.cej.2021.131462

[262] Elfeky AS, Salem SS, Elzaref AS, Owda ME, Eladawy HA, Saeed AM, Awad MA, Abou-Zeid RE, Fouda A (2020) Multifunctional cellulose nanocrystal/metal oxide hybrid, photo-degradation, antibacterial and larvicidal activities. Carbohydr Polym 230:115711. https://doi.org/10.1016/j.carbpol.2019.115711

[263] Zhou WM, Sun SC, Jiang YF, Zhang MX, Lawan I, Fernando GF, Wang LW, Yuan ZH (2019) Template in situ synthesis of flower-like BiOBr/microcrystalline cellulose composites with highly visible-light photocatalytic activity.

Cellulose 26(18):9529–9541. https://doi.org/10.1007/s10570-019-02722-4

[264] Zhang D, Zhang M, Chen S, Liang Q, Sheng N, Han Z, Cai Y, Wang H (2021) Scalable, self-cleaning and self-floating bi-layered bacterial cellulose biofoam for efficient solar evaporator with photocatalytic purification. Desalination 500:114899. https://doi.org/10.1016/j.desal.2020.114899

[265] Zhang D, Cai Y, Liang Q, Wu Z, Sheng N, Zhang M, Wang B, Chen S (2020) Scalable, flexible, durable, and salt-tolerant CuS/bacterial cellulose gel membranes for efficient interfacial solar evaporation. ACS Sustain Chem Eng 8(24):9017–9026. https://doi.org/10.1021/acssuschemeng.0c01707

[266] Ghim D, Jiang QS, Cao SS, Singamaneni S, Jun YS (2018) Mechanically interlocked 1T/2H phases of MoS2 nanosheets for solar thermal water purification. Nano Energy 53:949–957. https://doi.org/10.1016/j.nanoen.2018.09.038

[267] Li XQ, Xu WC, Tang MY, Zhou L, Zhu B, Zhu SN, Zhu J (2016) Graphene oxide-based efficient and scalable solar desalination under one sun with a confined 2D water path. Proc Natl Acad Sci USA 113(49):13953–13958. https://doi.org/10.1073/pnas.1613031113

[268] Didone M, Tosello G (2019) Moulded pulp products manufacturing with thermoforming. Packag Technol Sci 32(1):7–22. https://doi.org/10.1002/pts.2412

[269] Boldizar A, Klason C, Kubát J, Näslund P, Sáha P (1987) Prehydrolyzed cellulose as reinforcing filler for thermoplastics. Int J Polym Mater Polym Biomater 11(4):229–262. https://doi.org/10.1080/00914038708078665

[270] Favier V, Chanzy H, Cavaille JY (1995) Polymer nanocomposites reinforced by cellulose whiskers. Macromolecules 28(18):6365–6367

[271] Favier V, Canova GR, Cavaillé JY, Chanzy H, Dufresne A, Gauthier C (1995) Nanocomposite materials from latex and cellulose whiskers. Polym Adv Technol 6(5):351–355. https://doi.org/10.1002/pat.1995.220060514

[272] Azizi Samir MAS, Alloin F, Dufresne A (2005) Review of recent research into cellulosic whiskers, their properties and their application in nanocomposite field. Biomacromolecules 6(2):612–626. https://doi.org/10.1021/bm0493685

[273] Nakagaito AN, Yano H (2005) Novel high-strength biocomposites based on microfibrillated cellulose having nano-order-unit web-like network structure. Appl Phys A Mater Sci Process 80(1):155–159. https://doi.org/10.1007/s00339-003-2225-2

[274] Yano H, Sugiyama J, Nakagaito AN, Nogi M, Matsuura T, Hikita M, Handa K (2005) Optically transparent composites reinforced with networks of bacterial nanofibers. Adv

Mater 17(2):153–155. https://doi.org/10.1002/adma.200400597

[275] Ansari F, Galland S, Johansson M, Plummer CJG, Berglund LA (2014) Cellulose nanofiber network for moisture stable, strong and ductile biocomposites and increased epoxy curing rate. Compos A Appl Sci Manuf 63:35–44. https://doi.org/10.1016/j.compositesa.2014.03.017

[276] Ansari F, Skrifvars M, Berglund L (2015) Nanostructured biocomposites based on unsaturated polyester resin and a cellulose nanofiber network. Compos Sci Technol 117:298–306. https://doi.org/10.1016/j.compscitech.2015.07.004

[277] Ansari F, Berglund LA (2018) Toward semistructural cellulose nanocomposites: the need for scalable processing and interface tailoring. Biomacromol 19(7):2341–2350. https://doi.org/10.1021/acs.biomac.8b00142

[278] Lee KY, Aitomäki Y, Berglund LA, Oksman K, Bismarck A (2014) On the use of nanocellulose as reinforcement in polymer matrix composites. Compos Sci Technol 105:15–27. https://doi.org/10.1016/j.compscitech.2014.08.032

[279] Arvidsson R, Nguyen D, Svanström M (2015) Life cycle assessment of cellulose nanofibrils production by mechanical treatment and two different pretreatment processes. Environ Sci Technol 49(11):6881–6890. https://doi.org/10.1021/acs.est.5b00888

[280] Yang X, Reid MS, Olsén P, Berglund LA (2020) Eco-friendly cellulose nanofibrils designed by nature: effects from preserving native state. ACS Nano 14(1):724–735. https://doi.org/10.1021/acsnano.9b07659

[281] Dufresne A, Dupeyre D, Vignon MR (2000) Cellulose microfibrils from potato tuber cells: processing and characterization of starch-cellulose microfibril composites. J Appl Polym Sci 76(14):2080–2092. https://doi.org/10.1002/(SICI)1097-4628(20000628)76:14%3c2080::AID-APP12%3e3.0.CO;2-U

[282] Svagan AJ, Azizi Samir MAS, Berglund LA (2007) Biomimetic polysaccharide nanocomposites of high cellulose content and high toughness. Biomacromolecules 8 (8):2556–2563. https://doi.org/10.1021/bm0703160

[283] Larsson K, Berglund LA, Ankerfors M, Lindström T (2012) Polylactide latex/nanofibrillated cellulose bio-nanocomposites of high nanofibrillated cellulose content and nanopaper network structure prepared by a paper-making route. J Appl Polym Sci 125(3):2460–2466. https://doi.org/10.1002/app.36413

[284] Igarashi Y, Sato A, Okumura H, Nakatsubo F, Yano H (2018) Manufacturing process centered on dry-pulp direct kneading method opens a door for commercialization of cellulose nanofiber reinforced composites. Chem Eng J 354:563–568. https://doi.org/10.1016/j.cej.2018.08.020

[285] Nogi M, Abe K, Handa K, Nakatsubo F, Ifuku S, Yano H (2006) Property enhancement of optically transparent bio-nanofiber composites by acetylation. Appl Phys Lett 89 (23):233123–233123. https://doi.org/10.1063/1.2403901

[286] Cunha AG, Zhou Q, Larsson PT, Berglund LA (2014) Topochemical acetylation of cellulose nanopaper structures for biocomposites: mechanisms for reduced water vapour sorption. Cellulose 21(4):2773–2787. https://doi.org/10.1007/s10570-014-0334-z

[287] Oksman K, Mathew AP, Bismarck A, Rojas O, Sain M (2014) Handbook of green materials: processing technologies, properties and applications. World Scientific Pub Co Pte, Singapore

[288] Oksman K, Aitomaki Y, Mathew AP, Siqueira G, Zhou Q, Butylina S, Tanpichai S, Zhou X, Hooshmand S (2016) Review of the recent developments in cellulose nanocomposite processing. Compos Part A-Appl Sci Manuf 83:2–18. https://doi.org/10.1016/j.compositesa.2015.10.041

[289] Wang L, Gardner DJ, Wang J, Yang Y, Tekinalp HL, Tajvidi M, Li K, Zhao X, Neivandt DJ, Han Y, Ozcan S, Anderson J (2020) Towards industrial-scale production of cellulose nanocomposites using melt processing: a critical review on structure-processing-property relationships. Compos B Eng 201:108297–108297. https://doi.org/10.1016/j.compositesb.2020.108297

[290] Zheng T, Pilla S (2020) Melt processing of cellulose nanocrystal-filled composites: toward reinforcement and foam nucleation. Ind Eng Chem Res 59(18):8511–8531. https://doi.org/10.1021/acs.iecr.0c00170

[291] Clemons C, Sabo R (2021) A review of wet compounding of cellulose nanocomposites. Polymers 13(6):911–911. https://doi.org/10.3390/polym13060911

[292] Karger-Kocsis J, Kmetty Á, Lendvai L, Drakopoulos SX, Bárány T (2015) Water-assisted production of thermoplastic nanocomposites: a review. Materials 8(1):72–95

[293] Oksman K, Mathew AP, Bondeson D, Kvien I (2006) Manufacturing process of cellulose whiskers/polylactic acid nanocomposites. Compos Sci Technol 66(15):2776–2784. https://doi.org/10.1016/j.compscitech.2006.03.002

[294] Bondeson D, Syre P, Niska KO (2007) All cellulose nanocomposites produced by extrusion. J Biobased Mater Bioenergy 1(3):367–371. https://doi.org/10.1166/jbmb.2007.011

[295] Herrera N, Singh AA, Salaberria AM, Labidi J, Mathew AP, Oksman K (2017) Triethyl citrate (TEC) as a dispersing aid in polylactic acid/chitin nanocomposites prepared via liquid-assisted extrusion. Polymers 9(9):406–406

[296] Geng S, Wloch D, Herrera N, Oksman K (2020) Large-scale manufacturing of ultra-strong, strain-responsive poly (lactic acid)-based nanocomposites reinforced with

cellulose nanocrystals. Compos Sci Technol 194:108144–108144. https://doi.org/10.1016/j.compscitech.2020.108144

[297] Bondeson D, Oksman K (2007) Polylactic acid/cellulose whisker nanocomposites modified by polyvinyl alcohol. Compos A Appl Sci Manuf 38(12):2486–2492. https://doi.org/10.1016/j.compositesa.2007.08.001

[298] Peng J, Walsh PJ, Sabo RC, Turng L-S, Clemons CM (2016) Water-assisted compounding of cellulose nanocrystals into polyamide 6 for use as a nucleating agent for microcellular foaming. Polymer 84:158–166. https://doi.org/10.1016/j.polymer.2015.12.050

[299] Herrera N, Salaberria AM, Mathew AP, Oksman K (2016) Plasticized polylactic acid nanocomposite films with cellulose and chitin nanocrystals prepared using extrusion and compression molding with two cooling rates: effects on mechanical, thermal and optical properties. Compos A Appl Sci Manuf 83:89–97. https://doi.org/10.1016/j.compositesa.2015.05.024

[300] Herrera N, Mathew AP, Oksman K (2015) Plasticized polylactic acid/cellulose nanocomposites prepared using melt-extrusion and liquid feeding: mechanical, thermal and optical properties. Compos Sci Technol 106:149–155. https://doi.org/10.1016/j.compscitech.2014.11.012

[301] Hietala M, Mathew AP, Oksman K (2013) Bionanocomposites of thermoplastic starch and cellulose nanofibers manufactured using twin-screw extrusion. Eur Polymer J 49(4):950–956. https://doi.org/10.1016/j.eurpolymj.2012.10.016

[302] Yasim-Anuar TAT, Ariffin H, Norrrahim MNF, Hassan MA, Andou Y, Tsukegi T, Nishida H (2020) Well-dispersed cellulose nanofiber in low density polyethylene nanocomposite by liquid-assisted extrusion. Polymers 12(4):927–927

[303] Bondeson D, Oksman K (2007) Dispersion and characteristics of surfactant modified cellulose whiskers nanocomposites. Compos Interfaces 14(7–9):617–630. https://doi.org/10.1163/156855407782106519

[304] Wang L, Gramlich WM, Gardner DJ, Han Y, Tajvidi M (2018) Spray-dried cellulose nanofibril-reinforced polypropylene composites for extrusion-based additive manufacturing: Nonisothermal crystallization kinetics and thermal expansion. J Compos Sci 2(1):7–7. https://doi.org/10.3390/jcs2010007

[305] Venkatraman P, Gohn AM, Rhoades AM, Foster EJ (2019) Developing high performance PA 11/cellulose nanocomposites for industrial-scale melt processing. Compos B Eng 174:106988–106988. https://doi.org/10.1016/j.compositesb.2019.106988

[306] Leão RM, Jesus LCC, Bertuoli PT, Zattera AJ, Maia JMLL, del Menezzi CHS, Amico SC, da Luz SM (2020) Production and characterization of cellulose nanocrystals/acrylonitrile butadiene styrene nanocomposites. J Compos Mater 54(27):4207–4214. https://doi.org/10.1177/0021998320927773

[307] Sarul DS, Arslan D, Vatansever E, Kahraman Y, Durmus A, Salehiyan R, Nofar M (2021) Preparation and characterization of PLA/PBAT/CNC blend nanocomposites. Colloid Polym Sci 299(6):987–998. https://doi.org/10.1007/s00396-021-04822-9

[308] Jonoobi M, Harun J, Mathew AP, Oksman K (2010) Mechanical properties of cellulose nanofiber (CNF) reinforced polylactic acid (PLA) prepared by twin screw extrusion. Compos Sci Technol 70(12):1742–1747. https://doi.org/10.1016/j.compscitech.2010.07.005

[309] Gong G, Pyo J, Mathew AP, Oksman K (2011) Tensile behavior, morphology and viscoelastic analysis of cellulose nanofiber-reinforced (CNF) polyvinyl acetate (PVAc). Compos A Appl Sci Manuf 42(9):1275–1282. https://doi.org/10.1016/j.compositesa.2011.05.009

[310] Gong G, Mathew AP, Oksman K (2011) Toughening effect of cellulose nanowhiskers on polyvinyl acetate: fracture toughness and viscoelastic analysis. Polym Compos 32(10):1492–1498. https://doi.org/10.1002/pc.21170

[311] Jonoobi M, Mathew AP, Abdi MM, Makinejad MD, Oksman K (2012) A comparison of modified and unmodified cellulose nanofiber reinforced polylactic acid (PLA) prepared by twin screw extrusion. J Polym Environ 20(4):991–997. https://doi.org/10.1007/s10924-012-0503-9

[312] Corrêa AC, de Morais TE, Carmona VB, Teodoro KBR, Ribeiro C, Mattoso LHC, Marconcini JM (2014) Obtaining nanocomposites of polyamide 6 and cellulose whiskers via extrusion and injection molding. Cellulose 21(1):311–322. https://doi.org/10.1007/s10570-013-0132-z

[313] Sato A, Kabusaki D, Okumura H, Nakatani T, Nakatsubo F, Yano H (2016) Surface modification of cellulose nanofibers with alkenyl succinic anhydride for high-density polyethylene reinforcement. Compos A Appl Sci Manuf 83:72–79. https://doi.org/10.1016/j.compositesa.2015.11.009

[314] Suzuki K, Sato A, Okumura H, Hashimoto T, Nakagaito AN, Yano H (2014) Novel high-strength, micro fibrillated cellulose-reinforced polypropylene composites using a cationic polymer as compatibilizer. Cellulose 21(1):507–518. https://doi.org/10.1007/s10570-013-0143-9

[315] Semba T, Ito A, Kitagawa K, Kataoka H, Nakatsubo F, Kuboki T, Yano H (2021) Polyamide 6 composites reinforced with nanofibrillated cellulose formed during compounding: effect of acetyl group degree of substitution.

Compos A Appl Sci Manuf 145:106385–106385. https://doi.org/10.1016/j.compositesa.2021.106385

[316] Suzuki K, Okumura H, Kitagawa K, Sato S, Nakagaito AN, Yano H (2013) Development of continuous process enabling nanofibrillation of pulp and melt compounding. Cellulose 20(1):201–210. https://doi.org/10.1007/s10570-012-9843-9

[317] Iwamoto S, Yamamoto S, Lee S-H, Endo T (2014) Solid-state shear pulverization as effective treatment for dispersing lignocellulose nanofibers in polypropylene composites. Cellulose 21(3):1573–1580. https://doi.org/10.1007/s10570-014-0195-5

[318] Iyer KA, Schueneman GT, Torkelson JM (2015) Cellulose nanocrystal/polyolefin biocomposites prepared by solid-state shear pulverization: Superior dispersion leading to synergistic property enhancements. Polymer 56:464–475. https://doi.org/10.1016/j.polymer.2014.11.017

[319] Venkatraman P, Trotto E, Burgoyne I, Foster EJ (2020) Premixed cellulose nanocrystal reinforcement of polyamide 6 for melt processing. Polym Compos 41(10):4353–4361. https://doi.org/10.1002/pc.25717

[320] Oliveira GHM, Maia THS, Talabi SI, Canto LB, Lucas AA (2021) Characterization of cellulose nano/microfibril reinforced polypropylene composites processed via solid-state shear pulverization. Polym Compos 42(3):1371–1382. https://doi.org/10.1002/pc.25907

[321] Sridhara PK, Vilaseca F (2021) High performance PA 6/cellulose nanocomposites in the interest of industrial scale melt processing. Polymers 13(9):1495–1495

[322] Johns MA, Lewandowska AE, Green E, Eichhorn SJ (2020) Employing photoluminescence to rapidly follow aggregation and dispersion of cellulose nanofibrils. Analyst 145(14):4836–4843. https://doi.org/10.1039/d0an00868k

[323] Lewandowska AE, Inai NH, Ghita OR, Eichhorn SJ (2018) Quantitative analysis of the distribution and mixing of cellulose nanocrystals in thermoplastic composites using Raman chemical imaging. RSC Adv 8(62):35831–35839. https://doi.org/10.1039/C8RA06674D

[324] Palange C, Johns MA, Scurr DJ, Phipps JS, Eichhorn SJ (2019) The effect of the dispersion of microfibrillated cellulose on the mechanical properties of melt-compounded polypropylene–polyethylene copolymer. Cellulose 26 (18):9645–9659. https://doi.org/10.1007/s10570-019-02756-8

[325] The Global Market for Cellulose Nanofibres to 2030, Future Markets Inc. (2018). https://www.marketresearch.com/Future-Markets-Inc-v3760/Global-Cellulose-Nanofibers-12045523/

[326] Dourado F, Fontao AI, Leal M, Rodrigues AC, Gama M (2018) Process modelling and techno-economic evaluation of an industrial airlift bacterial cellulose fermentation process. In: Lee KY (ed) Nanocellulose and Sustainability: production, properties, applications and case studies. Taylor Francis/CRC Press, Boca Raton, FL, pp 1–16

[327] Fortea-Verdejo M, Bumbaris E, Burgstaller C, Bismarck A, Lee K-Y (2017) Plant fibre-reinforced polymers: where do we stand in terms of tensile properties? Int Mater Rev 62 (8):441–464. https://doi.org/10.1080/09506608.2016.1271089

[328] Kumar V, Tyagi L, Sinha S (2011) Wood flour–reinforced plastic composites: a review. Rev Chem Eng 27(5–6):253–264. https://doi.org/10.1515/REVCE.2011.006

[329] Ramamoorthy SK, Skrifvars M, Persson A (2015) A review of natural fibers used in biocomposites: plant, animal and regenerated cellulose fibers. Polym Rev 55(1):107–162. https://doi.org/10.1080/15583724.2014.971124

[330] Chan CM, Vandi L-J, Pratt S, Halley P, Richardson D, Werker A, Laycock B (2018) Composites of wood and biodegradable thermoplastics: a review. Polym Rev 58 (3):444–494. https://doi.org/10.1080/15583724.2017.1380039

[331] Sato H, Iba H, Naganuma T, Kagawa Y (2002) Effects of the difference between the refractive indices of constituent materials on the light transmittance of glass-particle-dispersed epoxy-matrix optical composites. Philos Magaz B 82(13):1369–1386. https://doi.org/10.1080/13642810208220726

[332] Brown RM Jr, Willison JH, Richardson CL (1976) Cellulose biosynthesis in Acetobacter xylinum: visualization of the site of synthesis and direct measurement of the in vivo process. Proc Natl Acad Sci USA 73(12):4565–4569. https://doi.org/10.1073/pnas.73.12.4565

[333] Yamanaka S, Watanabe K, Kitamura N, Iguchi M, Mitsuhashi S, Nishi Y, Uryu M (1989) The structure and mechanical properties of sheets prepared from bacterial cellulose. J Mater Sci 24(9):3141–3145. https://doi.org/10.1007/BF01139032

[334] Wang S-S, Han Y-H, Ye Y-X, Shi X-X, Xiang P, Chen D-L, Li M (2017) Physicochemical characterization of high-quality bacterial cellulose produced by Komagataeibacter sp. strain W1 and identification of the associated genes in bacterial cellulose production. RSC Adv 7(71):45145–45155. https://doi.org/10.1039/C7RA08391B

[335] Lee K-Y, Qian H, Tay FH, Blaker JJ, Kazarian SG, Bismarck A (2013) Bacterial cellulose as source for activated nanosized carbon for electric double layer capacitors. J Mater Sci 48(1):367–376. https://doi.org/10.1007/s10853-012-6754-y

[336] Chashiro K, Iwasaki S, Hasegawa T, Maruyama J, Maruyama S, Pal A, Nandi M, Uyama H (2021) Integrating

polyacrylonitrile (PAN) nanoparticles with porous bacterial cellulose hydrogel to produce activated carbon electrodes for electric double-layer capacitors. Microporous Mesoporous Mater 323:111209–111209. https://doi.org/10.1016/j.micromeso.2021.111209

[337] Kondor A, Santmarti A, Mautner A, Williams D, Bismarck A, Lee K-Y (2021) On the BET surface area of nanocellulose determined using volumetric, gravimetric and chromatographic adsorption methods. Front Chem Eng 3 (45):738995. https://doi.org/10.3389/fceng.2021.738995

[338] Santmarti A, Teh JW, Lee K-Y (2019) Transparent poly (methyl methacrylate) composites based on bacterial cellulose nanofiber networks with improved fracture resistance and impact strength. ACS Omega 4(6):9896–9903. https://doi.org/10.1021/acsomega.9b00388

[339] Santmarti A, Zhang H, Lappalainen T, Lee K-Y (2020) Cellulose nanocomposites reinforced with bacterial cellulose sheets prepared from pristine and disintegrated pellicle. Compos A Appl Sci Manuf 130:105766–105766. https://doi.org/10.1016/j.compositesa.2020.105766

[340] Herráez M, Fernández A, Lopes CS, González C (2016) Strength and toughness of structural fibres for composite material reinforcement. Philos Trans Royal Soc A: Math Phys Eng Sci 374(2071):20150274–20150274. https://doi.org/10.1098/rsta.2015.0274

[341] Mautner A, Lee KY, Lahtinen P, Hakalahti M, Tammelin T, Li K, Bismarck A (2014) Nanopapers for organic solvent nanofiltration. Chem Commun 50(43):5778–5781. https://doi.org/10.1039/C4CC00467A

[342] Rivers G, Cronin D (2019) Influence of moisture and thermal cycling on delamination flaws in transparent armor materials: thermoplastic polyurethane bonded glass-polycarbonate laminates. Mater Des 182:108026–108026. https://doi.org/10.1016/j.matdes.2019.108026

[343] Oliaei E, Berthold F, Berglund LA, Lindström T (2021) Eco-friendly high-strength composites based on hot-pressed lignocellulose microfibrils or fibers. ACS Sustain Chem Eng 9(4):1899–1910

[344] Hill CAS (2007) Wood modification: chemical, thermal and other processes. John Wiley & Sons, Chichester

[345] Berglund LA, Burgert I (2018) Bioinspired wood nanotechnology for functional materials. Adv Mater 30 (19):1704285. https://doi.org/10.1002/adma.201704285

[346] Zhu M, Song J, Li T, Gong A, Wang Y, Dai J, Yao Y, Luo W, Henderson D, Hu L (2016) Highly anisotropic, highly transparent wood composites. Adv Mater 28(26):5181–5187. https://doi.org/10.1002/adma.201600427

[347] Li Y, Fu Q, Yu S, Yan M, Berglund L (2016) Optically transparent wood from a nanoporous cellulosic template: Combining functional and structural performance.

Biomacromolecules 17(4):1358–1364. https://doi.org/10.1021/acs.biomac.6b00145

[348] Yang X, Berglund LA (2018) Water-based approach to high-strength all-cellulose material with optical transparency. ACS Sustain Chem Eng 6(1):501–510. https://doi.org/10.1021/acssuschemeng.7b02755

[349] Wu Y, Wang Y, Yang F, Wang J, Wang X (2020) Study on the properties of transparent bamboo prepared by epoxy resin impregnation. Polymers 12(4):863. https://doi.org/10.3390/polym12040863

[350] Li Y, Vasileva E, Sychugov I, Popov S, Berglund L (2018) Optically transparent wood: recent progress, opportunities, and challenges. Adv Opt Mater 6(14):1800059. https://doi.org/10.1002/adom.201800059

[351] Yano H (2001) Potential strength for resin-impregnated compressed wood. J Mater Sci Lett 20(12):1127–1129

[352] Li Y, Fu Q, Rojas R, Yan M, Lawoko M, Berglund L (2017) Lignin-retaining transparent wood. ChemSusChem 10:3445–3451. https://doi.org/10.1002/cssc.201701089

[353] Fink S (1992) Transparent wood—a new approach in the functional study of wood structure. Holzforschung 46 (5):403–408. https://doi.org/10.1515/hfsg.1992.46.5.403

[354] Höglund M, Johansson M, Sychugov I, Berglund LA (2020) Transparent wood biocomposites by fast UV-curing for reduced light-scattering through wood/thiol–ene interface design. ACS Appl Mater Interfaces 12(41):46914–46922. https://doi.org/10.1021/acsami.0c12505

[355] Chen L, Xu Z, Wang F, Duan G, Xu W, Zhang G, Yang H, Liu J, Jiang S (2020) A flame-retardant and transparent wood/polyimide composite with excellent mechanical strength. Compos Commun 20:100355. https://doi.org/10.1016/j.coco.2020.05.001

[356] Chen H, Montanari C, Yan M, Popov S, Li Y, Sychugov I, Berglund LA (2020) Refractive index of delignified wood for transparent biocomposites. RSC Adv 10(67):40719–40724. https://doi.org/10.1039/D0RA07409H

[357] Pang J, Baitenov A, Montanari C, Samanta A, Berglund L, Popov S, Zozoulenko I (2021) Light propagation in transparent wood: Efficient ray-tracing simulation and retrieving an effective refractive index of wood scaffold. Adv Photon Res 2(11):2100135. https://doi.org/10.1002/adpr.202100135

[358] Montanari C, Olsén P, Berglund LA (2020) Interface tailoring by a versatile functionalization platform for nanostructured wood biocomposites. Green Chem 22(22):8012–8023. https://doi.org/10.1039/D0GC02768E

[359] Montanari C, Ogawa Y, Olsén P, Berglund LA (2021) High performance, fully bio-based, and optically transparent wood biocomposites. Adv Sci 8(12):2100559. https://doi.org/10.1002/advs.202100559

[360] Jungstedt E, Montanari C, Östlund S, Berglund L (2020) Mechanical properties of transparent high strength biocomposites from delignified wood veneer. Compos A Appl Sci Manuf 133:105853. https://doi.org/10.1016/j.compositesa.2020.105853

[361] Vasileva E, Chen H, Li Y, Sychugov I, Yan M, Berglund L, Popov S (2018) Light scattering by structurally anisotropic media: a benchmark with transparent wood. Adv Opt Mater 6(23):1800999. https://doi.org/10.1002/adom.201800999

[362] Vasileva E, Baitenov A, Chen H, Li Y, Sychugov I, Yan M, Berglund L, Popov S (2019) Effect of transparent wood on the polarization degree of light. Opt Lett 44(12):2962–2965. https://doi.org/10.1364/OL.44.002962

[363] Li T, Zhu M, Yang Z, Song J, Dai J, Yao Y, Luo W, Pastel G, Yang B, Hu L (2016) Wood composite as an energy efficient building material: guided sunlight transmittance and effective thermal insulation. Adv Energy Mater 6(22):1601122. https://doi.org/10.1002/aenm.201601122

[364] Chen H, Baitenov A, Li Y, Vasileva E, Popov S, Sychugov I, Yan M, Berglund L (2019) Thickness dependence of optical transmittance of transparent wood: chemical modification effects. ACS Appl Mater Interfaces 11(38):35451–35457. https://doi.org/10.1021/acsami.9b11816

[365] Li Y, Yang X, Fu Q, Rojas R, Yan M, Berglund L (2018) Towards centimeter thick transparent wood through interface manipulation. J Mater Chem A 6(3):1094–1101. https://doi.org/10.1039/C7TA09973H

[366] Chen P, Li Y, Nishiyama Y, Pingali SV, O'Neill HM, Zhang Q, Berglund LA (2021) Small angle neutron scattering shows nanoscale PMMA distribution in transparent wood biocomposites. Nano Lett 21(7):2883–2890. https://doi.org/10.1021/acs.nanolett.0c05038

[367] Fu Q, Yan M, Jungstedt E, Yang X, Li Y, Berglund LA (2018) Transparent plywood as a load-bearing and luminescent biocomposite. Compos Sci Technol 164:296–303. https://doi.org/10.1016/j.compscitech.2018.06.001

[368] Wu Y, Wang Y, Yang F (2021) Comparison of multilayer transparent wood and single layer transparent wood with the same thickness. Front Mater 8:41. https://doi.org/10.3389/fmats.2021.633345

[369] Montanari C, Li Y, Chen H, Yan M, Berglund LA (2019) Transparent wood for thermal energy storage and reversible optical transmittance. ACS Appl Mater Interfaces 11(22):20465–20472. https://doi.org/10.1021/acsami.9b05525

[370] Yu Z, Yao Y, Yao J, Zhang L, Chen Z, Gao Y, Luo H (2017) Transparent wood containing CsxWO3 nanoparticles for heat-shielding window applications. J Mater Chem A 5(13):6019–6024. https://doi.org/10.1039/C7TA00261K

[371] Gan W, Gao L, Xiao S, Zhang W, Zhan X, Li J (2017) Transparent magnetic wood composites based on immobilizing Fe3O4 nanoparticles into a delignified wood template. J Mater Sci 52(6):3321–3329. https://doi.org/10.1007/s10853-016-0619-8

[372] Höglund M, Garemark J, Nero M, Willhammar T, Popov S, Berglund LA (2021) Facile processing of transparent wood nanocomposites with structural color from plasmonic nanoparticles. Chem Mater 33(10):3736–3745. https://doi.org/10.1021/acs.chemmater.1c00806

[373] Lang AW, Li Y, De Keersmaecker M, Shen DE, Österholm AM, Berglund L, Reynolds JR (2018) Transparent wood smart windows: Polymer electrochromic devices based on poly(3,4-ethylenedioxythiophene):poly(styrene sulfonate) electrodes. ChemSusChem 11(5):854–863. https://doi.org/10.1002/cssc.201702026

[374] Li Y, Yu S, Veinot JGC, Linnros J, Berglund L, Sychugov I (2017) Luminescent transparent wood. Adv Opt Mater 5(1):1600834. https://doi.org/10.1002/adom.201600834

[375] Samanta A, Chen H, Samanta P, Popov S, Sychugov I, Berglund LA (2021) Reversible dual-stimuli-responsive chromic transparent wood biocomposites for smart window applications. ACS Appl Mater Interfaces 13(2):3270–3277. https://doi.org/10.1021/acsami.0c21369

[376] Li Y, Gu X, Gao H, Li J (2020) Photoresponsive wood composite for photoluminescence and ultraviolet absorption. Constr Build Mater 261:119984. https://doi.org/10.1016/j.conbuildmat.2020.119984

[377] Zhu M, Li T, Davis CS, Yao Y, Dai J, Wang Y, AlQatari F, Gilman JW, Hu L (2016) Transparent and haze wood composites for highly efficient broadband light management in solar cells. Nano Energy 26:332–339. https://doi.org/10.1016/j.nanoen.2016.05.020

[378] Li Y, Cheng M, Jungstedt E, Xu B, Sun L, Berglund L (2019) Optically transparent wood substrate for perovskite solar cells. ACS Sustain Chem Eng 7(6):6061–6067. https://doi.org/10.1021/acssuschemeng.8b06248

[379] Foster KEO, Jones R, Miyake GM, Srubar Iii WV (2021) Mechanics, optics, and thermodynamics of water transport in chemically modified transparent wood composites. Compos Sci Technol 208:108737–108737

[380] Bisht P, Pandey KK, Barshilia HC (2021) Photostable transparent wood composite functionalized with an UV-absorber. Polym Degrad Stab 189:109600. https://doi.org/10.1016/j.polymdegradstab.2021.109600

[381] Vasileva E, Li Y, Sychugov I, Mensi M, Berglund L, Popov S (2017) Lasing from organic dye molecules embedded in transparent wood. Adv Opt Mater 5(10):1700057. https://doi.org/10.1002/adom.201700057

[382] Bu L, Himmel ME, Crowley MF (2015) The molecular origins of twist in cellulose I-beta. Carbohyd Polym 125:146–152. https://doi.org/10.1016/J.CARBPOL.2015.02.023

[383] Parker RM, Guidetti G, Williams CA, Zhao T, Narkevicius A, Vignolini S, Frka-Petesic B (2018) The self-assembly of cellulose nanocrystals: Hierarchical design of visual appearance. Adv Mater 30(19):1704477–1704477. https://doi.org/10.1002/adma.201704477

[384] Schütz C, Bruckner JR, Honorato-Rios C, Tosheva Z, Anyfantakis M, Lagerwall JPF (2020) From equilibrium liquid crystal formation and kinetic arrest to photonic bandgap films using suspensions of cellulose nanocrystals. Curr Comput-Aided Drug Des 10(3):199–199. https://doi.org/10.3390/cryst10030199

[385] Revol JF, Marchessault RH (1993) In vitro chiral nematic ordering of chitin crystallites. Int J Biol Macromol 15(6):329–329. https://doi.org/10.1016/0141-8130(93)90049-R

[386] Revol J-F, Godbout DL, Gray DG (1998) Solid self-assembled films of cellulose with chiral nematic order and optically variable properties. J Pulp Pap Sci 24(5):146–146

[387] Guidetti G, Atifi S, Vignolini S, Hamad WY (2016) Flexible photonic cellulose nanocrystal films. Adv Mater 28(45):10042–10047. https://doi.org/10.1002/adma.201603386

[388] Yao K, Meng Q, Bulone V, Zhou Q (2017) Flexible and responsive chiral nematic cellulose nanocrystal/poly(ethylene glycol) composite films with uniform and tunable structural color. Adv Mater 29(28):1701323–1701323. https://doi.org/10.1002/adma.201701323

[389] Walters CM, Boott CE, Nguyen TD, Hamad WY, Maclachlan MJ (2020) Iridescent cellulose nanocrystal films modified with hydroxypropyl cellulose. Biomacromol 21(3):1295–1302. https://doi.org/10.1021/acs.biomac.0c00056

[390] Saraiva DV, Chagas R, de Abreu BM, Gouveia CN, Silva PES, Godinho MH, Fernandes SN (2020) Flexible and structural coloured composite films from cellulose nanocrystals/hydroxypropyl cellulose lyotropic suspensions. Curr Comput-Aided Drug Des 10(2):122–122. https://doi.org/10.3390/cryst10020122

[391] Guidetti G, Sun H, Ivanova A, Marelli B, Frka-Petesic B (2021) Co-assembly of cellulose nanocrystals and silk fibroin into photonic cholesteric films. Adv Sustain Syst 5(6):2000272–2000272. https://doi.org/10.1002/ADSU.202000272

[392] Shopsowitz KE, Qi H, Hamad WY, MacLachlan MJ (2010) Free-standing mesoporous silica films with tunable chiral nematic structures. Nature 468(7322):422–425. https://doi.org/10.1038/nature09540

[393] Frka-Petesic B, Kelly JA, Jacucci G, Guidetti G, Kamita G, Crossette NP, Hamad WY, MacLachlan MJ, Vignolini S (2020) Retrieving the coassembly pathway of composite cellulose nanocrystal photonic films from their angular optical response. Adv Mater 32(19):1906889–1906889. https://doi.org/10.1002/adma.201906889

[394] Frka-Petesic B, Kamita G, Guidetti G, Vignolini S (2019) Angular optical response of cellulose nanocrystal films explained by the distortion of the arrested suspension upon drying. Phys Rev Mater 3(4):045601–045601. https://doi.org/10.1103/PhysRevMaterials.3.045601

[395] Gu M, Jiang C, Liu D, Prempeh N, Smalyukh II (2016) Cellulose nanocrystal/poly(ethylene glycol) composite as an iridescent coating on polymer substrates: structure-color and interface adhesion. ACS Appl Mater Interfaces 8(47):32565–32573. https://doi.org/10.1021/acsami.6b12044

[396] Espinha A, Guidetti G, Serrano MC, Frka-Petesic B, Dumanli AG, Hamad WY, Blanco Á, López C, Vignolini S (2016) Shape memory cellulose-based photonic reflectors. ACS Appl Mater Interfaces 8(46):31935–31940. https://doi.org/10.1021/acsami.6b10611

[397] Boott CE, Tran A, Hamad WY, MacLachlan MJ (2020) Cellulose nanocrystal elastomers with reversible visible color. Angew Chem 132(1):232–237. https://doi.org/10.1002/ange.201911468

[398] Tran A, Hamad WY, MacLachlan MJ (2018) Tactoid annealing improves order in self-assembled cellulose nanocrystal films with chiral nematic structures. Langmuir 34(2):646–652. https://doi.org/10.1021/acs.langmuir.7b03920

[399] Boott CE, Soto MA, Hamad WY, MacLachlan MJ (2021) Shape-memory photonic thermoplastics from cellulose nanocrystals. Adv Func Mater 31(43):2103268–2103268. https://doi.org/10.1002/ADFM.202103268

[400] Chowdhury RA, Clarkson C, Youngblood J (2018) Continuous roll-to-roll fabrication of transparent cellulose nanocrystal (CNC) coatings with controlled anisotropy. Cellulose 25:1769–1781. https://doi.org/10.1007/s10570-018-1688-4

[401] Koppolu R, Abitbol T, Kumar V, Jaiswal AK, Swerin A, Toivakka M (2018) Continuous roll-to-roll coating of cellulose nanocrystals onto paperboard. Cellulose 25(10):6055–6069. https://doi.org/10.1007/s10570-018-1958-1

[402] Droguet B, Liang H-L, Parker RM, Frka-Petesic B, De Volder M, Baumberg J, Vignolini S (2021) Large-scale fabrication of structurally coloured cellulose nanocrystal films and effect pigments. Nature Materials. https://doi.org/10.1038/s41563-021-01135-8

[403] Klockars KW, Tardy BL, Borghei M, Tripathi A, Greca LG, Rojas OJ (2018) Effect of anisotropy of cellulose nanocrystal suspensions on stratification, domain structure formation, and structural colors. Biomacromolecules 19(7):2931–2943. https://doi.org/10.1021/acs.biomac.8b00497

[404] Honorato-Rios C, Lehr C, Schütz C, Sanctuary R, Osipov MA, Baller J, Lagerwall JPF (2018) Fractionation of cellulose nanocrystals: enhancing liquid crystal ordering without promoting gelation. NPG Asia Materials 10 (5):455–465. https://doi.org/10.1038/s41427-018-0046-1

[405] Zhao TH, Parker RM, Williams CA, Lim KTP, Frka-Petesic B, Vignolini S (2019) Printing of responsive photonic cellulose nanocrystal microfilm arrays. Adv Func Mater 29(21):1804531–1804531. https://doi.org/10.1002/adfm.201804531

[406] Parker RM, Frka-Petesic B, Guidetti G, Kamita G, Consani G, Abell C, Vignolini S (2016) Hierarchical self-assembly of cellulose nanocrystals in a confined geometry. ACS Nano 10(9):8443–8449. https://doi.org/10.1021/acsnano.6b03355

[407] Parker MR, Zhao TH, Frka-Petesic B, Vignolini S (2021) Cellulose photonic pigments. https://arxiv.org/abs/2110.00410

[408] Fang Z, Gong AS, Hu L (2020) Chapter 10 - Wood cellulose paper for solar cells. In: Filpponen I, Peresin MS, Nypelö T (eds) Lignocellulosics. Elsevier, Amsterdam, pp 279–295

[409] Reimer M, Zollfrank C (2021) Cellulose for light manipulation: methods, applications, and prospects. Adv Energy Mater 11(43):2003866. https://doi.org/10.1002/aenm.202003866

[410] Brunetti F, Operamolla A, Castro-Hermosa S, Lucarelli G, Manca V, Farinola GM, Brown TM (2019) Printed solar cells and energy storage devices on paper substrates. Adv Func Mater 29(21):1806798–1806798. https://doi.org/10.1002/adfm.201806798

[411] Vicente AT, Araújo A, Mendes MJ, Nunes D, Oliveira MJ, Sanchez-Sobrado O, Ferreira MP, Águas H, Fortunato E, Martins R (2018) Multifunctional cellulose-paper for light harvesting and smart sensing applications. J Mater Chem C 6(13):3143–3181. https://doi.org/10.1039/c7tc05271e

[412] Yao YG, Tao JS, Zou JH, Zhang B, Li T, Dai JQ, Zhu MW, Wang S, Fu KK, Henderson D, Hitz E, Peng JB, Hu LB (2016) Light management in plastic–paper hybrid substrate towards high-performance optoelectronics. Energy Environ Sci 9(7):2278–2285. https://doi.org/10.1039/C6EE01011C

[413] Jia C, Li T, Chen CJ, Dai JQ, Kierzewski IM, Song JW, Li YJ, Yang CP, Wang CW, Hu LB (2017) Scalable, anisotropic transparent paper directly from wood for light management in solar cells. Nano Energy 36:366–373. https://doi.org/10.1016/j.nanoen.2017.04.059

[414] Águas H, Mateus T, Vicente A, Gaspar D, Mendes MJ, Schmidt WA, Pereira L, Fortunato E, Martins R (2015) Thin film silicon photovoltaic cells on paper for flexible indoor applications. Adv Func Mater 25(23):3592–3598. https://doi.org/10.1002/adfm.201500636

[415] Tobjörk D, Österbacka R (2011) Paper electronics. Adv Mater 23(17):1935–1961. https://doi.org/10.1002/adma.201004692

[416] Chen W, Yu H, Lee S-Y, Wei T, Li J, Fan Z (2018) Nanocellulose: a promising nanomaterial for advanced electrochemical energy storage. Chem Soc Rev 47 (8):2837–2872. https://doi.org/10.1039/C7CS00790F

[417] Zhu Z, Xu Z (2020) The rational design of biomass-derived carbon materials towards next-generation energy storage: a review. Renew Sust Energ Rev 134:110308–110308. https://doi.org/10.1016/j.rser.2020.110308

[418] Kim J-H, Lee D, Lee Y-H, Chen W, Lee S-Y (2019) Nanocellulose for energy storage systems: beyond the limits of synthetic materials. Adv Mater 31(20):1804826. https://doi.org/10.1002/adma.201804826

[419] Jacucci G, Schertel L, Zhang Y, Yang H, Vignolini S (2021) Light management with natural materials: from whiteness to transparency. Adv Mater 33(28):2001215. https://doi.org/10.1002/adma.202001215

[420] Nogi M, Iwamoto S, Nakagaito AN, Yano H (2009) Optically transparent nanofiber paper. Adv Mater 21 (16):1595–1598. https://doi.org/10.1002/adma.200803174

[421] Fang ZQ, Hou GY, Chen CJ, Hu LB (2019) Nanocellulose-based films and their emerging applications. Curr Opin Solid State Mater Sci 23(4):100764–100764. https://doi.org/10.1016/j.cossms.2019.07.003

[422] Fang ZQ, Zhu HL, Preston C, Hu LB (2014) Development, application and commercialization of transparent paper. Transl Mater Res 1(1):15004–15004. https://doi.org/10.1088/2053-1613/1/1/015004

[423] Hu LB, Zheng G, Yao J, Liu N, Weil B, Eskilsson M, Karabulut E, Ruan ZC, Fan SH, Bloking JT, McGehee MD, Wågberg L, Cui Y (2013) Transparent and conductive paper from nanocellulose fibers. Energy Environ Sci 6 (2):513–518. https://doi.org/10.1039/c2ee23635d

[424] Zhou YH, Fuentes-Hernandez C, Khan TM, Liu JC, Hsu J, Shim JW, Dindar A, Youngblood JP, Moon RJ, Kippelen B (2013) Recyclable organic solar cells on cellulose nanocrystal substrates. Sci Rep 3(1):1536–1536. https://doi.org/10.1038/srep01536

[425] Gao L, Chao LF, Hou MH, Liang J, Chen YH, Yu HD, Huang W (2019) Flexible, transparent nanocellulose paper-based perovskite solar cells. NPJ Flex Electron 3(1):4–4. https://doi.org/10.1038/s41528-019-0048-2

[426] Barr MC, Rowehl JA, Lunt RR, Xu J, Wang A, Boyce CM, Im SG, Bulović V, Gleason KK (2011) Direct monolithic integration of organic photovoltaic circuits on unmodified paper. Adv Mater 23(31):3500–3505. https://doi.org/10.1002/adma.201101263

[427] Zhou Y, Khan TM, Liu J-C, Fuentes-Hernandez C, Shim JW, Najafabadi E, Youngblood JP, Moon RJ, Kippelen B (2014) Efficient recyclable organic solar cells on cellulose nanocrystal substrates with a conducting polymer top electrode deposited by film-transfer lamination. Org Electron 15(3):661–666. https://doi.org/10.1016/j.orgel.2013.12.018

[428] Yang L, Xiong Q, Li Y, Gao P, Xu B, Lin H, Li X, Miyasaka T (2021) Artemisinin-passivated mixed-cation perovskite films for durable flexible perovskite solar cells with over 21% efficiency. J Mater Chem A 9(3):1574–1582. https://doi.org/10.1039/D0TA10717D

[429] Ning HL, Zeng Y, Kuang Y, Zheng ZK, Zhou PP, Yao RH, Zhang HK, Bao WZ, Chen G, Fang ZQ, Peng JB (2017) Room-temperature fabrication of high-performance amorphous In-Ga-Zn-O/Al2O3 thin-film transistors on ultrasmooth and clear nanopaper. ACS Appl Mater Interfaces 9(33):27792–27800. https://doi.org/10.1021/acsami.7b07525

[430] Fang ZQ, Zhu HL, Yuan YB, Ha DH, Zhu S, Preston C, Chen QX, Li YY, Han XG, Lee SW, Chen G, Li T, Munday J, Huang JS, Hu LB (2014) Novel nanostructured paper with ultrahigh transparency and ultrahigh haze for solar cells. Nano Lett 14(2):765–773. https://doi.org/10.1021/nl404101p

[431] Fang ZQ, Zhu HL, Bao W, Preston C, Liu Z, Dai JQ, Li YY, Hu LB (2014) Highly transparent paper with tunable haze for green electronics. Energy Environ Sci 7(10):3313–3319. https://doi.org/10.1039/C4EE02236J

[432] Hu W, Chen G, Liu Y, Liu YY, Li B, Fang ZQ (2018) Transparent and hazy all-cellulose composite films with superior mechanical properties. ACS Sustain Chem Eng 6(5):6974–6980. https://doi.org/10.1021/acssuschemeng.8b00814

[433] Hou G, Liu Y, Zhang D, Li G, Xie H, Fang Z (2020) Approaching theoretical haze of highly transparent all-cellulose composite films. ACS Appl Mater Interfaces 12(28):31998–32005. https://doi.org/10.1021/acsami.0c08586

[434] Zhu HL, Fang ZQ, Wang Z, Dai JQ, Yao YG, Shen F, Preston C, Wu WX, Peng P, Jang N, Yu QK, Yu ZF, Hu LB (2016) Extreme light management in mesoporous wood cellulose paper for optoelectronics. ACS Nano 10(1):1369–1377. https://doi.org/10.1021/acsnano.5b06781

[435] Simon P, Gogotsi Y, Dunn B (2014) Where do batteries end and supercapacitors begin? Science 343(6176):1210–1211. https://doi.org/10.1126/science.1249625

[436] Choi NS, Chen Z, Freunberger SA, Ji X, Sun YK, Amine K, Yushin G, Nazar LF, Cho J, Bruce PG (2012) Challenges facing lithium batteries and electrical double-layer capacitors. Angew Chem Int Edn 51(40):9994–10024. https://doi.org/10.1002/anie.201201429

[437] Chen C, Hu L (2018) Nanocellulose toward advanced energy storage devices: structure and electrochemistry. Acc Chem Res 51(12):3154–3165. https://doi.org/10.1021/acs.accounts.8b00391

[438] Li T, Chen C, Brozena AH, Zhu JY, Xu L, Driemeier C, Dai J, Rojas OJ, Isogai A, Wågberg L, Hu L (2021) Developing fibrillated cellulose as a sustainable technological material. Nature 590(7844):47–56. https://doi.org/10.1038/s41586-020-03167-7

[439] Chen C, Hu L (2021) Nanoscale Ion Regulation in Wood-Based Structures and Their Device Applications. Adv Mater 33(28):2002890. https://doi.org/10.1002/adma.202002890

[440] Wang Z, Lee YH, Kim SW, Seo JY, Lee SY, Nyholm L (2021) Why cellulose-based electrochemical energy storage devices? Adv Mater 33(28):2000892. https://doi.org/10.1002/adma.202000892

[441] Wang X, Yao C, Wang F, Li Z (2017) Cellulose-based nanomaterials for energy applications. Small 13(42):1702240. https://doi.org/10.1002/smll.201702240

[442] Wang Z, Tammela P, Strømme M, Nyholm L (2017) Cellulose-based supercapacitors: material and performance considerations. Adv Energy Mater 7(18):1700130. https://doi.org/10.1002/aenm.201700130

[443] Zou F, Manthiram A (2020) A Review of the design of advanced binders for high-performance batteries. Adv Energy Mater 10(45):2002508. https://doi.org/10.1002/aenm.202002508

[444] Liu J, Yuan H, Tao X, Liang Y, Yang SJ, Huang JQ, Yuan TQ, Titirici MM, Zhang Q (2020) Recent progress on biomass-derived ecomaterials toward advanced rechargeable lithium batteries. EcoMat 2(1):e12019. https://doi.org/10.1002/eom2.12019

[445] Kuang Y, Chen C, Pastel G, Li Y, Song J, Mi R, Kong W, Liu B, Jiang Y, Yang K, Hu L (2018) Conductive cellulose nanofiber enabled thick electrode for compact and flexible energy storage devices. Adv Energy Mater 8(33):1802398. https://doi.org/10.1002/aenm.201802398

[446] Cao D, Xing Y, Tantratian K, Wang X, Ma Y, Mukhopadhyay A, Cheng Z, Zhang Q, Jiao Y, Chen L (2019) 3D printed high-performance lithium metal microbatteries enabled by nanocellulose. Adv Mater 31(14):1807313. https://doi.org/10.1002/adma.201807313

[447] Li Y, Zhu H, Wang Y, Ray U, Zhu S, Dai J, Chen C, Fu K, Jang S-H, Henderson D, Li T, Hu L (2017) Cellulose-

nanofiber-enabled 3D printing of a carbon-nanotube microfiber network. Small Methods 1(10):1700222. https://doi.org/10.1002/smtd.201700222

[448] Gonçalves R, Lizundia E, Silva MM, Costa CM, Lanceros-Méndez S (2019) Mesoporous cellulose nanocrystal membranes as battery separators for environmentally safer lithium-ion batteries. ACS Appl Energy Mater 2(5):3749–3761. https://doi.org/10.1021/acsaem.9b00458

[449] Battery separator (2019). Nippon Kodoshi corporation https://www.kodoshi.co.jp/english/product/battery_separator.html,

[450] Hou M, Hu Y, Xu M, Li B (2020) Nanocellulose based flexible and highly conductive film and its application in supercapacitors. Cellulose 27(16):9457–9466. https://doi.org/10.1007/s10570-020-03420-2

[451] Li YM, Hu YS, Titirici MM, Chen LQ, Huang XJ (2016) Hard carbon microtubes made from renewable cotton as high-performance anode material for sodium-ion batteries. Adv Energy Mater 6(18):1600659–1600659. https://doi.org/10.1002/aenm.201600659

[452] Xu Z, Xie F, Wang J, Au H, Tebyetekerwa M, Guo Z, Yang S, Hu YS, Titirici MM (2019) All-cellulose-based quasi-solid-state sodium-ion hybrid capacitors enabled by structural hierarchy. Adv Func Mater 29(39):1903895–1903895. https://doi.org/10.1002/adfm.201903895

[453] Xu Z, Guo Z, Madhu R, Xie F, Chen R, Wang J, Tebyetekerwa M, Hu YS, Titirici MM (2021) Homogenous metallic deposition regulated by defect-rich skeletons for sodium metal batteries. Energy Environ Sci 14(12):6381–6393. https://doi.org/10.1039/D1EE01346G

[454] Guo R, Zhang L, Lu Y, Zhang X, Yang D (2020) Research progress of nanocellulose for electrochemical energy storage: a review. J Energy Chem 51:342–361. https://doi.org/10.1016/j.jechem.2020.04.029

[455] Yang C, Wu Q, Xie W, Zhang X, Brozena A, Zheng J, Garaga MN, Ko BH, Mao Y, He S, Gao Y (2021) Copper-coordinated cellulose ion conductors for solid-state batteries. Nature 598(7882):590–596. https://doi.org/10.1038/s41586-021-03885-6

Publisher's Note Springer Nature remains neutral with regard to jurisdictional claims in published maps and institutional affiliations.

Authors and Affiliations

S. J. Eichhorn[1] · A. Etale[1] · J. Wang[1] · L. A. Berglund[2] · Y. Li[2] · Y. Cai[3] · C. Chen[4] · E. D. Cranston[5,6] · M. A. Johns[5] · Z. Fang[7] · G. Li[7] · L. Hu[8] · M. Khandelwal[9] · K.-Y. Lee[10] · K. Oksman[11] · S. Pinitsoontorn[12] · F. Quero[13,14] · A. Sebastian[15] · M. M. Titirici[16] · Z. Xu[16] · S. Vignolini[17] · B. Frka-Petesic[17]

[1]School of Civil, Aerospace and Mechanical Engineering, Bristol Composites Institute, University of Bristol, University Walk, Bristol BS8 1TR, UK

[2]Department of Fiber and Polymer Technology, Wallenberg Wood Science Center, Royal Institute of Technology (KTH), 10044 Stockholm, Sweden

[3]State Key Laboratory for Modification of Chemical Fibers and Polymer Materials, Key Laboratory of High-Performance Fibers and Products, Ministry of Education, College of Materials Science and Engineering, Donghua University, Shanghai 201620, China

[4]School of Resource and Environmental Sciences, Wuhan University, Wuhan 430079, China

[5]Department of Wood Science, The University of British Columbia, 2424 Main Mall, Vancouver, BC V6T 1Z4, Canada

[6]Department of Chemical and Biological Engineering, The University of British Columbia, 2360 East Mall, Vancouver, BC V6T 1Z3, Canada

[7]State Key Laboratory of Pulp and Paper Engineering, South China University of Technology, Guangzhou 510640, Guangdong, China

[8]Department of Materials Science and Engineering, University of Maryland, College Park, MD 20742, USA

[9]Department of Materials Science and Metallurgical Engineering, Indian Institute of Technology Hyderabad, Hyderabad, India

[10]Department of Aeronautics and Institute for Molecular Science and Engineering, Imperial College London, South Kensington Campus, London SW7 2AZ, UK

[11]Division of Materials Science, Department of Engineering Sciences and Mathematics, Luleå University of Technology, SE 97187, Luleå, Sweden

[12]Institute of Nanomaterials Research and Innovation for Energy (IN-RIE), Department of Physics, Faculty of Science, Khon

Kaen University, Khon Kaen 40002, Thailand

[13]Laboratory of Nanocellulose and Biomaterials, Department of Chemical Engineering, Biotechnology and Materials, Faculty of Physical Sciences and Mathematics, University of Chile, Avenida Beauchef 851, 8370456 Santiago, Chile

[14]Millennium Nucleus in Smart Soft Mechanical Metamaterials, Avenida Beauchef 851, 8370456 Santiago, Chile

[15]CIPET: Institute of Plastics Technology, IPT, Kochi, India

[16]Department of Chemical Engineering, Imperial College London, London SW7 2AZ, UK

[17]Yusuf Hamied Department of Chemistry, University of Cambridge, Lensfield Road, Cambridge CB2 1EW, UK